University of New Orleans

## ScholarWorks@UNO

University of New Orleans Theses and Dissertations

Dissertations and Theses

Spring 5-19-2017

# Tidal Creek Equilibrium: Barataria Bay

Bryan Carter
bcarter4@uno.edu

Follow this and additional works at: https://scholarworks.uno.edu/td

Part of the Other Environmental Sciences Commons

# Tidal Creek Equilibrium: Barataria Bay

A Thesis

Submitted to the Graduate Faculty of the
University of New Orleans
In partial fulfillment of the
Requirements for the degree of

Master of Science
in
Earth and Environmental Sciences
Coastal Geology

by

Bryan T. Carter

B.A. Millsaps College, 1999

May, 2017

# Acknowledgements

I would like to take this opportunity to thank the Earth and Environmental Sciences department at the University of New Orleans. I would especially like to thank my advisor Dr. Mark Kulp. Dr. Ioannis Georgiou and Dr. Martin O'Connell, I appreciate your willingness to join Dr. Kulp and serve on my thesis committee. I would also like to extend my thanks to Tara Yocum for her assistance with fieldwork and data processing. Finally, I would like to thank my amazing wife and son for their support and encouragement.

# Table of Contents

# List of Figures

# List of Tables

# Abstract

Louisiana's wetlands are losing land in response to sea level changes, anthropogenic influences and natural marine processes. Historical satellite image analysis reveals that between 2005 and 2015, fifteen tidal creeks in Barataria Bay, Louisiana eroded at the rate of 1.80 m/yr ($\pm$ 1.98 m), and the open water area behind these creeks enlarged at the rate of 530.00 m$^2$/yr ($\pm$ 204.80 m$^2$). This research revealed that selected tidal creeks within the estuary have cross-sectional areas larger (2639% larger) than established ocean-inlet equilibrium models would predict. This work suggests that tidal prism to tidal creek cross-sectional area relationships in Barataria Bay are most strongly shaped by creek exposure to waves and secondarily by tide range and currents. A trend of increased inlet erosion rates due to large fetch distances is evident, but impacts from storm driven subtidal variations also play an important role.

*Keywords: Tidal prism; Louisiana coastal erosion; Barataria Bay; tidal creeks*

# Introduction

## Introduction

The loss of intermediate through saline wetlands across coastal Louisiana is well documented and many of the physical processes that contribute to the losses have been widely investigated (Delaune et al., 1983; Day et al., 1988; Penland and Ramsey, 1990; Penland et al., 2000; Day et al., 2000; Penland et al., 2002; Georgiou et al., 2005; Barras et al., 2008; and Couvillon et al, 2011). An array of studies have identified how wave action, subsidence, sea level rise and insufficient sediment supply individually and collectively contribute toward marsh erosion (e.g. Day et al., 2001; Wilson and Mead, 2008; Georgiou et al., 2005; Yuill et al. 2009).  To date, however, there has been no examination of Louisiana's interior tidal creek evolution and erosion in response to conversion of land to open water. Tidal creeks, an important dimension to tidal marsh ecosystems, serve the vital role of connecting open water bodies to interior marsh ponds. This connection allows for the delivery of nutrients and sediments which benefit the overall health of the marsh ecosystem (Adam, 1990).This project evaluates the possible causes and contributing factors to tidal creek erosion through time with special attention given to the relationship between tidal prism passing through tidal creeks and their cross sectional area.

Subsidence, wave driven erosion and  anthropogenic interactions (e.g. dredging) have contributed to the disappearance of Louisiana's wetland (e.g. Hatton et al., 1983; Gagliano et al., 1981; DeLaune et al., 1994; Day et al., 2001; Day et al., 2007) at the estimated rate of 26.7 km$^2$/yr) from 1985 to 2010 (Couvillion et al., 2011). The creation of open water along the Louisiana coast leads to an increase in tidal prism that increases the amount of water that will flow through tidal creeks and channels. Numerous studies have documented that the amount of

water that flows through an inlet during a tidal cycle directly affects the inlet cross sectional area (O'Brien, 1930; Escoffier, 1940; Bruun and Gerritsen, 1960; O'Brien, 1969; Jarrett, 1976; Fitzgerald et al., 1984; Knaus, 1998; Fitzgerald et al., 2003; Van de Kreeke, 2004; FitzGerald et al., 2006; Stive et al. 2009).

This study contributes to marsh inlet erosion research by using equilibrium models developed for open-water oceanic inlets to evaluate the relationship between interior marsh tidal creeks and the open water area behind them. To accomplish this, 15 tidal creeks located along a 3 to 30-km up basin trend from inlets connected to the Gulf of Mexico have been examined. In Louisiana, this is of particular importance due to the fact that marsh is being converted to open water (Couvillion et al., 2011). The impact of open water expansion to tidal creeks should result in an increased cross sectional area as open water expands. Historical analysis revealed that each of the creek mouths of this study has increased in width during the last 10 years at the average rate of 1.80 m/yr (± 1.98 m). Moreover, at each of the sites, the open water area behind the tidal creeks has increased at an average rate of 530.00 $m^2$/yr (± 204.80 $m^2$). The conversion of marsh to open water is easily attributed to wave forces where large fetch distances facilitate wave erosion , however, at many of these research sites, limited fetch and shallow depths (<1 m) hinder wave erosion. This research will evaluate each contributor to the erosion of these creeks and assess the role of tidal prism equilibrium.

Louisiana's loss of wetlands in the last 100 years provides the perfect backdrop for evaluating the effects of wetland conversion to open water on tidal creeks. Perhaps one of the best locations, because of the numerous interior ponds, tidal creeks, high rates of wetland loss and numerous studies on the seaward tidal inlets, is within Barataria Bay (Figure 1). Previous studies within Barataria Bay (FitzGerald et al., 2004) similar to work done on the Frisian Islands

in the Netherlands (Van de Kreeke et al., 2004) show that as tidal prism changes due to land loss (Barataria Bay) or land gains (Frisian Islands) there are measurable changes to the cross sectional area of these inlets. Accordingly, an increase in open water area behind tidal creeks, which drives tidal prism increase, will result in an increase in cross sectional area of the creeks. This research investigates this relationship by identifying: 1) open water area and marsh inlet cross sectional area rates of erosion, 2) other contributing factors to creek edge erosion (e.g. waves, anthropogenic causes) and,3) calculating theoretical and actual tidal prism to tidal creek cross sectional area relationships. All this in an effort to identify the impact open water expansion has on tidal creeks in Barataria Bay, Louisiana.

Factors that contribute to the wetland loss in Louisiana have been investigated to quantify their contribution to tidal creek erosion. Quantifying the contributing erosional mechanisms allows the tidal prism to tidal creek cross sectional area relationship (P-A relationship) influence to be differentiated from overall erosion rates. Wave action is a driving force for marsh edge erosion (Moeller et al., 1993; Snedden, 2007; and Wilson and Mead, 2008) and will be accounted for in this study by comparing erosion rates at creek mouths with various fetch distances. Storm influences through surge and increased wave height due to high winds also play a role in Louisiana land loss (Georgiou et al., 2005; Snedden et al., 2007; Feng and Li, 2010). The influence of storm-generated wind on water level is of particular importance to this study, in that, tide range in Louisiana is influenced by wind direction and force (Chang and Wiseman, 1983; Snedden, 2007; Feng and Li, 2010). The contribution of hydroperiod (duration of marsh platform inundation) to the overall health of the marsh vegetation is also a known contributing factor to wetland erosion and accretion (DeLaune et al., 1983; Stevenson et al., 1986; Reed, 1995).

3

## Scientific Questions and Hypotheses

This project addresses the following scientific questions:

1) Do Barataria Bay, Louisiana -interior tidal creek cross sectional area to tidal prism equilibrium relationships follow oceanic tidal-inlet equilibrium models as expressed in the formula: $A_e = C (P)^n$?

2) Are differences and/or similarities between marsh interior and ocean tidal relationships a result of specific stressors and processes identifiable?

3) What are the determining variables that affect how closely interior tidal creek models adhere or do not adhere to already established equilibrium models?

## Hypothesis

H1— Cross sectional area of marsh tidal creeks of Barataria Bay is partially determined by the tidal prism they convey. The cross sectional area of the creek mouth is also determined by forces such as waves and tide range.

H2—Tidal creeks exhibit an equilibrium model that is distinct from oceanic models. These creeks are larger than their tidal prism would indicate due to ebb tidal asymmetry that occurs as a result of marsh platform flooding. Marsh platform flooding contributes to tidal volume and in turn increases tidal current velocity as the marsh platform drains. This increase in current velocity contributes to channel edge erosion and scour.

# Background

## Tidal Prism Equilibrium Models

An interest in the morphodynamics of oceanic tidal inlets is rooted in the necessity to understand how environmental conditions can affect the location and cross sectional area of inlets. Impacts, such as inlet migration and inlet infilling can affect commerce, transportation and ecosystem health (Stive, 2009). A relationship exists between cross sectional area of tidal inlets that open to the coastal ocean and the tidal prism flowing through the inlets and into the backbarrier environments (O'Brien, 1930; Escoffier, 1940; O'Brien, 1969; Jarrett, 1976). Tidal prism is the volume of water that flows through the inlet during one half a tide cycle and is expressed by the following formula: $P = H(A)$; where P is tidal prism, H is the spring tidal range, and A is the area of open water that is serviced by the inlet. This equilibrium relationship between tidal inlets and tidal prism can be expressed by:

$$A = CP^k \ (1)$$

where A is the minimum cross-sectional inlet area, C and k are dimensionless values based on actual inlet to tidal prism relationship dimensions and P is the tidal prism (e.g. Escoffier, 1940; Brunn, 1967, 1978; O'brien, 1969; O'brien and Dean, 1972; Byrne et al., 1974; and Jarrett, 1976; and others). Jarrett (1976) contributed to the inlet equilibrium models of O'Brien (1930 and 1969), Escofier (1940), and Nayak (1971), by utilizing inlet cross sectional area and tidal prism data from multiple inlets located on the Atlantic, Gulf of Mexico and Pacific coasts. Increasing the total number of studied inlets and including different bodies of water with a range of hydrodynamic regimes contributed to the identification of factors that contribute to equilibrium models on each of these coasts.

The equilibrium models that Jarrett (1976) developed accounted for the following scenarios for the Atlantic, Pacific and Gulf of Mexico coastlines: 1) no jetty, 2) 1 jetty and, 3) two jetties (Jarrett, 1976). This work highlighted the fact that, although equilibrium models exist for inlets, the hydrodynamic environment as well as structures at the inlet opening contribute to variations in cross sectional area for individual inlets. Variations to large coastal inlet equilibrium models as a result of jetty placement demonstrate that there are factors in addition to hydrologic regime that contribute to the relationship of inlet to tidal prism. The existence or absence of jetty structures along these inlets highlights the variability that littoral drift can have on the P-A relationship. Further evidence of the role of littoral transport is found in the research of Reidel and Gorlay (1980) on protected inlet systems in Australia. As noted in their study, most work done by O'Brien (1969), Escoffier (1940 and 1977), and Jarrett (1976) concentrates on open water inlets. Open water inlets, Reidel and Gorlay argue, are more impacted by wave driven sediment transport than protected inlets. Increased sediment transport along unprotected coastlines requires greater tide range in order to maintain the cross sectional area of the inlet. Protected inlets, on the other hand, do not have the same contribution of sediment as a result of littoral transport, thus cross sectional areas were larger than unprotected inlets given the same tidal prism values (Reidel and Gorlay, 1980). Additionally, Krauss (1998) identified the need for process-based evaluation of tidal inlet equilibrium, noting that protected inlets behave differently than exposed inlets due to lack of sediment transport.

## Variability to Tidal Prism and Inlet Equilibrium

Research on oceanic tidal inlets has shown that accurate description of wave driven littoral transports is critical to the construction of theoretical models that are aligned with empirical data (Escoffier, 1940; O'Brien, 1969; Jarrett, 1976; Van de Kreeke, 1985; Van de Kreeke, 1992;

Krauss, 1998; Van de Kreeke, 2004). Stive et al. (2009) found, with a review of well-known theoretical models for determining cross sectional area of tide inlet entrances to tidal prism relationships, that empirical results do not sufficiently support theoretical results. The Stive et al. (2009) review highlights that in order for inlet cross sectional area to adhere to a given theoretical equilibrium model, the empirical data must come from similar hydrodynamic and morphological conditions. Inlets that share similar tidal prism values may differ in cross sectional area due to these variations that result in small to the value of $k$ in equation (1) and may result in significant variations in the cross sectional area of tidal entrances (Stive et al., 2009). Variability within equilibrium model results demonstrates the fact that controlling factors such as sediment supply, wave climate and tide range determine how equilibrium conditions manifest in the morphology of the inlet.

Inlet equilibrium is achieved when tidal currents have the ability to transport sediment effectively into and out of the inlet, thus the cross sectional area of the inlet remains the same through time as ebb tides remove flood tide deposits of wave driven sediment (Van de Kreeke, 1992; Kraus, 1998; Van de Kreeke, 2004; Stive et al., 2009). Muddy, wave protected tidal creeks do not share these attributes (Reidel and Gorlay, 1980). It is expected that the sites chosen for this research will fall outside the theoretical equilibrium models.

## Contributing Factors to Tidal Prism Increase

Tidal wetlands are complex systems of salt marsh, intertidal flats and tidal creeks that respond to the ever-changing water levels caused by tidal forces (Adam, 1990). Tidal creeks serve this complex system by connecting marsh ecosystems to open water environments thus performing the important task of transporting organisms and nutrients throughout the ecosystem (Zedler and Callaway, 2001). The estuary system of Barataria Bay consists of bays, lakes, ponds

7

and creek systems that ultimately feed into the Gulf of Mexico through myriad inlets. Research has been done documenting the changes to Gulf inlet cross sectional area as a response to increases in tidal prism within the bay (Fitzgerald et al., 2003). This work has shown that inlets connecting the Gulf of Mexico to Barataria Bay have increased in cross sectional area as the tidal prism of the Bay has increased. Large-scale erosion throughout the estuary (Couvillion et al., 2010) has been suggested as the reason for tidal prism increase through time (Fitzgerald et al., 2003).

# Methods

## General Methods

Five separate datasets were developed to evaluate the relationship between tidal creek cross sectional area and tide prism at the Barataria Bay research sites:

1) Historic satellite imagery to quantify erosion rates at each site.

2) Creek mouth cross section area measured with an Acoustic Doppler current profiler (ADCP) along specific transects.

3) Tidal range and current velocity from *YSI* sensors, *RBR* sensors and aquadopp current profilers.

4) Hydroperiod and water level data from Coastwide Reference Monitoring System (CRMS).

5)  Meteorological and tide data from the National Oceanic and Atmospheric Administration (NOAA),

This project focused on 15 geographically and morphologically distinct sites (Figure 1). Each research site was subjected to identical techniques of measurement to determine historical evolution; however, six sites were chosen to collect additional data through instrument deployment and fieldwork. General methodology will cover all of the techniques and strategies used throughout the research sites. Once the general methodology has been described, each site will individually be assessed and described based on strategies used for that site.

## Historical Analysis
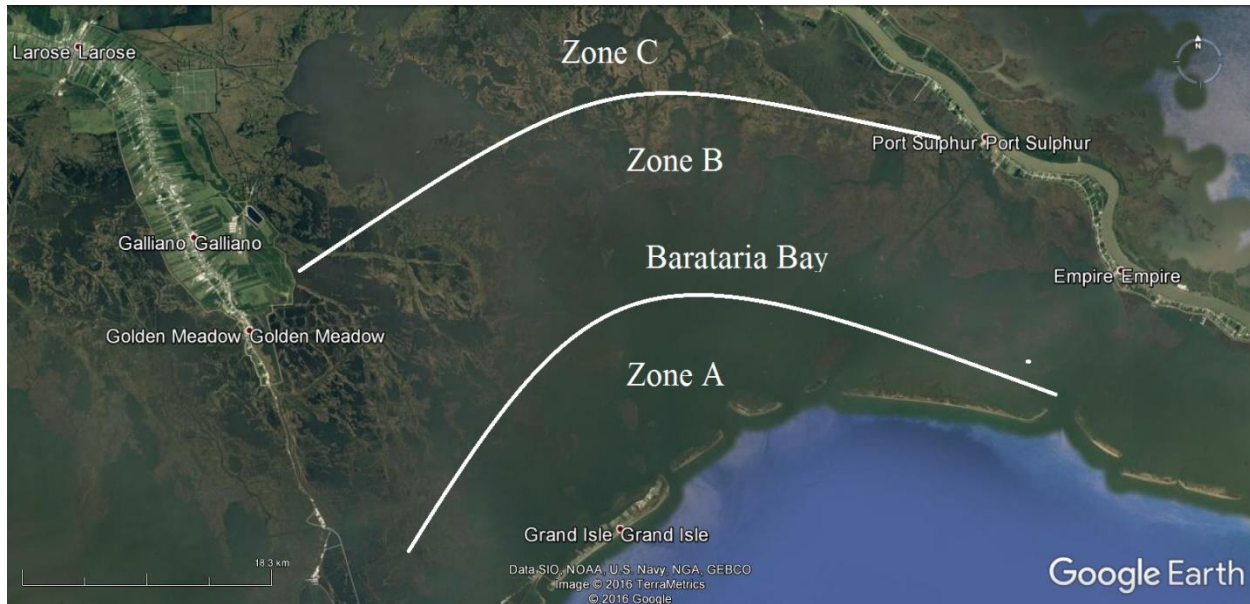


*Figure 1. Site locations broken down into Zones A, B, and C based on proximity to Gulf inlets. Barataria Bay and the surrounding cities are identified for scale and location. Three sites were chosen from Zone A, and six from Zones B and C (2016 image from Google Earth).*

## *Site Selection*

Barataria Bay was chosen as the location for research site based on erosion rates that are among the highest in Louisiana (Couvillion, 2011). Research areas were chosen based on proximity to the Gulf of Mexico and the number of tidal creeks servicing the area. The three areas chosen were 8-3km (A), 20-16km (B) and 38-33km (C) from inlets connecting the Gulf of Mexico to Barataria Bay. Six sites were chosen in Zones B and C and three sites were chosen in Zone A. Efforts were made to select sites within the zones of varying size, yet maintaining a minimal (<2) numbers of inlets.

## Google Earth and Historical Imagery

The research sites were analyzed individually based on historical images obtained through Google Earth imagery. Reviewing satellite images through time reveals that each site has certain dates that are of better quality than others. Image dates were selected on an individual basis to account for quality issues such as image contrast and cloud interference. Image quality did not always allow for identical image dates between all sites. The images of 10/29/2012 and 01/27/2015 were consistently of high quality and all sites used these two image dates. Efforts were made to be as consistent with image selection as possible. Based on comparing images from different dates, it was found that two calendar years between image dates provided enough time for measurable changes to occur.

### *Google Earth Spatial Resolution*

*Google Earth* is the global geographic information platform owned by *Google.* The platform was originally designed by a Central Intelligence Agency (CIA) funded program named Keyhole, Inc. Google purchase the platform in 2004 and *Google Earth* was online that same year. The platform uses a combination of satellite imagery, aerial photography and GIS 3D Globe (Mohamed et al., 2013). The difficulty in utilizing *Google Earth* imagery and obtaining accurate information on the images used is due to the fact that the system is constantly updating and accuracy varies spatially and temporally.

The satellite imagery used to perform the historical analysis for this project is dated from 2005 to 2015. During this timeframe, according to the imagery stamps on the lower portion of the images, *Google Earth* was using images from the *Landsat 7* and *Quickbird* satellite (via *Digital Globe, 2016)* programs. The *Landsat 7* satellite has a spatial resolution of 15 m for

11

panchromatic images (https://landsat.gsfc.nasa.gov/landsat-7, April 20, 2017) while the

*Quickbird* satellite images are 2.4 m resolution

(https://www.digitalglobe.com/resources/satellite-information, 2017, April 20, 2017). To resolve

the differences between the resolution disparity between images from 2005 (15 m resolution) and

the remaining images from 2010- 2015 (2.4 m resolution) ten measurements were taken from the

same research site (1C) from the two resolutions. These measurements were used to calculate a

digitization error value. For sites with 15 m resolution the error is ± .20 m and the error value for

2.4 m resolution is ± .15 m.

## *Measurements Taken and Strategies for Consistency*

Establishing the relationship between open water area and tidal creek inlets required

measuring inlet width at the mouth of the inlet as well as the open water area servicing the inlet.

Changes to the relationship between inlet mouth width and open water areas were measured

through time. These changes were used to calculate erosion rates for both inlet mouth width and

open water areas servicing them. The erosion rates were used to determine if open water rates

coincide with creek inlet mouth width erosion rates. Google Earth Pro imagery and the

measuring tools provided through the software were used to measure 4 images from various

dates for each research sites.  Inlet mouth widths were measured using the following procedures:

1) Starting with the latest image (in every case this was 1/27/2015), the site image was
   zoomed to fill screen.

2) Using the 'add' feature for the selected site folder (within the sidebar), 'path' was
   chosen. The 'add new path' measurement box pops up. For each site the following
   steps were taken within the 'path' pop up:

12

a. Name was designated by date of imagery (e.g. 1/27/2015)

b. Style, color was chosen. Newest images were given a red path followed by green, blue and pink respectfully.

c. Measurement set to meters.

d. Each site is measured across the widest opening of the channel. Once the 'path' is drawn it is saved under the site location (A, B, or C) and the date of image (Figure 2).

e. The satellite image is then changed to the next newest date selected for that site (e.g. 10/29/2012). While leaving the previous measurement in place as a reference point for the next measurement (Figure 3), procedures 'a' through 'd' are repeated (Figure 4).
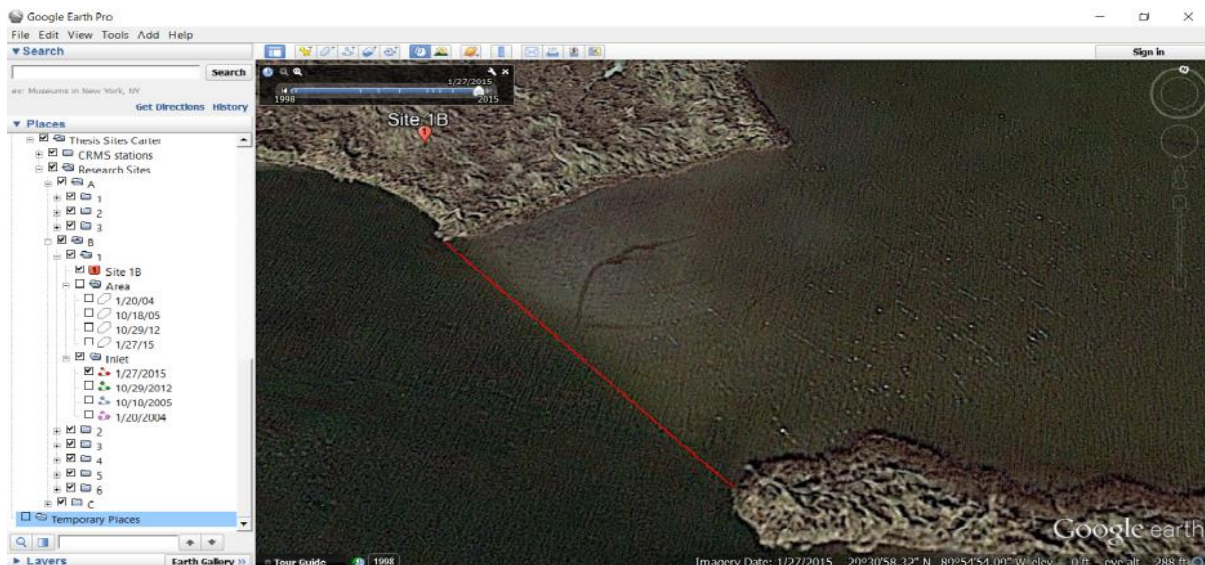


*Figure 2. This image demonstrates method used to measure satellite imagery of channel inlet width. This initial measurement will serve as a reference point for subsequent measurements (2016 image from Google Earth).*
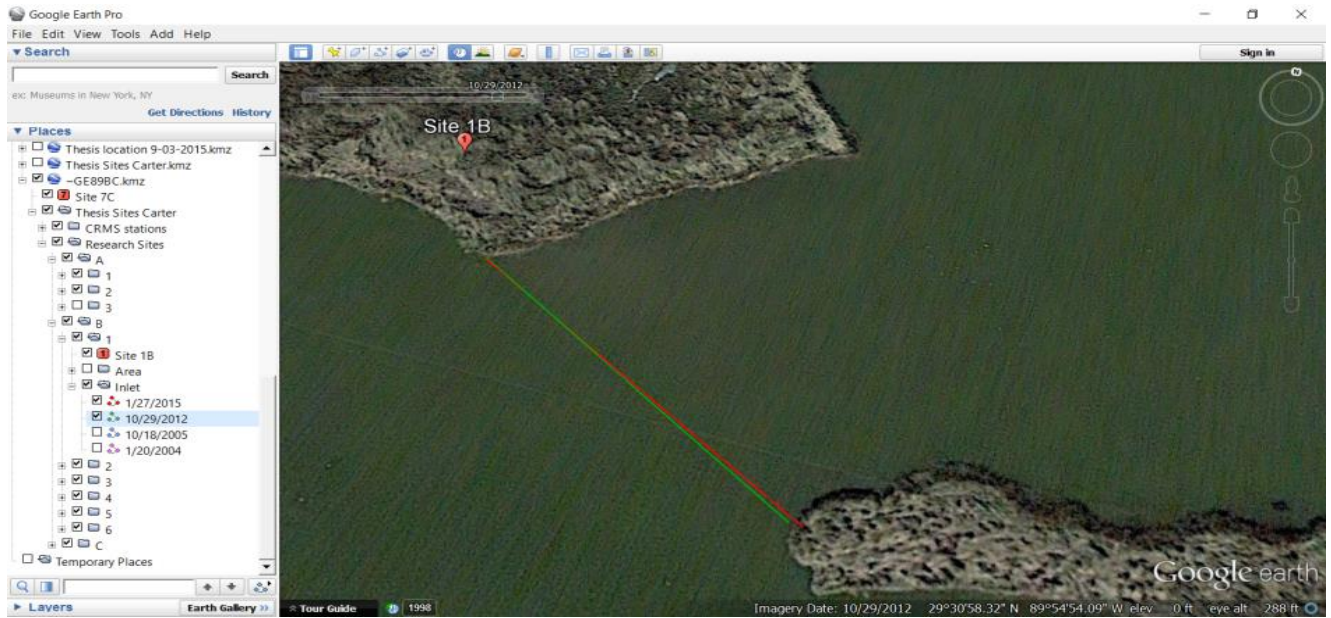
*Figure 3. Comparison of 2 different inlet width measurements. The red line represents 1/27/2015 inlet location and width and the green line is the measurement of the same inlet on 10/29/2012 (2016 image from Google Earth).*



*Figure 4. This image shows all four inlet width measurements on the newest satellite image.*

*To measure open water area behind the inlet the following procedures were used (2016 image from Google Earth).*

Open water area was measured using the following procedure:

1) Starting with the latest image (1/27/2015), image was zoomed to between 450 and 550 feet. Throughout the measurement process the goal is to keep the zoom consistent between the different image dates.

2) Using the 'add' feature for the selected site folder (within the sidebar), 'polygon' was chosen. The 'add new polygon' measurement box pops up. For each site the following steps were taken.

   a. Name designated by date of imagery (e.g. 1/27/2015)

   b. Style, color was chosen. Newest images were given a red path followed by green, blue and pink respectfully

   c. Measurement set to meters.

   d. Beginning from the inlet measurement path for the chosen image date, the polygon measurement is started.

   e. The area is figured by outlining the shoreline as closely as possible (Figure 5). Once the entire open water area is outlined the measurement is save under the site location and the date of the image (Figure 6 and Figure 7).

   f. Steps 'a' through 'e' are repeated for each image date



*Figure 5. This image shows the outlining of open water area for Site 1B (2016 image from Google Earth).*
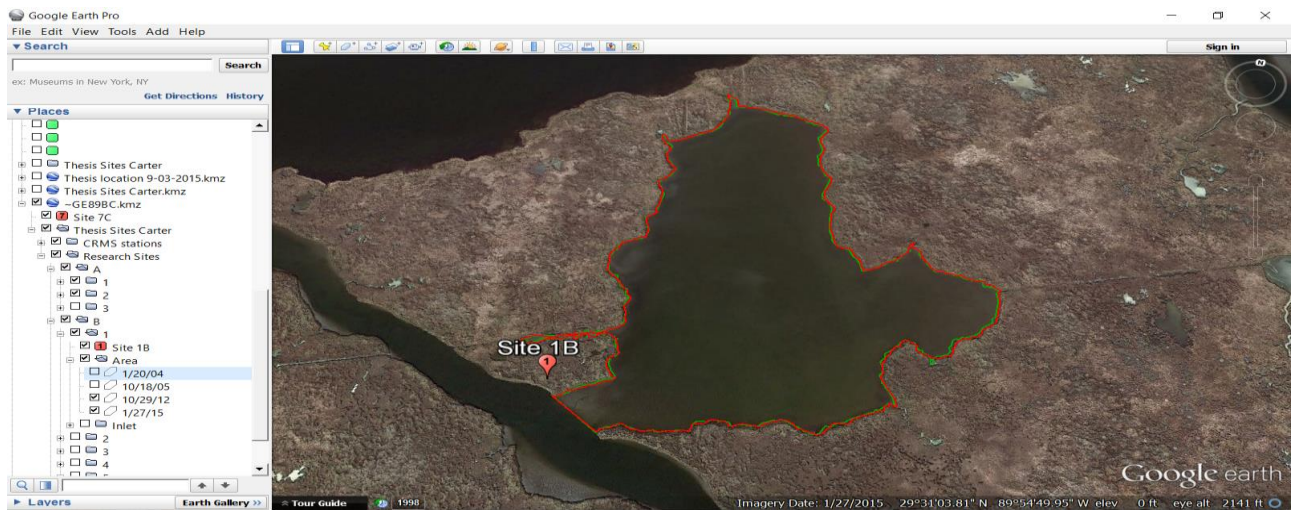
*Figure 6. this image shows the area measurement of two different time images. 10/29/2012 is in green and 1/27/2015 is in red. The sidebar menu in this image shows organization of different sites and image dates (2016 image from Google Earth).*



*Figure 7. this image shows area measurements from the different image dates. Viewing measurements together demonstrates erosion of shorelines and channel inlet changes through time (2016 image from Google Earth).*

## Fetch

In order to account for wave erosion for each of the research locations measurements were taken to document the open water fetch distances. Each site was evaluated based on the latest available imagery. Sixteen measurements were taken from the approximate center of the inlet mouth and followed compass directions in 360 degrees (Figure 8). The open water fetch distances were then used to create a graphical representation of each site (Figure 8). Historical wind data were acquired from the National Oceanic and Atmospheric Administration (NOAA) wind and tide gauges at Grand Isle, Louisiana (Station ID: 8761724 GISL1). Wind data from the last 10 years was compiled and used to establish prevailing wind direction and speed.
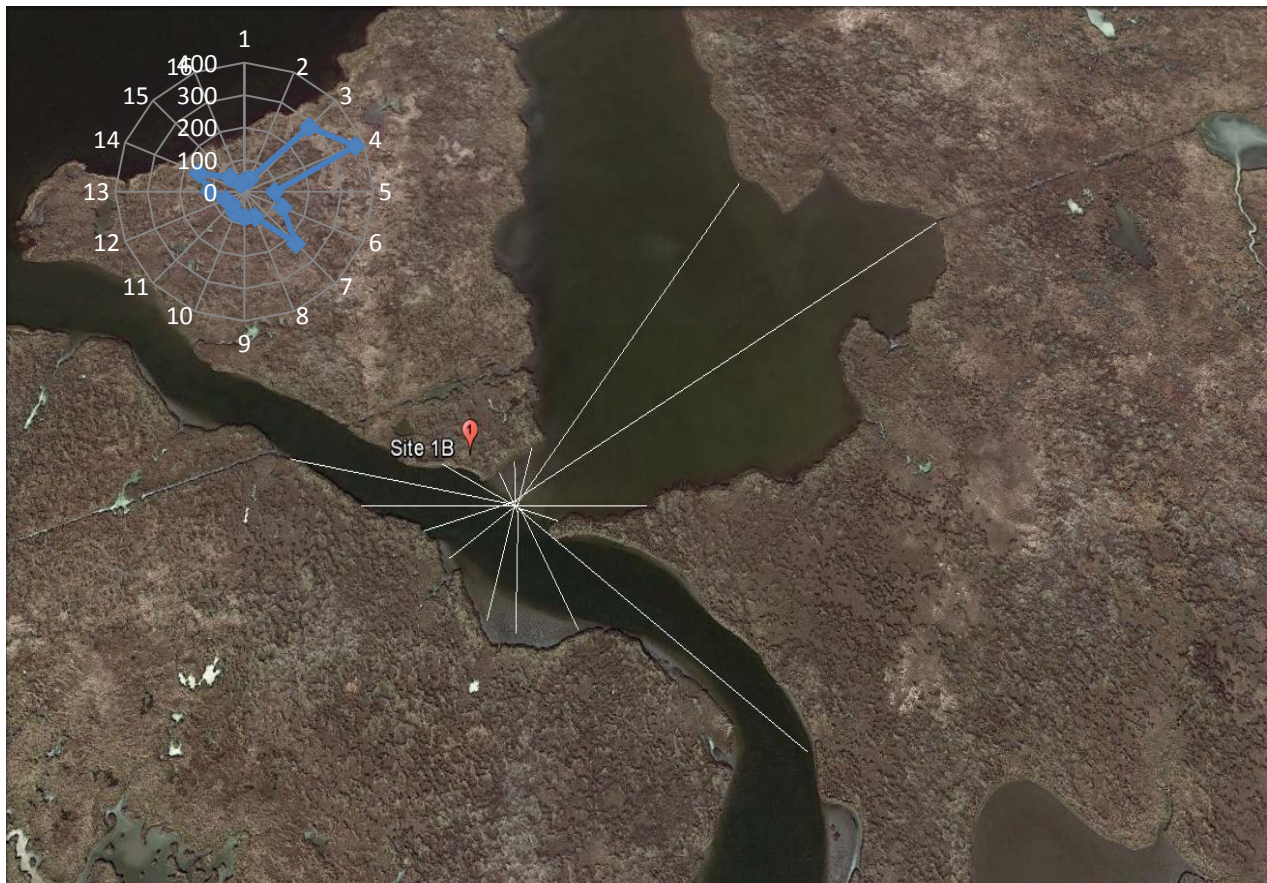


*Figure 8. Image of fetch measurements with the graphic representation of the measured distances imbedded. Measurements are in meters (2016 image from Google Earth).*

17

**Field Work**

*ADCP Transects*

All ADCP transects were taken on July 21$^{st}$, 2016 from the RV Mudlump. Six sites were selected based on location and size (Figure 9). The two most inland zones (C and B) were chosen to conduct the fieldwork. Within these zones, inlet sites were chosen based on relative size within the respective zone. Zone 'C' had a small (5C), medium (1C) and large (6C) inlet width chosen. Zone 'B' had similar selections small (3B), medium (2B) and large (1B) sites selected for ADCP transects. Transect length and location was based on historical analysis measurements derived from satellite imagery. Care was taken to reproduce the same measurements acquired from imagery measurements; however, sites 2B and 5C required measurements different from satellite imagery due to shallow depth and erosion since the imagery date. Updates to inlet width measurements were made after fieldwork. The ADCP was set in a down looking position and held in place off the side of the RV Mudlump with a custom adjustable arm. ADCP transects were taken across the selected inlets at as slow a speed as possible and still maintain proper heading. Low current speed and light winds during fieldwork made this possible (Figure 10).

*Figure 9. Sites chosen for ADCP transect and boat path taken to each site (2016 image from Google Earth).*
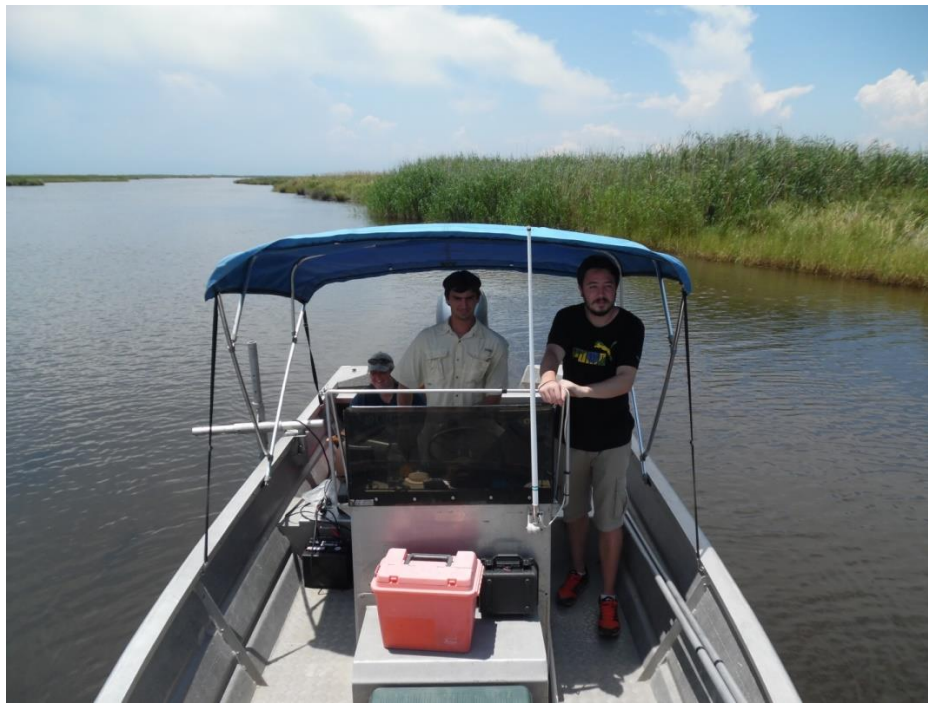


*Figure 10. Transect being measured at slow speed and all researchers in transect measuring position.*

### *Tide Data and Current Velocity*

Fieldwork to acquire tide data was performed on August 23, 2016. Instrumentation

deployed consisted of three *YSI* sensors, one *RBR* (TWR-2050) and one *Aquadopp* current

profiler (*Nortec* AS, serial # AQD1749). One site (site 1C), was instrumented with the *RBR* and

*Aquadopp* current profiler on a single deployment platform. This instrument cluster was

positioned at the mouth of the tidal creek in 1.5 m of water (Figure 11). The *Aquadopp*

equipment was position sensitive and required the 'Z' axis of the sensor be facing towards the

surface and perpendicular to the current. This meant that the deployment sled was orientated

with sensors facing west in the thalweg of the creek at site 1C.

YSI deployment was done at site 4C, 1B and 2B. 4C was instrumented with *YSI* meter

"Starsky", while sensors "039" and "Hutch" were deployed at sites 1B and 2B respectfully.

"Starsky" was placed at the back of the open water area servicing 4C's inlet, in 2 m of water

(Figure 11). Sites 1B and 2B deployment occurred (Figure 12). Three of these locations (1B, 2B

and 4C) had *YSI* pressure sensors placed at the mouth of the tide channels. The deployment

process began on August 22nd when instrumentation was setup to begin recording pressure

changes. The *YSI* instrumentation was secured to instrument sleds and deployed the following

day. Researchers placed instrumentation platforms within 20 m of the shoreline in the deepest

(using onboard transducers) section of tidal creeks. The instrumentation was left in the field until

September 12th, 2016.
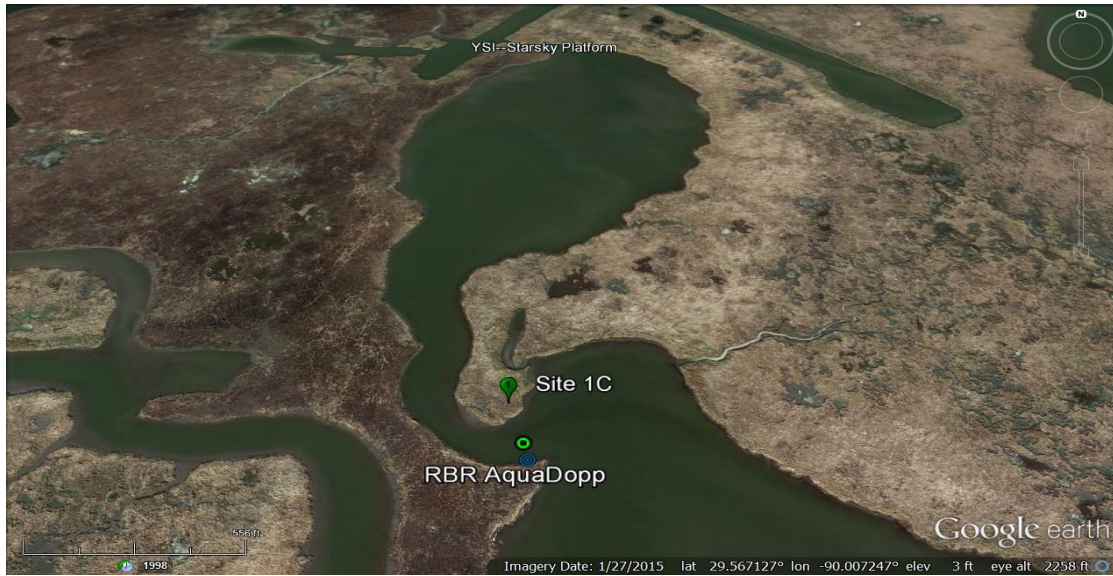
*Figure 11. Location of instrumentation that documented tidal current and range at site 1C (2016 image from Google Earth).*
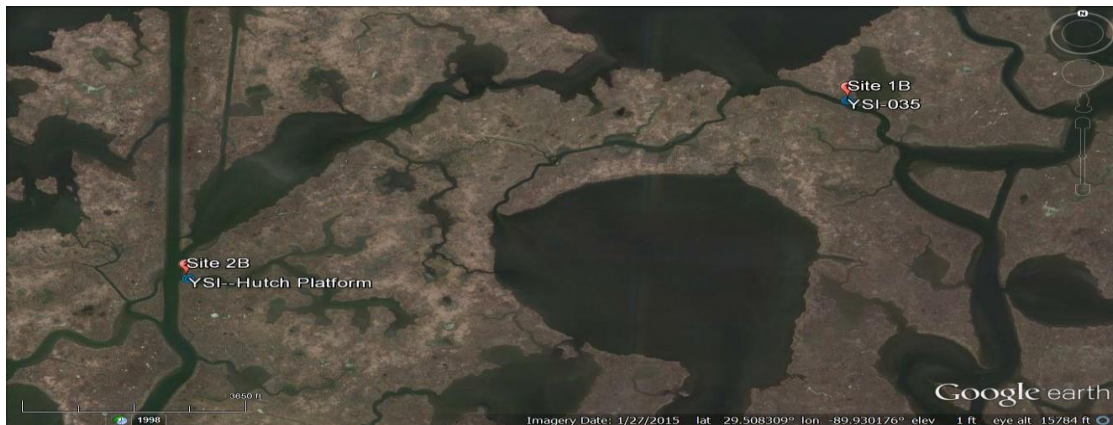


*Figure 12. Location of YSI at sites 1B and 2B. Sensors were deployed in the thalweg of the tidal creek being researched (2016 image from Google Earth).*

## Data Processing

All measurements taken through historical imagery analysis were processed to calculated erosion rates for inlet width, erosion rates for open water area and theoretical tidal prism for each

image time. Microsoft *Excel* was used to organize and process the various calculations needed to accomplish the data processing. To begin processing, a blank worksheet (Figure 13) was created that allowed for simple input of data and creation of all needed computations. The data used were divided into the four different time categories for images. Time 1, 2, 3 and 4 were used to designate the different images. *Excel* software calculated days between site images, this was used to calculate erosion rates per day.
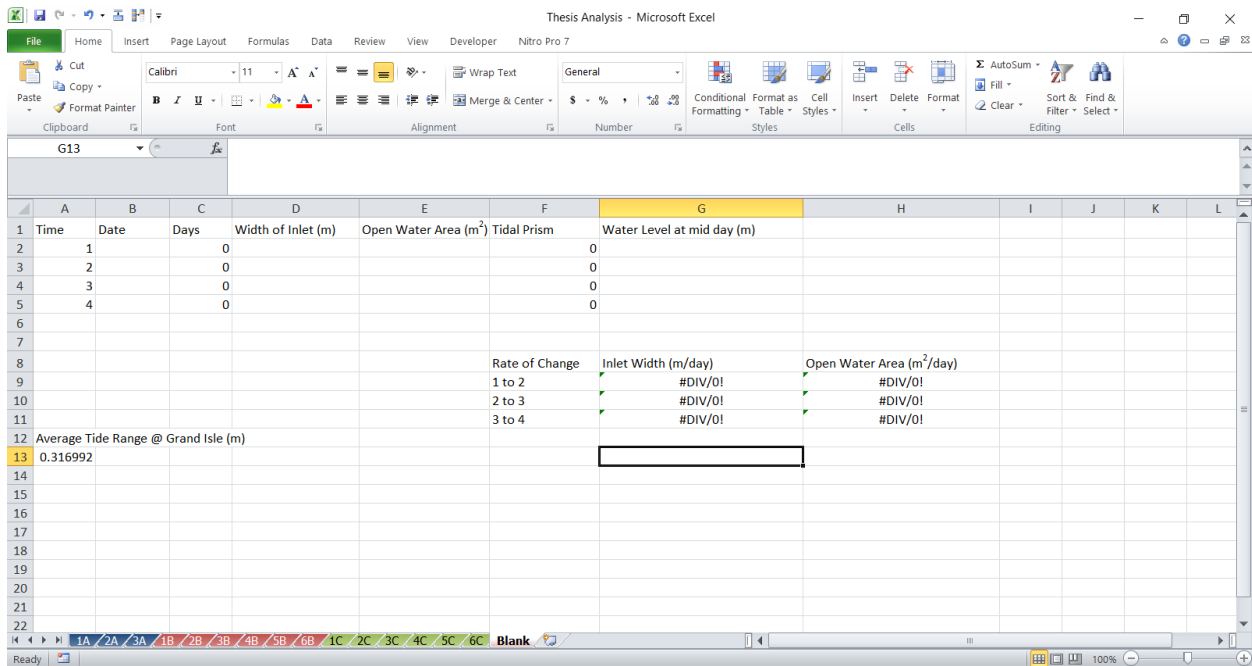


*Figure 13. Excel worksheet used to calculate tidal prism, days between images and rates of change for both inlet width and open water area.*

The formulas used in this worksheet are as follows:

Tidal Prism:

$$P = A \ (T)$$

Where *P* is tidal prism and *A* is open water area behind the channel and *T* is the mean tide range for either a flood or ebb tide.

Rate of Change (Inlet width and open water area):

$$(W1-W2)/D$$

Where *W1* is inlet width at time 1 and *W2* is inlet width at time 2 and *D* is the number of days between *W1* and *W2*.

$$(A1-A2)/D$$

Where *A1* is open water area at time 1 and *A2* is open water area at time 2 and *D* is the number of days between time 1 and time 2.

## *Tide Range and Current Profile*

The data collected by field instruments was downloaded and processed through *Excel* spreadsheets. The *YSI* and *RBR* data was adjusted to a baseline of '0' by subtracting the water depth at the time of deployment from all measurements. This step ensured that sensor data was tracking water-level variations during the deployment periods and, therefore, could be temporally compared to sensor data between various sites. To establish the height of the marsh platform, observations at the time of deployment estimated the water level 2 cm below the marsh platform for all sites.

The water level data were plotted according to time. All measurements prior to 14:00.00 hours on August 23, 2016 were removed from the data and that time became the starting point of the deployment period since all sensors were in place and recording data at that time. The *YSI* sensor, by default, recorded data every 5 minutes, whereas the *RBR* recorded data every 10 minutes. To compare the two datasets every other reading from the YSI data was removed. Measurements were continually taken until 14:00:00 hours September 12, 2016, which became the cut off time for all data acquisition.

## *Aquadopp Data Analysis*

Data acquired during the *Aquadopp* deployment (August 23, 2016 -September 12, 2016) was processed through MATLAB and Microsoft *Excel* software. The *Aquadopp* sensor is capable of recording current velocity along three different axes. The current entering and leaving the tidal creek is the only data of interest to this study and is represented by 'Z' axis data. The data was collected such that ebb tide velocities were positive and flood tide velocities were negative. At the time of deployment surface current velocity at site 1C was visually assessed to be approximately 0.2 m/s and falling.

## **CRMS and NOAA Data**

The Coastwide Reference Monitoring System (CRMS) provided water levels for areas surrounding the research sites. CRMS sites 3601, 3617, 0237, 0171, and 0178 (Figure 14) provided annual hydroperiod percentages and historic water level ranges. Cross-referencing CRMS water level data with wind data from the National Oceanic and Atmospheric Administration (NOAA) wind and tide station at Grand Isle, allowed for an evaluation of meteorological forcing on water levels and tide range. Cross-referencing meteorological events with water levels provided an opportunity to assess annual erosion rates in relationship to subtidal forces.

*Figure 14. CRMS sites in relationship to the location of research zones A, B and C. CRMS data allowed for historical analysis of tide range through the estuary as well as corroboration of data acquired during sensor deployment (2016 image from Google Earth).*

## Tidal Prism Calculations

The *YSI* and *RBR* data provided the opportunity to determine actual tide range for zones B and C. Further, the use of CRMS and NOAA data provided tide range data for zone 'A' tidal prism calculations, as well as corroborate *YSI* and *RBR* data. The average spring tide range was calculated from the four largest tide cycles during the deployment.

## Statistical Analysis

Statistical analysis was employed to determine if measurements taken across the three zones were statistically significant to one another. The null hypothesis being tested is that Zone A, Zone B and Zone C share similar tidal creek cross sectional area to tidal prism relationships.

25

$$H_o = TC/TP_A = TC/TP_B = TC/TP_C$$

Where $H_o$ is the null hypothesis and TC/TP is the tidal creek cross sectional area to tidal prism ration. The tidal creek cross sectional area for sites where ADCP transects were not taken is calculated from the average water depth across the sites that were surveyed. Additional statistics were also performed comparing measured tidal creek cross sectional area and tidal prism relationships.

# RESULTS

Research sites are represented by 'Zones' (Figure 15) that denote the geographic location of the site. Results for individual sites are presented with respect to these 'Zones' and are individually described in terms of historical analysis, water level, current and ADCP measurements and fetch distances. The individual site results for this study are divided into five categories:

1) Historical analysis and rate of change

2) Water level and tide gauge data

3) Current profile and ADCP transects

4) Meteorological conditions during study period

5) Fetch distances
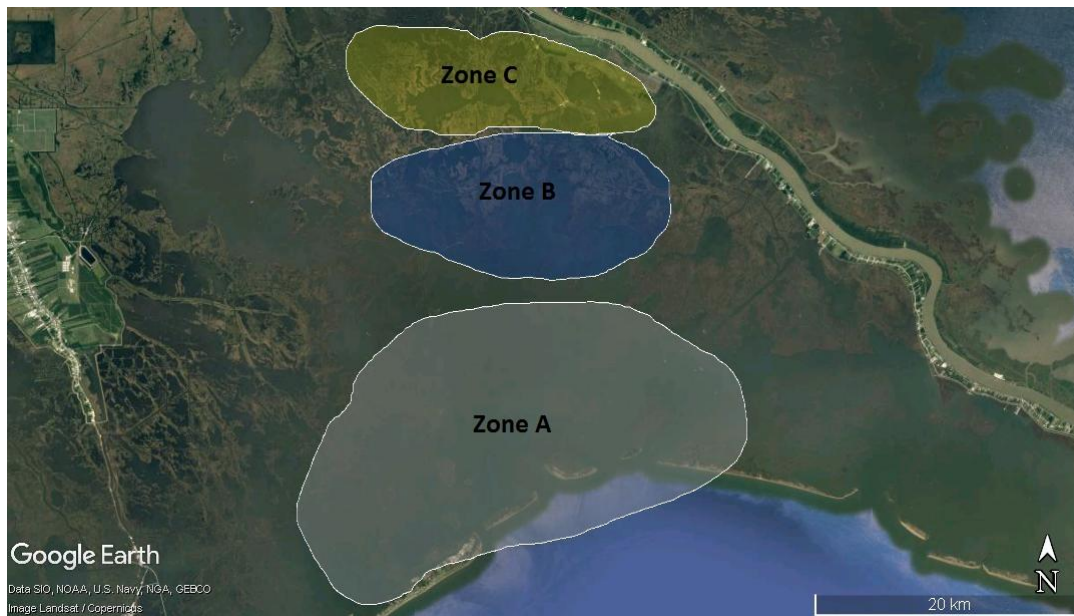


*Figure 15. For this study, research sites are differentiated by their location. The location of each site can be found in one of the three zones depicted in this image (2016 image from Google Earth).*

## Zone A

### *Overview*

Geographically, zone A represents sites closest to the Gulf of Mexico (Figure 15). Three sites were chosen ranging from 3-8 km from inlets that connect Barataria Bay to the Gulf of Mexico (Figure 16). Within this range site selection was based on the number of tidal creeks and the size of the open water area behind those creeks. Sites with fewer than two tidal creeks and open water pond areas ranged in size from 1,500 $m^2$ to 22,000 $m^2$ were chosen.

The research sites located in zone 'A' were measured and these measurements through time were used to calculate erosion rates. Zone 'A' sites had the lowest rates of erosion in this study (Table 1). An examination of the temporal variability of erosion rates reveals that inlet widths have widened at all sites in this zone. Additionally, measurements of satellite imagery reveals that, with the exception of site 2A, open water area has also increased at these sites. Detailed site results are presented for site 1A and similar techniques were used for all sites. Results for the remaining sites in zone A can be found in Appendix A.

*Figure 16. Overview of Zone A reasearch sites. The location of these sites was determined by their distance from Gulf inlets as well as the number of tidal creeks servicing the pond area at the site (2016 image from Google Earth).*

| Site | Inlet Width Rate of Change (m/yr) | Open Water Conversion Rate (m$^2$/yr) |
|---|---|---|
| 1A | -0.23 ($\pm$ 0.48 m) | -16.59 ($\pm$ 40.44 m$^2$) |
| 2A | -0.45 ($\pm$ 0.24 m) | 123.84 ($\pm$ 322.22 m$^2$) |
| 3A | -0.22 ($\pm$ 0.10 m) | -26.99 ($\pm$ 14.86 m$^2$) |

*Table 1. Average erosion rates for both open water and inlet width for zone 'A' sites. Historical analysis of satellite imagery revealed that inlet width increased for all sites and open water area increased for sites 1A and 3A but decreased for site 2A. Standard deviation is given for the average erosion rates for each site.*

## Detailed Site Results

### Site 1A

Site 1 is located in the interior of an island due north of Grand Isle, Louisiana, at N 29.2414˚W 90.0111˚(Figure 17). The site represents the smallest geographic area in Zone 'A'. The open-water area behind the single tidal creek currently (1/27/2015) measures 547 $m^2$ according to measurements taken from satellite imagery and the tidal creek mouth measured 9.4 m. The largest fetch distance from the center of the creek mouth is to the SSW and measures 19.1 m. The creek mouth is protected to the south by a section of marsh that is less than 10-m wide and the creek connect the pond to the north and a natural bayou to the south. The site is flanked to the west and east by Caminada Pass (5.6 km from creek) and Barataria Pass (6.8 km from creek) respectfully.



*Figure 17. Location and latest image available for site 1A. Image shows open water area and tidal creek (2016 image from Google Earth).*

*Historical Analysis*

The earliest satellite image reviewed for site 1A was 10/18/2005. At this time, the creek mouth measured 9.3 m wide. Additional measurements were taken from images on 3/02/2010, 10/29/2012 and 1/27/2015 (Table 2).

*Inlet Widths*

During the historical analysis period, (2005-2015) the inlet mouth width at site 1A increased between 2005 and 2012, but decreased in size between 2012 and 2015. Erosion of the shoreline on either side of the creek mouth is responsible for the decrease in inlet width from 2012 to 2015 (Figure 18). Investigating the imagery reveals that the mouth of the inlet retreated and thus exposed a narrower section of creek as the creek mouth.

| Date | Width of Inlet (m) | Erosion Rate Inlet (m/yr) | Open Water Area (m$^2$) | Erosion Rate Open Water Area (m$^2$/yr) |
|---|---|---|---|---|
| 10/18/2005 | 9.30 (± 0.20m) | --- | 1539.00 (±0.20m) | --- |
| 3/2/2010 | 10.30 (± 0.15 m) | -0.23 | 1717.00 (±0.15 m) | -40.71 |
| 10/29/2012 | 11.20 (± 0.15 m) | -0.34 | 1611.00 (±0.15 m) | 39.80 |
| 1/27/2015 | 10.50 (± 0.15 m) | 0.31 | 1597.00 (±0.15 m) | 6.23 |

*Table 2. Historical measurements and erosion rates derived from measurements of the inlet width and interior pond open water area from satellite imagery of site 1A.Dashed lines indicate no erosion rate data available for the earliest imagery dates. Digitization error is included in parentheses.*

*Figure 18. Image shows the narrowing of inlet due to shoreline retreat. As the shoreline adjacent to the mouth of the inlet eroded, narrower sections of inlet were exposed resulting in decreasing erosion measurements (2016 image from Google Earth).*

### *Interior Pond Area*

Open-water erosion measurements were taken from the exact same satellite imagery as the creek-mouth erosion measurements (Table 2). Interestingly, the open-water area during the period of analysis fluctuated in a fashion somewhat similar to inlet widths. Open water area increased from 2005 to 2010 and then decreased from 2010 to 2015.

### *Tidal Prism*

The average tide range, 2010 to 2015at the closest CRMS station (CRMS 0178) is 0.36 m. Multiplication of open water area by the average tide range indicates tidal prism values ranging from 569.60 m$^3$ (2005) to 728.40 (2010) (Table 3). The fluctuation of tidal prism values follows a similar pattern as the creek mouth width. Tidal prism increases from 2005 to 2010 then decreases from 2012 to 2015.

| Date | Tidal Prism (m³) |
|---|---|
| 10/18/2005 | 554.04 |
| 3/2/2010 | 618.12 |
| 10/29/2012 | 579.96 |
| 1/27/2015 | 574.92 |

*Table 3. Tidal prism calculation for site 1A. Calculations were based on tide range data from CRMS station 0178.*

### *Fetch Measurements*

From the center of the creek mouth fetch measurements were taken to the closest land mass that would disrupt wave action (Figure 19). This site has an average fetch distance of 25.90 m (± 23.64 m) and has the longest stretch of open water is 67.80 m toward the WSW.
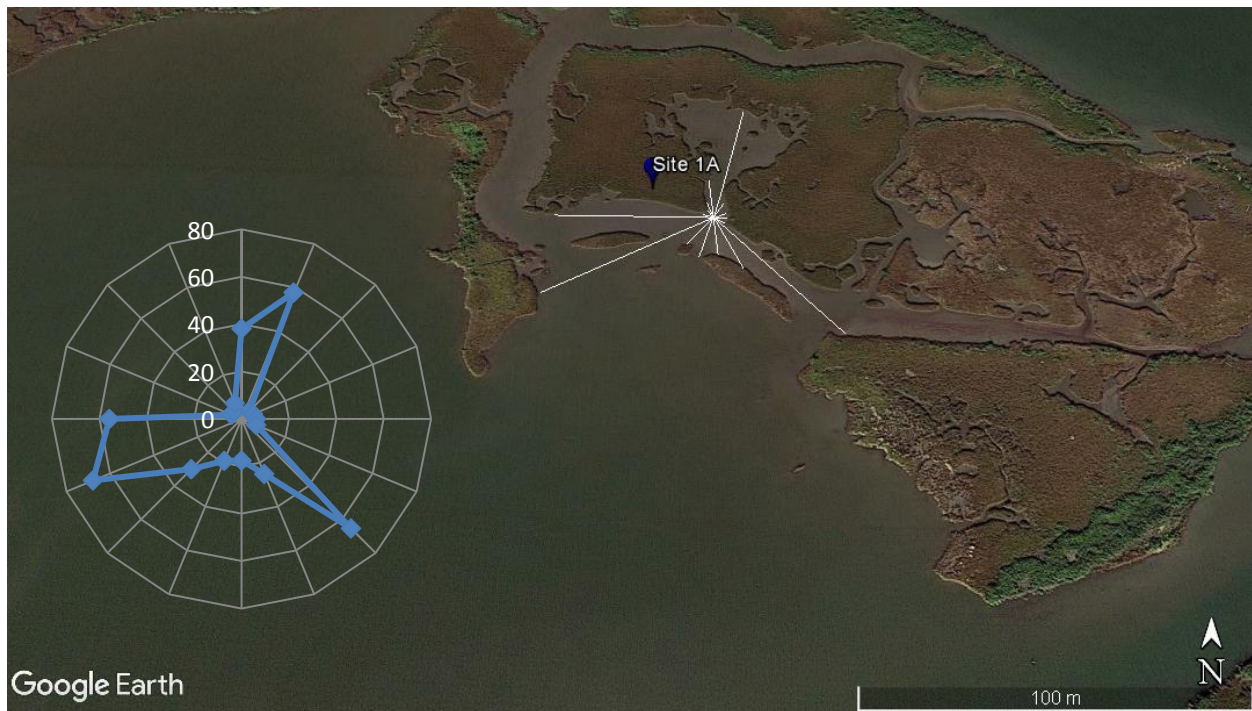


*Figure 19. This image depicts fetch distances and directions as they relate to the mouth of the inlet located at site 1A Distance (in meters) from the center of the inlet mouth to the nearest shoreline is depicted as the blue line in the inset graph (2016 image from Google Earth).*

## Zone B

### Overview

Zone B research sites are located further inland than zone A. The sites range from 15 - 25 km landward of inlets connecting Barataria Bay and the Gulf of Mexico (Figure 20). Selection of sites was done through satellite image analysis of the location with emphasis placed on the number of tidal creeks servicing an open water pond area. Bias was placed on locations with two or less tidal creeks. Between the six chosen locations the size of open water areas varies from 12,596 $m^2$ to 678,095 $m^2$. Efforts were made in the selection process to choose locations with various sized open water areas. Historical satellite imagery analysis was done on the six research sites located in zone 'B'. In addition to the historical analysis, three sites were selected to deploy instrumentation in order to measure tide range and bathymetry.

Historical evaluation revealed that, as a whole, zone 'B' (Table 4) experienced greater erosion rates than zone 'A'. The highest rates of inlet width change occur at sites 1B and 4B. The location of 4B makes it clear that the unprotected nature of the shoreline plays a role in the advanced erosion rates for the inlet. 1B, on the other hand, experiences high inlet erosion rates while being protected. Erosion rates at 1B and 2B are very similar and both of these sites are adjacent to deep-water channels. Detailed site results are presented for site 1B and similar techniques were used for all sites. Results for the remaining sites in zone B can be found in Appendix A.

*Figure 20. Overview of location of Zone B research sites (2016 image from Google Earth).*

| Site | Inlet Width Change (m/year) | Open Water Change (m2/year) |
|------|------------------------------|------------------------------|
| 1B | -1.08 (± 1.02 m) | -347.90 (± 85.05 m$^2$) |
| 2B | -0.88 (± 0.85 m) | -893.56 (± 464.14 m$^2$) |
| 3B | -0.25 (± 0.13 m) | -66.79 (± 29.54 m$^2$) |
| 4B | -3.03 (± 2.23 m) | -1653.32 (± 1003.36 m$^2$) |
| 5B | -0.23 (± 0.15 m) | -228.07 (± 86.83 m$^2$) |
| 6B | -0.75 (± 0.48 m) | -1175.49 (± 800.50 m$^2$) |

*Table 4. Inlet Width and open water change for all sites located in Zone 'B'. Sites 1B and 4B had the largest inlet erosion rates and sites 2B and 4 B had the largest change in open water area. Standard deviation is given in for each average is given.*

## Detailed Site Results

### Site 1B

Located approximately 23 km north of Grand Terre Islands and Quatre Bayou Pass at N 29.5164˚W 89.9155˚, site 1B is the furthest from Gulf of Mexico inlets as any site in Zone B. The open water area that is serviced by the tidal channel is 86837 $m^2$ (Figure 21). The tidal channel is 50 m long and serves as a connection between a uniform pond/open water area and a natural bayou with 10 m of depth. 1B is one of three research sites in Zone B chosen to deploy additional instrumentation to acquire tide range data. An YSI pressure sensor was deployed 10 m west of the channel mouth in approximately 3 m of water. This site was also chosen to run ADCP transects to calculate cross sectional area of the mouth of the channel. The channel mouth is protected from wave action with the greatest fetch distances being to the north at 221 m. The open water area being serviced by the channel is 86,837 $m^2$.
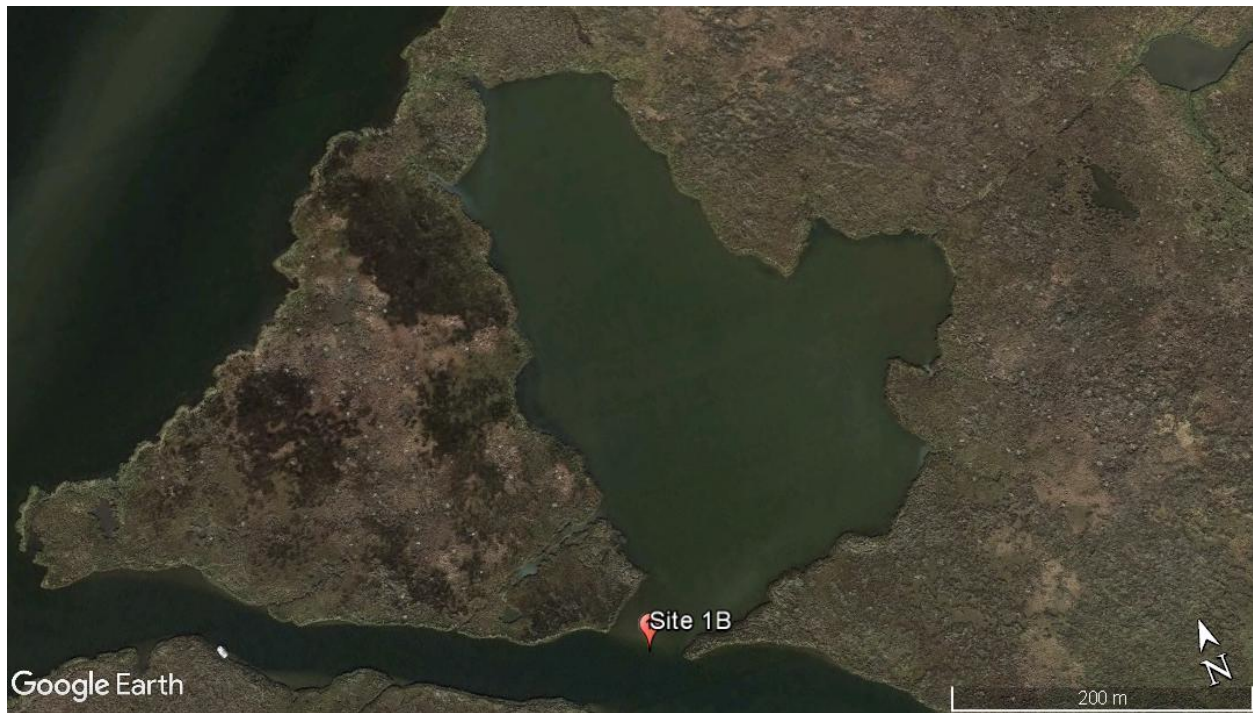
*Figure 21. Site 1B and location of YSI deployment location. TheYSI pressure gauge was deployed at the western edge of the inlet at site 1B in approximately 2.5 m of water (2016 image from Google Earth).*

### *Historical Analysis*

#### *Inlet Width*

The inlet mouth located at site 1B eroded between each of the satellite imagery dates.

Quality of available imagery dictated that 1/20/2004, 10/18/2005, 10/29/2012 and 1/27/2015

would be used to take historical measurements. The earliest satellite imagery reviewed for site

1B was 1/20/2004 during this time measurement of the inlet revealed the width of the creek

mouth was 46.6 m. Further measurements were taken on 10/18/2005, 10/29/2012 and 1/27/2015.

The latest measurement indicates the inlet mouth had widened to 53.9 m. The inlet at site 1B

experienced its greatest erosion from time 2004 to 2005 where it eroded at the rate of 2.46 m/yr.

### *Interior Pond Area*

Open water erosion measurements were taken during from the exact same satellite

imagery as the creek mouth erosion measurements. Similar to inlet measurements, there is

fluctuation in the open water area. Measurement shows an increase in open water area from 2005

to 2010, yet a decrease in 2010 to 2012 followed by another decrease from 2012 to 2015 (Table

5).

| Date | Width of Inlet (m) | Erosion Rates Inlet (m/yr) | Open Water Area (m²) | Erosion Rates Open Water Area (m2/yr) |
|---|---|---|---|---|
| 1/20/2004 | 46.60 (± 0.20 m) | --- | 82895.00 (± 0.20 m) | --- |
| 10/18/2005 | 50.90 (± 0.15 m) | -2.46 | 83344.00 (± 0.15 m) | -257.27 |
| 10/29/2012 | 52.70 (± 0.15 m) | -0.26 | 85880.00 (± 0.15 m) | -360.45 |
| 1/27/2015 | 53.90 (± 0.15 m) | -0.53 | 86837.00 (± 0.15 m) | -425.98 |

*Table 5. Inlet and open water area sizes and erosion rates for site 1B. Digitization error is presented in parentheses.*

### *Tidal Prism*

The tidal prism is calculated using the actual tide range average from the deployment of

YSI sensors at site 1B. The spring tide range at this site during the deployment period was .29 m.

Tidal prism values for site 1B range from 19065.85 $m^3$ to 19972.51 $m^3$ (Table 6).

| Date | Tidal Prism (m³) |
|---|---|
| 1/20/2004 | 19065.85 |
| 10/18/2005 | 19169.12 |
| 10/29/2012 | 19752.4 |
| 1/27/2015 | 19972.51 |

*Table 6. Tidal prism calculation for site 1B. Calculations were based on tide range data from YSI sensor '039'.*

### Fetch Measurements

Site 1B is most protected to the South. Evaluating fetch distances reveals the longest open water stretches are to the NE and extend to 372 m. The average fetch distance for this site is 117.6 m (± 97.24 m) (Figure 22).
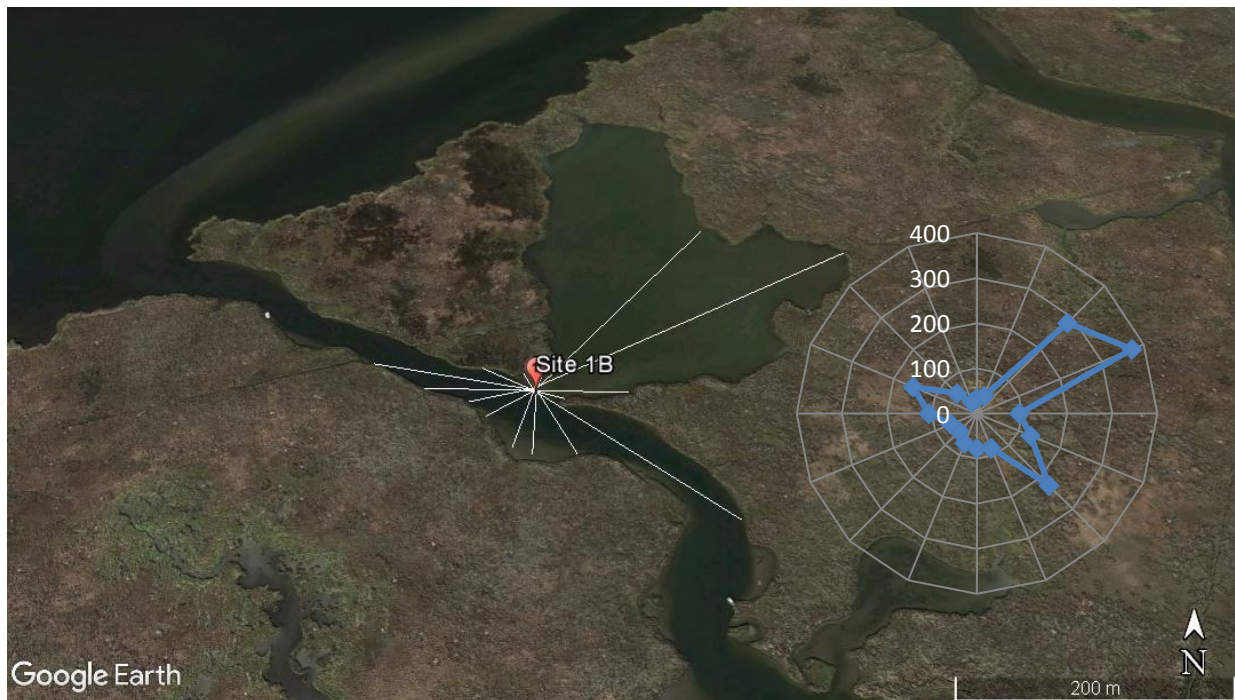


*Figure 22. This image depicts Fetch distances and directions as they relate to the mouth of the inlet located at site 1B. Distance (in meters) from the center of the inlet mouth to the nearest shoreline is depicted as the blue line in the inset graph (2016 image from Google Earth).*

### ADCP

There were four ADCP transects taken at site 1B but only three produced valid data. Between the three transects there was an average distance of 42.47 m (± 3.81 m) and an average depth of 1.15 m (± .28 m) (Table 7). The transect lengths vary slightly from the historical analysis measured width due to limited depth near the marsh edge that prevented equipment from being used across the entire inlet mouth.

| Transect # | 005 | 006 | 007 |
|---|---|---|---|
| | | | |
| Average Depth (m) | 1.01 | 1.20 | 1.20 |
| Transect Length (m) | 43.74 | 42.33 | 41.34 |
| Cross Sectional Area (m²) | 44.29 | 52.36 | 50.50 |
| Avg. Cross Sectional Area (m²) | 49.05 (± 13.73m²) | | |

*Table 7. Data from ADCP transects run at site 1B. Cross sectional area and averages were also calculated. Standard deviation is given for the average cross sectional area of the creek.*

### YSI and RBR

YSI deployment from August 23, 2016 until September 12, 2016 provided necessary data to calculate an average tide range for this site. The average water level was .24 m above the deployment depth and the averages of the spring tide cycles during the deployment time was .24 m (Figure 23).
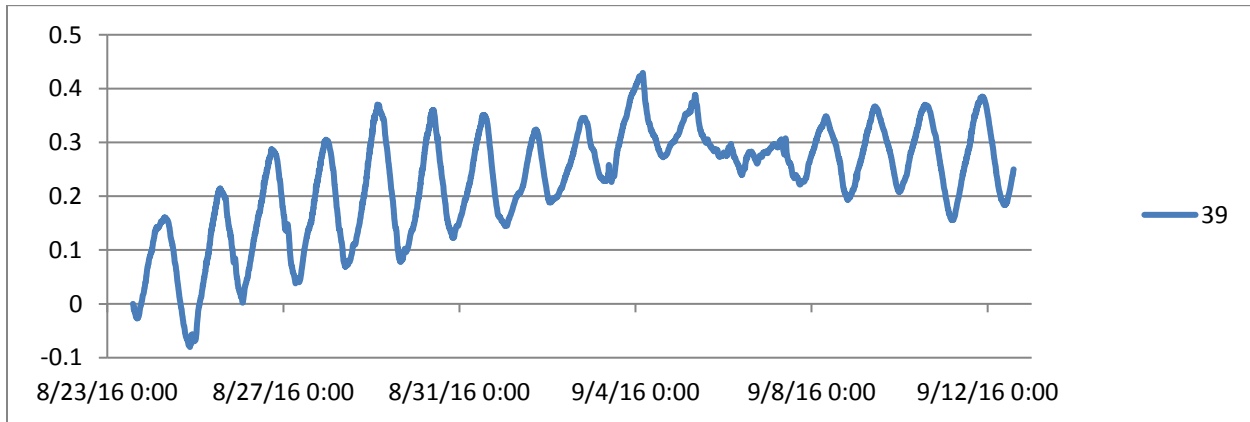
*Figure 23. Represents data acquired during YSI deployment from August 23, 2016 until September 12, 2016. Y-axis is tide range (m) and x-axis is date and time.*

## Zone C

### *Overview*

Ranging from 35-40 km from coastal inlets, sites within zone C are the furthest inland (Figure 24). Similar to 'A' and 'B' research sites, selection was done through historical analysis of satellite imagery with emphasis placed on the number of tidal creeks servicing an open water pond area. Bias was placed on location with two or less tidal creeks. Between the six chosen locations the size of open water areas varies from 2,674 m$^2$ to 167,763 m$^2$. Efforts were made in the selection process to choose locations with varied sized open water areas. Aside from historical evolution data, ADCP transects were taken from three sites and YSI, RBR and Aquadopp instrumentation were each deployed in one site within zone 'C'. Measurements through sites within zone 'C' show that the erosion rates for inlet width within this zone are the highest of any examples from this study (*Table 8*).

| Zone | Inlet (m/yr) | Open Water (m$^2$/yr) |
|:---:|:---:|:---:|
| C | -4.04 ($\pm$ 8.63 m) | -543.87 ($\pm$ 521.75 m$^2$) |
| B | -1.03 ($\pm$ 1.04 m) | -727.52 ($\pm$ 618.95 m$^2$) |
| A | -0.30 ($\pm$ 0.13 m) | -318.62 ($\pm$ 514.15 m$^2$) |

*Table 8. This table gives erosion rates for each zone in respect to inlet width and open water area behind the inlet. Measurements are in m and m$^2$ per year.*

As noted the erosion rates for the inlet width throughout zone 'C' are higher than the other research zones. The average rate of erosion of 4.04 m/yr ($\pm$ 8.63 m) is a 75% increase in erosion rate that occurred at the inlet mouth of zone 'B' sites. Site 6C skews the average for zone

C because the creation of the inlet occurs during the study period. When site 6C is removed from zone 'C' an erosion rate of -0.52 m/yr (± .41 m) becomes the new average (Table 9). Detailed site results are presented for site 1C and similar techniques were used for all sites. Results for the remaining sites in zone C can be found in Appendix A.

| Site | Inlet Width (m/yr) | Open Water (m$^2$/yr) | Original Inlet Width (m) | Final Inlet Width (m) |
|---|---|---|---|---|
| 1C | -0.74 (± 0.64 m) | -888.24 (± 1131.50 m) | 46.70 (± 0.20m) | 54.70 (± 0.15m) |
| 2C | -0.18 (± 0.02 m) | 194.61 (± 113.94 m) | 30.60 (± 0.20m) | 32.20 (± 0.15m) |
| 3C | -0.27 (± 0.21 m) | -47.12 (± 23.45 m) | 7.30 (± 0.20m) | 10.10 (± 0.15m) |
| 4C | -1.15 (± 1.38 m) | -888.25 (± 1131.50 m) | 0.95 (± 0.20m) | 9.56 (± 0.15m) |
| 5C | -0.27 (± 0.05 m) | -515.03 (± 393.15 m) | 11.70 (± 0.20m) | 14.30 (± 0.15m) |
| 6C | -21.64 (± 28.25 m) | -1119.17 (± 1569.22 m) | 5.50 (± 0.20m) | 106.40 (± 0.15m) |

*Table 9. Overview of sites researched in Zone'C'. With the exception of site 2C all sites within this zone underwent erosion through time. This Zone had the site (6C) with the largest erosion rates in this study. Sites 1C and 4C share an open water area, thus the open water erosion rates are the same. Standard deviation is given for Inlet width and open water erosion rate averages. Digitization error is given in paretheses for original and final inlet width measurements.*

*Figure 24. Zone 'C' site locations. 'C' sites are located the furthest from coastal inlet (2016 image from Google Earth).*

## *Detailed Site Results*

### *Site 1C*

Located approximately 5 km west from Wilkinson Canal at N 29.5651˚ W 90.0074˚, site 1C can be found in the northwest corner of Round Lake 9 km from the town of Myrtle Grove, Louisiana. This tidal creek services an open water area of 167763 m$^2$. Although 1C is protected from wave action in most directions, a fetch distance of 2.9 km can be found to the SE of the channel mouth. ADCP instrumentation was used to calculate the cross sectional area of the creek mouth and YSI, Aquadopp and RBR sensors were deployed to measure water level and current

velocity (Figure 25). The open water area behind the channel is a uniform pond structure that has a channel in the NW corner. This channel is site 4C in this study.
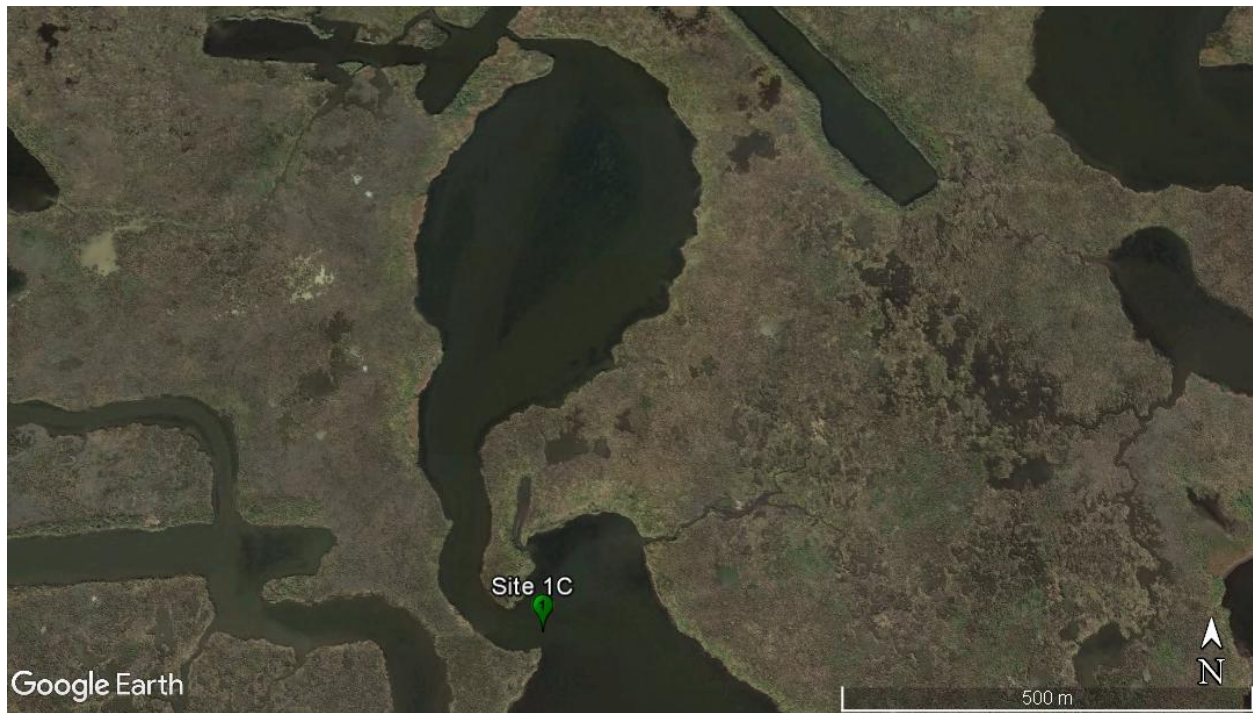


*Figure 25.  Location and latest image available for site 1C. Image shows open water area and tidal channel (2016 image from Google Earth).*

### *Historical Analysis*

The earliest image date used for site 1C is from 10/18/ 2005. Subsequent images were analyzed and measured from 2010, 2012 and 2015.

### *Inlet Width*

Measurements show that the inlet mouth and open water area at site 1C continued to erode between each image date studied. The largest rates of erosion for the inlet width occurred between 2005 and 2010. The mouth of this inlet consists of a thin point (approximately 5 m at the tip) on the southern end of the inlet that separates the inlet from Bay Round and a southerly

44

facing shoreline to the north. Most of the erosion at this inlet occurred to the point of the inlet mouth. Through time (2005-2015), the point eroded 16.75 m to the southwest.

### *Interior Pond Area*

The pond area at this site eroded between each time period. The greatest erosion rates occurred between 2005 and 2010. Erosion in the northeastern portion of the pond is responsible for most of the land loss between 2005 and 2010. An additional inlet is located in this portion of the pond and its establishment contributed to the increase in open water at this site. Additional contributions to open water area increases came from shoreline retreat time along all shorelines surrounding this pond area.

| Date | Width of Inlet (m) | Erosion Rates Inlet (m/yr) | Open Water Area (m²) | Erosion Rates Open Water Area (m²/yr) |
|---|---|---|---|---|
| 10/18/2005 | 46.7 (± 0.20m) | --- | 159167.00 (± 0.20 m²) | --- |
| 3/13/2010 | 52.7 (± 0.15m) | -1.36 | 166619.00 (± 0.15 m²) | -1692.58 |
| 10/29/2012 | 53.1 (± 0.15m) | -0.15 | 167220.00 (± 0.15 m²) | -228.26 |
| 1/27/2015 | 54.7 (± 0.15m) | -0.71 | 167763.00 (± 0.15 m²) | -241.70 |

*Table 10. Inlet and open water area sizes and erosion rates for site 1C. Digitization error is given in parentheses for both inlet width and open water area.*

### *Tidal Prism*

Tide range from RBR deployed at site 1C was used to calculate tidal prism. .22 m average spring tide was multiplied by the open water area behind the inlet at site 1C. Tidal prism at site 1C ranged from 34530.32 m$^3$ in 2005 to 36907.86 m$^3$ in 2015.

| Date | Tidal Prism (m³) |
|---|---|
| 10/18/2005 | 34530.32 |
| 3/13/2010 | 36656.18 |
| 10/29/2012 | 36788.40 |
| 1/27/2015 | 36907.86 |

*Table 11. Tidal prism calculations for site 1C based on open water area and tide range. Tide range values were calculated from data acquired during deployment of RBR sensors.*

### Fetch Measurements

The inlet at site is unprotected to the east southeast and south southeast. The greatest fetch distances are to the southeast with 2910 m of open water. The average fetch distance from the center of the inlet at site 1C is 363.96 m ($\pm$ 742.20 m).
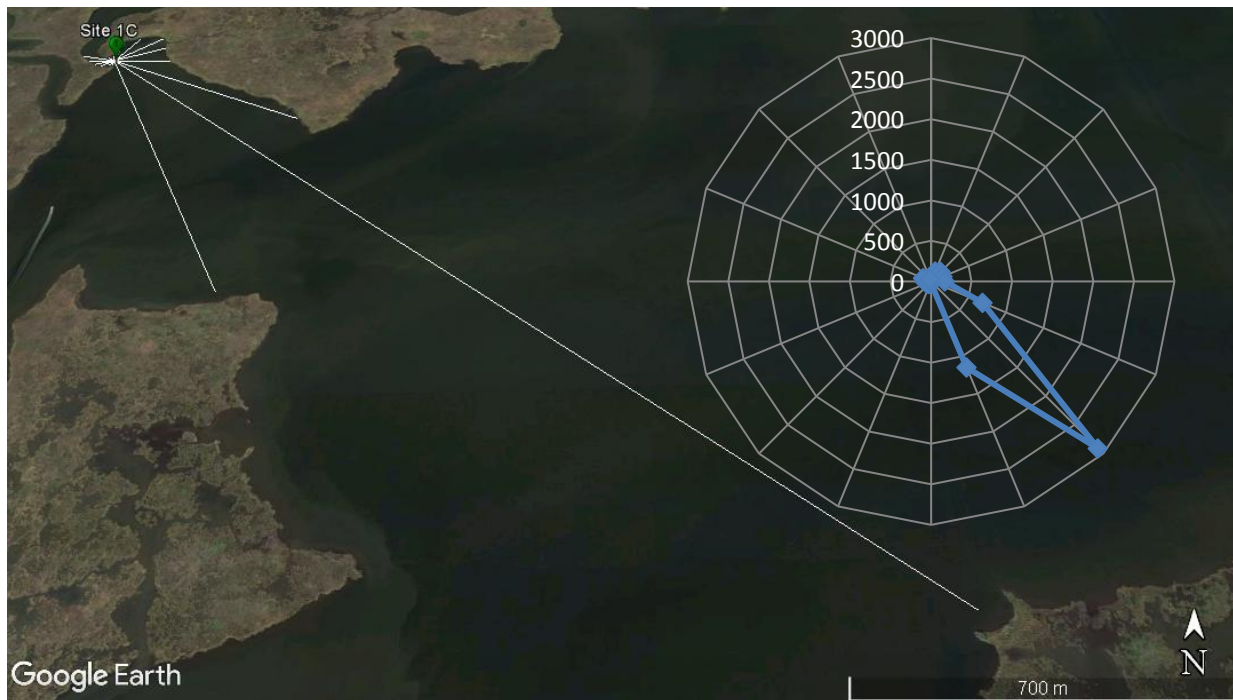


*Figure 26. This image depicts Fetch distances and directions as they relate to the mouth of the inlet located at site 1C (2016 image from Google Earth).*

*ADCP*

Two transects were measured for site 1C. Both measurements were aided by light winds and slow currents during field work. Average depth for all transects measured at the inlet mouth was 1.16m (± .02 m).

| Transect # | 006 | 007 |
|---|---|---|
| Average Depth (m) | 1.18 | 1.141 |
| Transect Length (m) | 54.79 | 57.30 |
| Actual Cross Sectional Area (m2) | 64.38 | 65.36 |

*Table 12. Results from ADCP transects from site 1C.*

### *YSI and RBR*

The RBR sensor was placed in the thalweg of the inlet on 8/23/2016 and remained in place until 9/12/2016. At the time of deployment the tide was falling and surface current velocity was visually measured at .02 m/s (Figure 27). Average water level during deployment period was .2 m above the water level at the beginning of the deployment.
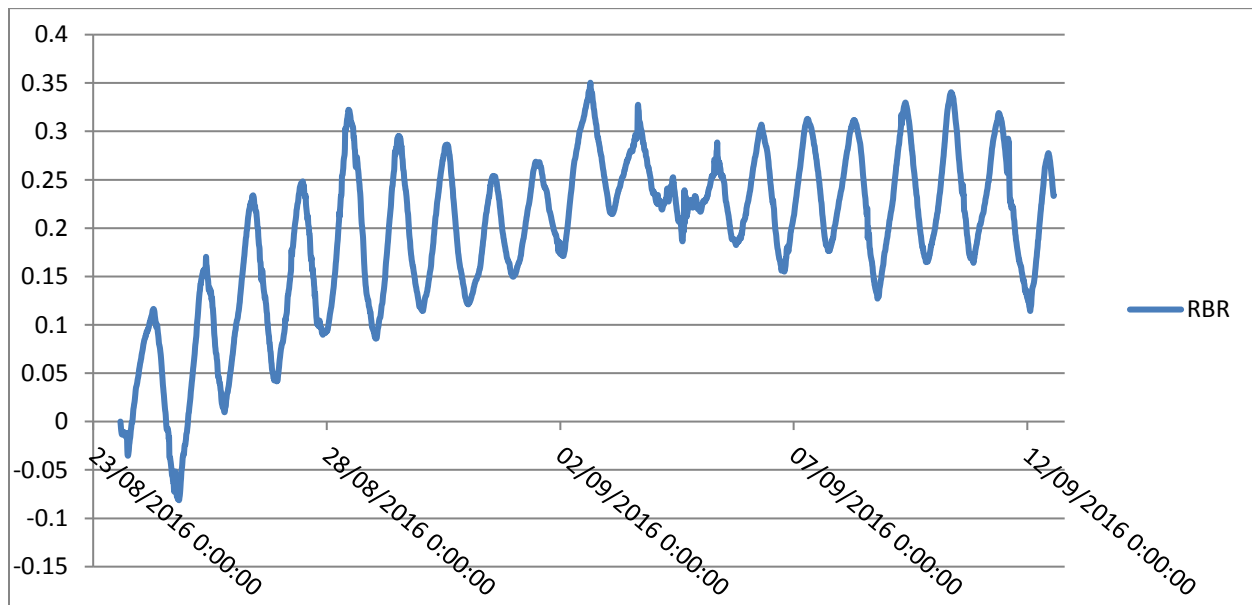


*Figure 27. RBR data from site 1C. Y-axis is tide range in m and x-axis is date and time.*

*Aquadopp*

An Aquadopp current velocity profiler was deployed from 8/23/2016 until 9/12/2016 at the thalweg of the inlet at site 1C. Average flood tide velocity was .064 m/sec and average ebb tide velocity was .177 m/sec.
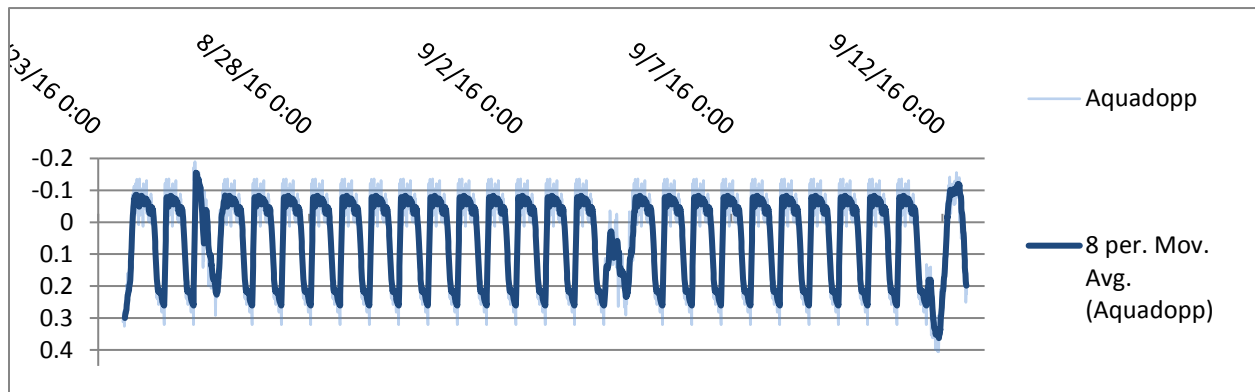


*Figure 28. Current velocity at site 1C. Y-axis is velocity in m/s and x-axis is date and time. Negative values represent the flood tide and positive number indicate ebb tide.*

# Regional Wind Data

## *NOAA Meteorological and Water Level Observations*

During the study period the water levels at the Grand Isle data buoy were higher than predicted by NOAA. The average tide level at the gauge was .47 m. Additionally, between 8/26 and 9/3 water levels were consistently .30m above predicted levels as a result of Hurricane Hermine that entered the Gulf of Mexico on August 27, 2016 and made land fall in the Florida Panhandle on Sept 2, 2016 (https://www.wunderground.com/hurricane/atlantic/2016/Tropical-Storm-Hermine) (Figure 29).
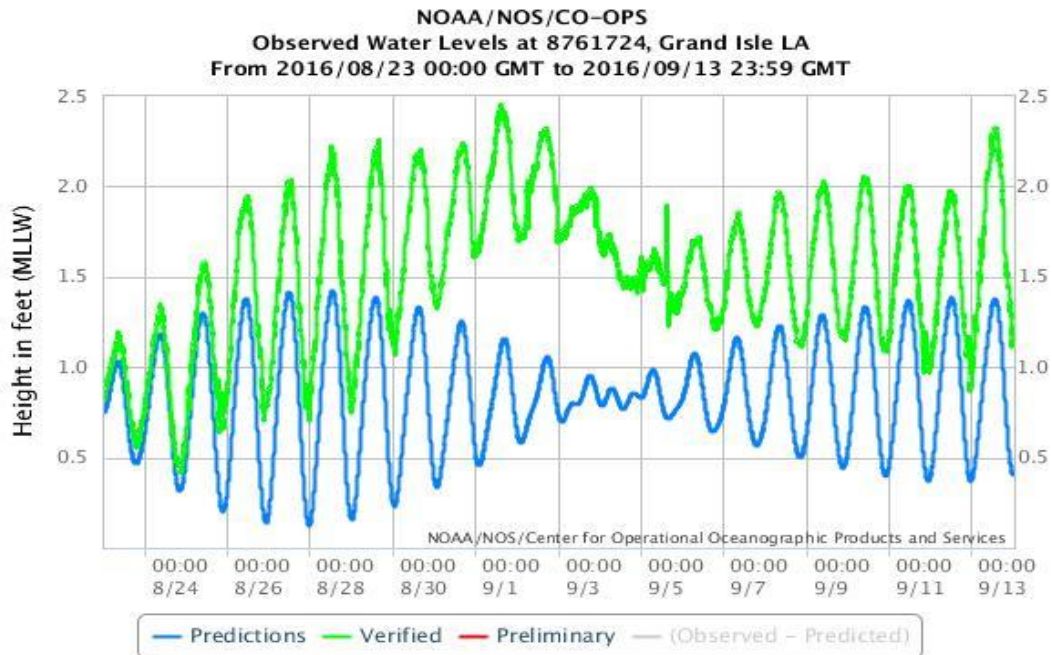
*Figure 29. Water levels at the Grand Isle tide station during the deployment of YSI, RBR and Aquadopp sensors in the Barataria study sites.  Note the elevated water levels during deployment period that coincide with Hurricane Hermine entering the Gulf of Mexico(NOAA, 2016).*
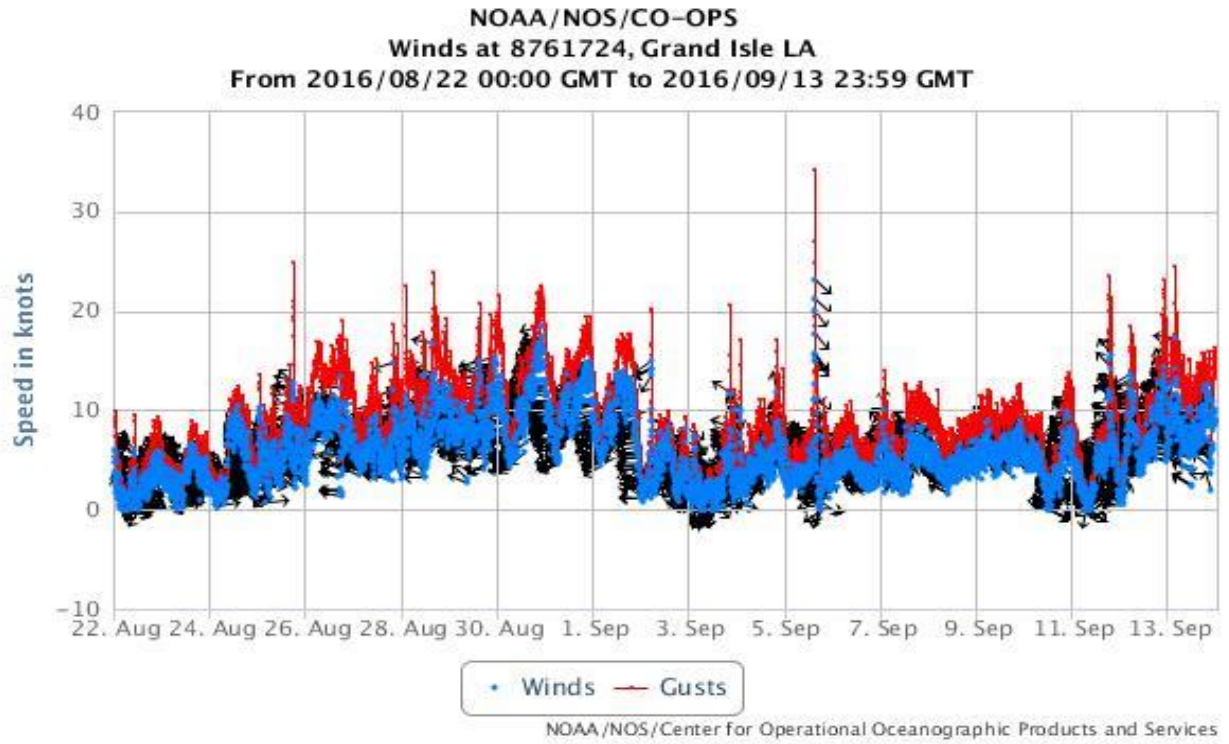
*Figure 30. The wind direction and speed during instrument deployment. The highest sustained winds occurred between 08/30/2016-09/02/2016 (2016, NOAA).*
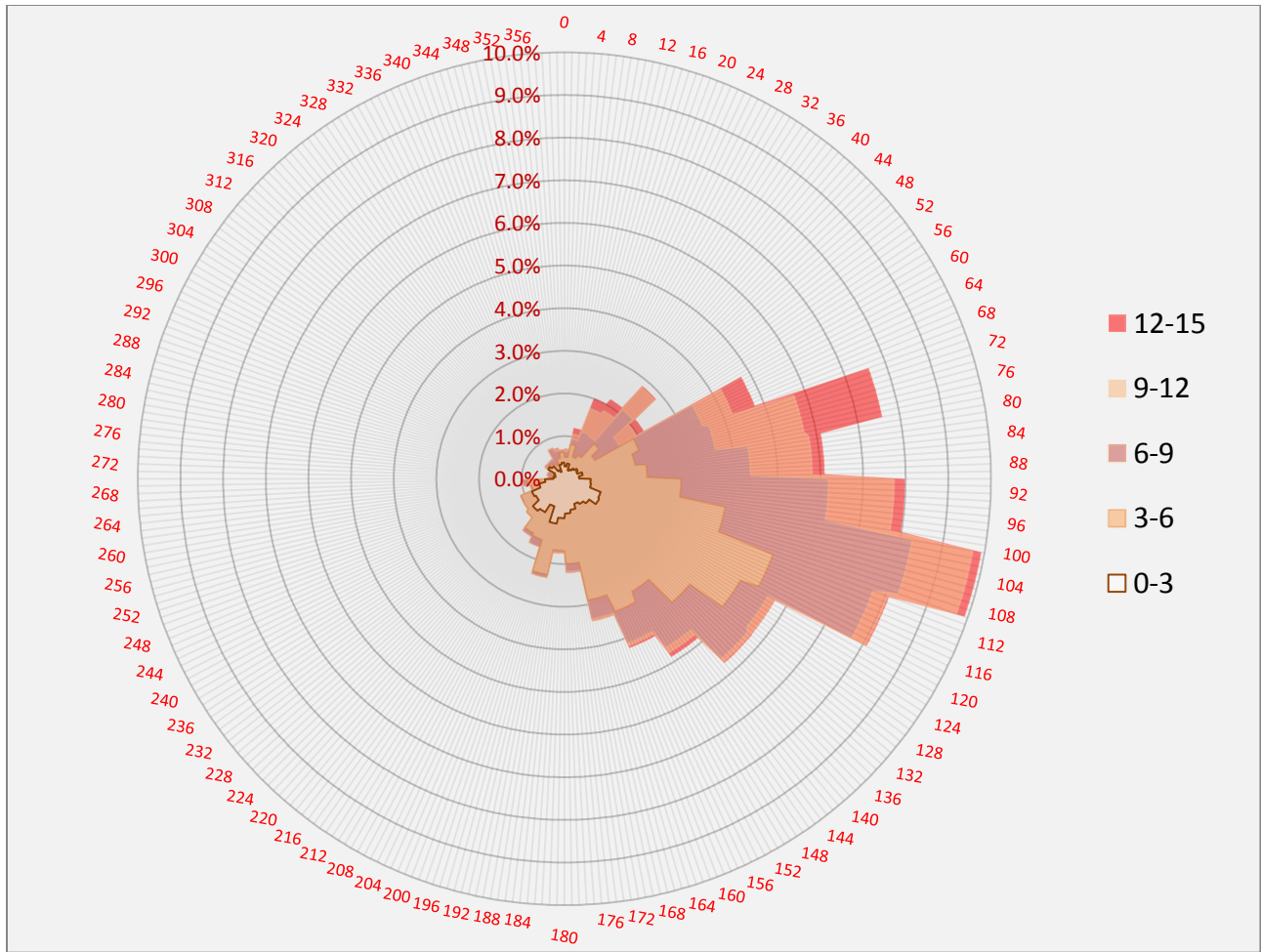
*Figure 31.This wind rose depicts the wind direction during the deployment period between 08/23/2016 and 9/12/2016. Wind direction is depicted by the percentage of time the wind was from that direction and wind speed is indicated by color as well as percentage of time spent at that speed. Speed measurements are in meters per second .*

## Prevailing Wind during Historical Analysis

The velocity and direction of wind, as well as fetch and water depth, dictate the

wavelength and amplitude of waves in open water bodies and waves, in turn, contribute to

shoreline erosion (Day et al., 1988; Day et al., 2000; Georgiou et al., 2005). Satellite imagery

used to document the geomorphology of the ponds and creeks represents a 10-yr period between

October 2005 and January 2015. An examination of wind data for this period from NOAA

indicates that the predominant wind direction was from 160-190 degrees and accounted for 15.76

% of the wind direction during the period studied. The next most prevalent wind direction was

between 0 and 30 degrees and accounted for 13.68% of the days studied.  . The strongest winds,

within 6-9 ms$^{-1}$ category, were predominantly North to Northeasterly. NOAA wind data suggests

that research sites exposed to the southeast and northeast are most susceptible to wave erosion

(Figure 32).
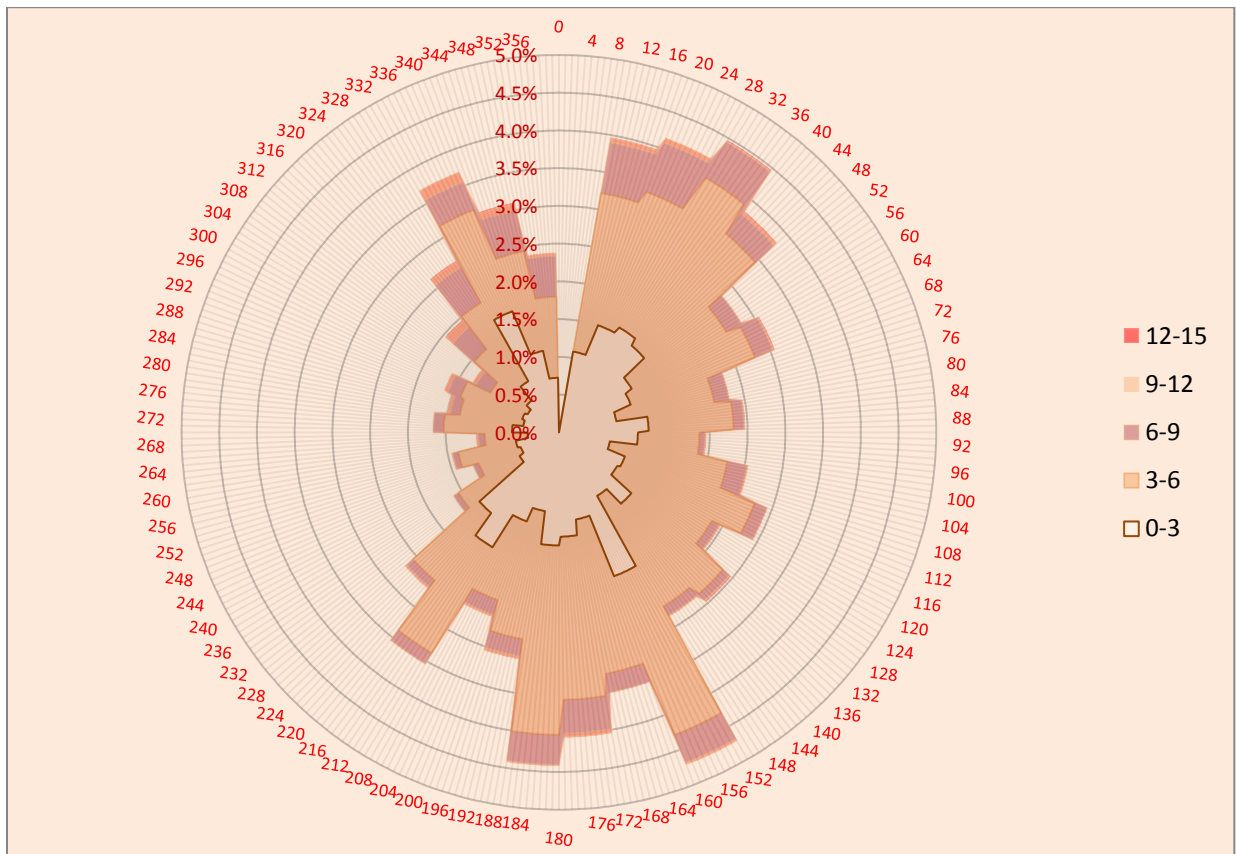


*Figure 32.  Wind rose with wind data collected at New Orleans regional airport over the last 10 years.*

## *Statistical Analysis*

The statistical analysis performed for this study evaluated whether the tidal prism to tidal creek width relationship was equal across the different research zones. An Anova single factor test produced a p-value of .31 (Table 13); therefore, it is apparent that the tidal creek cross sectional area to tidal prism relationship is not statistically significant between the three zones. Further tests were performed to determine if the sites with actual cross sectional measurements were statistically significant and it was also found that the compared sites were not significant (P-value = .17).

SUMMARY

| Groups | Count | Sum | Average | Variance |
|---|---|---|---|---|
| Row 1 | 3 | 0.033515 | 0.011172 | 7.28E-05 |
| Row 2 | 6 | 0.015428 | 0.002571 | 4.33E-06 |
| Row 3 | 6 | 0.076955 | 0.012826 | 0.000284 |

ANOVA

| Source of Variation | SS | df | MS | F | P-value | F crit |
|---|---|---|---|---|---|---|
| Between Groups | 0.000344 | 2 | 0.000172 | 1.303133 | 0.307505 | 3.885294 |
| Within Groups | 0.001586 | 12 | 0.000132 | | | |
| | | | | | | |
| Total | 0.00193 | 14 | | | | |

*Table 13. Anova test: single factor performed on the tide creek cross sectional area to tidal prism relationship. The P-value of .307505 means that the null hypothesis that all zones are statistically similar is rejected. These Zones are statistically insignificant.*

# Discussion

## Modeled Cross-Sectional Area versus Actual Cross Sectional Area

Bathymetry from ADCP transects at the inlets mouths was used to calculate the actual cross sectional area of the inlets at the six research sites. This cross sectional area was used to plot an inlet cross-sectional area to tidal prism relationship (PA relationship) (Table 14). The plot of the actual inlet cross sectional areas against the tidal prism values for each location indicates that the theoretical (Jarrett, 1976) P-A relationships diverge from the results on interior tidal creeks (Figure 33). Without exception, all tidal creeks fall outside the theoretical inlet cross sectional area plot found by using the tidal prism values of 20,000 m$^3$, 40,000 m$^3$, 60,000 m$^3$, and 80,000 m$^3$ in the Jarrett (1976) formula for Gulf Coast inlets:

$$A_e = 9.311 \; (10^{-4}) \; (P)^{.84}$$

| Location | All Inlets | | Unjettied, Single-Jettied | | Dual Jettied | |
|---|---|---|---|---|---|---|
| | $c$ | $n$ | $c$ | $n$ | $c$ | $n$ |
| All Inlets | $1.576 \times 10^{-4}$ | 0.95 | $3.797 \times 10^{-5}$ | 1.03 | $7.490 \times 10^{-4}$ | 0.86 |
| Atlantic Coast | $3.039 \times 10^{-5}$ | 1.05 | $2.261 \times 10^{-5}$ | 1.07 | $1.584 \times 10^{-4}$ | 0.95 |
| Gulf Coast | $9.311 \times 10^{-4}$ | 0.84 | $6.992 \times 10^{-4}$ | 0.86 | Insuff. Data | Insuff. data |
| Pacific Coast | $2.833 \times 10^{-4}$ | 0.91 | $8.950 \times 10^{-6}$ | 1.10 | $1.015 \times 10^{-3}$ | 0.85 |

*Table 14. Table showing Jarrett (1976) inlet cross sectional area to tidal prism calculation (from Kraus, 1998).*
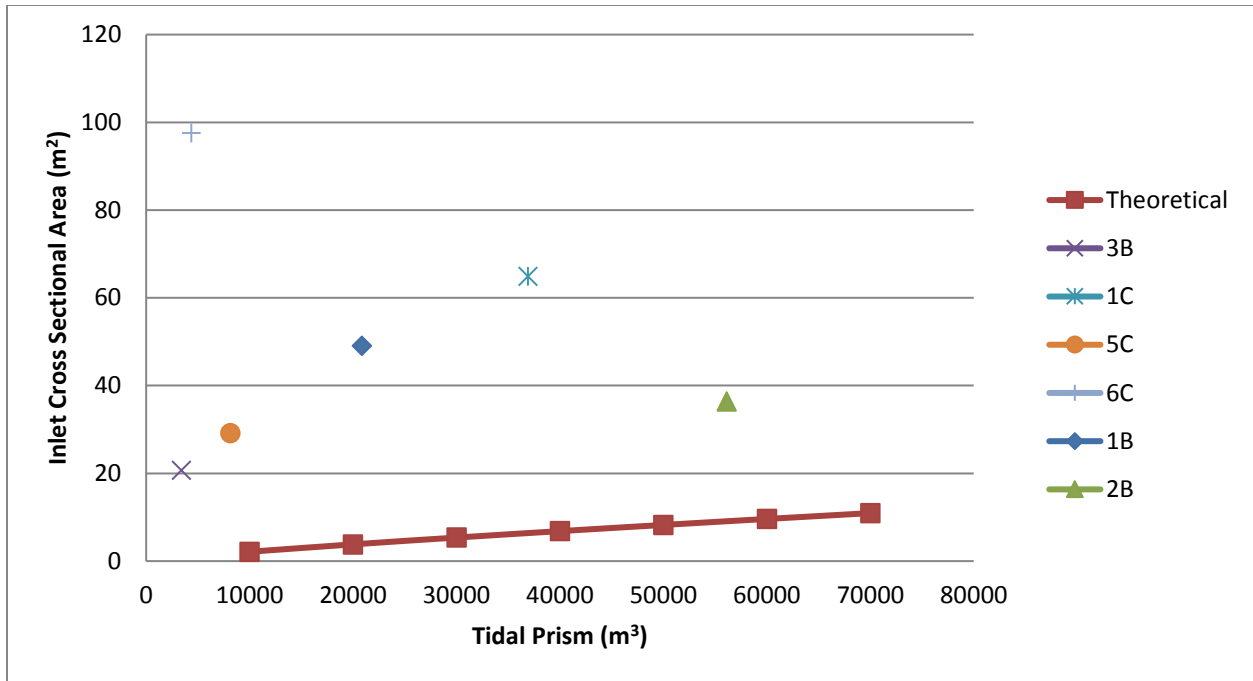
*Figure 33. Plot of inlet cross sectional areas against tidal prisms for six study sites (labled data points) and the theoretical trend of similar relationshps derived from the Jarrett (1976) equation (lower solid line). The study sites of this project have a much larger inlet cross sectional area than equilibrium models indicate. Cross sectional areas of sites are on average 2639.80% larger than what would be expected from the theoretical models.*

A plot comparing theoretical modeled inlet cross sectional areas to a range of tidal prisms determined for the Barataria Bay study sites demonstrates that the tidal creeks of this study have a larger cross sectional area (2639.80 % greater on average) then oceanic inlet models would predict (Figure 33). Tidal prism impact on inlet cross sectional area can be established through understanding erosion trends from one site to the other.

## Erosion Rates and Historical Analysis

It can be seen that erosion rates are greatest for inlet width in zone C and open water area in zone B. Zone A has the lowest erosion rates within this study. Evaluating these erosion rates is essential to making a correlation between tidal prism increase and erosion rates at the inlet

because understanding the components to erosion rates allows for commentary on the role of

tidal prism increase. Understanding erosion rates begins by reviewing results from the historical

analysis. Sites will be evaluated based on fetch, erosion rates through time, tide range, and the

total area of the study site, will be examined in order to determine their impact on erosion rates.

Examining and comparing external forces impacting erosion rates will ultimately determine

whether tidal prism enlargement plays a significant role in expanding tidal creek cross sectional

area by eliminating other causes of erosion (Table 15).

| Zone | Erosion Rates Inlet (myr$^{-1}$) | Erosion Rates Open Water Area (m$^2$yr$^{-1}$) |
|---|---|---|
| C | -4.04 (±8.63 m) | -543.86 (± 521.75 m$^2$) |
| B | -1.04 (± 1.04 m) | -727.52 (± 618.95 m$^2$) |
| A | -0.30 (± .13 m) | -318.62 (± 514.15 m$^2$) |

*Table 15. Erosion rate comparison between the three zones studied for this project. Zones are divided by location from the Gulf of Mexico. Zone A is closest to Gulf inlets while Zone C is the furthest inland.Standard deviation is presented in paretheses.*

## *Outliers*

The erosion rates for zone C inlets are 388.5 % higher than zone B and 1346.7 % higher

than zone A. Zone C has a skewed inlet erosion rate because of the evolution of the inlet at site

6C. Prior to 2010 there was no inlet on the southern shoreline of the open water area of site 6C.

This can be seen in satellite imagery prior to 2010 that shows an open water area of

approximately 14,000 m$^2$ that was being serviced by a small tidal creek to the north of the study

area. The open water was connected sometime between 2008 and 2010 and expanded rapidly.

This rapid expansion from 5.5 m in 2010 to 106.4 m in 2015 is in contrast to other erosion rates

throughout the study. When site 6C is backed out of the zone erosion rate calculations the average rate of -.52 m/yr. Site 6C will be discussed individually to examine these higher erosion rates.

Site 4B has a similar effect on the erosion rates of zone B. While the inlet erosion rates for site 4B are from 280.6 % to 1377.27 % greater than other site in zone C, the biggest disparity in erosion rates is for open water. Site 4B has erosion rates for open water anywhere from 170.88 % to 2475.4 % greater erosion rates than other site in this zone. When open water and inlet width erosion rates for site 4B are removed from calculations the final erosion rates for zone B are -500.77 m$^2$/yr and -0.56 m/yr respectfully. 4B will be evaluated individually to examine these higher erosion rates.

## *Fetch*

Perhaps the largest distinction when it comes to erosion rates, fetch distances have the greatest impact on the erosion rates of inlet mouths. When the sites with large fetch distances (average fetch >200 m) are compared to sites with medium (100-200 m) and small (average<100 m) fetch distances it can be seen that large fetch sites have erosion rates 16 times greater than small fetch sites and 14 times greater than medium sites (Figure 34).
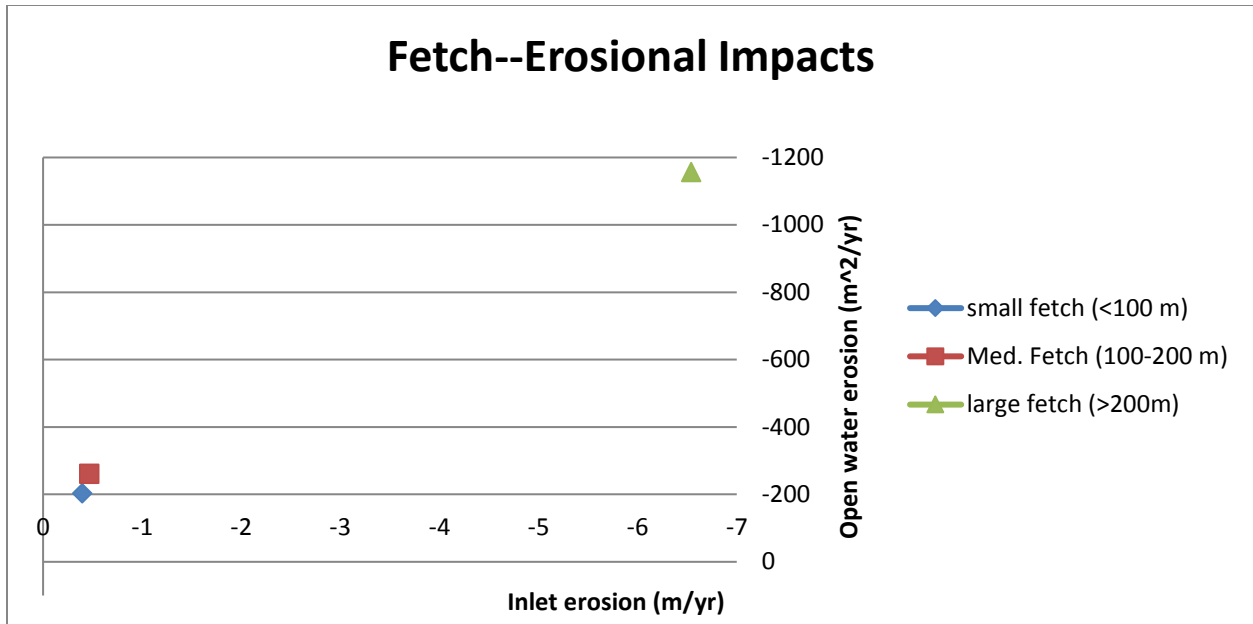
*Figure 34. This graph demonstrates the impact of fetch distance on the erosion rates of research sites.*

Furthermore; comparing the large fetch sites individually shows that fetch distance is directly proportional to erosion rates (Table 16). The only exception to this within this study is the aforementioned site 6C. Site 6C is unique to the study, in that, it was the only site that was created during the time frame of this study. The large fetch distance to the south of the site served to enhance the creation of this inlet, that shortly after its inception became more of a cove than an inlet, in the North shoreline of Bay Round.

| Large fetch (>200m) | Inlet Erosion (m/yr) | Area Erosion (m²/yr) | Average Fetch (m) |
|---|---|---|---|
| 4B | -3.03 (± 2.23 m) | -1653.00 (± 1003.36 m²) | 4317.50 (± 6073.11 m) |
| 6B | -0.75 (± 0.48 m) | -967.53 (± 800.50 m²) | 802.28 (± 1126.87 m) |
| 1C | -0.74 (± 0.61 m) | -888.25 (± 1131.50 m²) | 363.96 (± 742.20 m) |
| 6C | -21.64 (± 28.25 m) | -1119.17 (± 1569.22 m²) | 895.48(± 1210.05 m) |
| average | -6.54 (± 13.60 m) | -1156.99 (± 325.30 m²) | |

*Table 16. Erosion rates for research sites with large (>200m) average fetch distances.*

Fetch has an impact on both the inlet erosion rate and open water area erosion. Fetch distance impacts on erosion rates to open water area are greater at site with larger open water area, thus larger fetch distances. Table 16 shows the impact large fetch has on the research sites with fetch distances greater than 200 m. We can see that 4B and 6C have the highest inlet erosion rates and they also have the largest average fetch particularly from the south to east-southeast. As noted in Metrologic results prevailing winds for this region are from the southeast. 4B also has the highest erosion rates of open water area and this coincides with it also having the largest open water area. Site 6B has the second largest open water area and predictably has among the highest open water erosion rates. Site 1C has the lowest erosion rates at both the inlet and open water area. This also coincides with the overall open water area of the site as well as the smallest average fetch from sites with large (>200 m) average fetch distance (Figure 35).
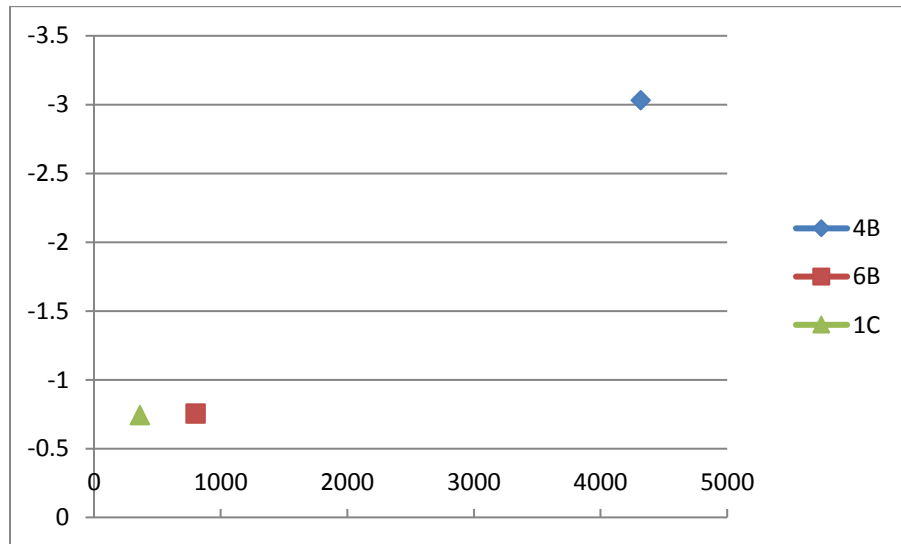


*Figure 35. Sites with large fetch distances compared to each other with respect to erosion rates. Y-axis is erosion rates (m/yr) and x-axis represents average fetch distance (m).Site 4B has the largest fetch distance as well as the largest erosion rates of sites with large fetch.*

## *Erosion with Respect to Time*

Impacts to erosion from meteorological events are well documented within this study. While these impacts would be regional and affect the research area similarly, it would not be possible to determine increased erosion on individual sites; however, the historical analysis will determine whether one period had higher erosion rates than others. Storm impacts to the region would affect sites similarly, thus erosion rates would be skewed based on when measurement are taken not where they are taken. Identifying whether erosion rates fluctuate between historical imagery would highlight meteorological impacts that could point to two processes important to this study:

1) If certain time periods have varying erosion rates than others, then there must be a regional erosional event contributing to the increase or decrease.

2) Erosion rate variations to open water area should coincide with inlet width erosion rates. If tidal prism determines inlet cross sectional area, then changes to erosion rates should manifest as changes to inlet width.

Historical analysis of satellite imagery took into account three time period for each site. From initial measurement to second image date is the first time period, the second image date to the third image is the second time period and the third image date to the last is time period three. While some of the dates varied there was commonly an image from 2005, 2010, 2012 and 2015. Comparing historical erosion rates for the three time periods reveals that for both Zones A and B had the highest erosion rates at the inlet mouth during the first time period and erosion rates dropped through time. Zone C, however, had an increase to erosion rates through time.
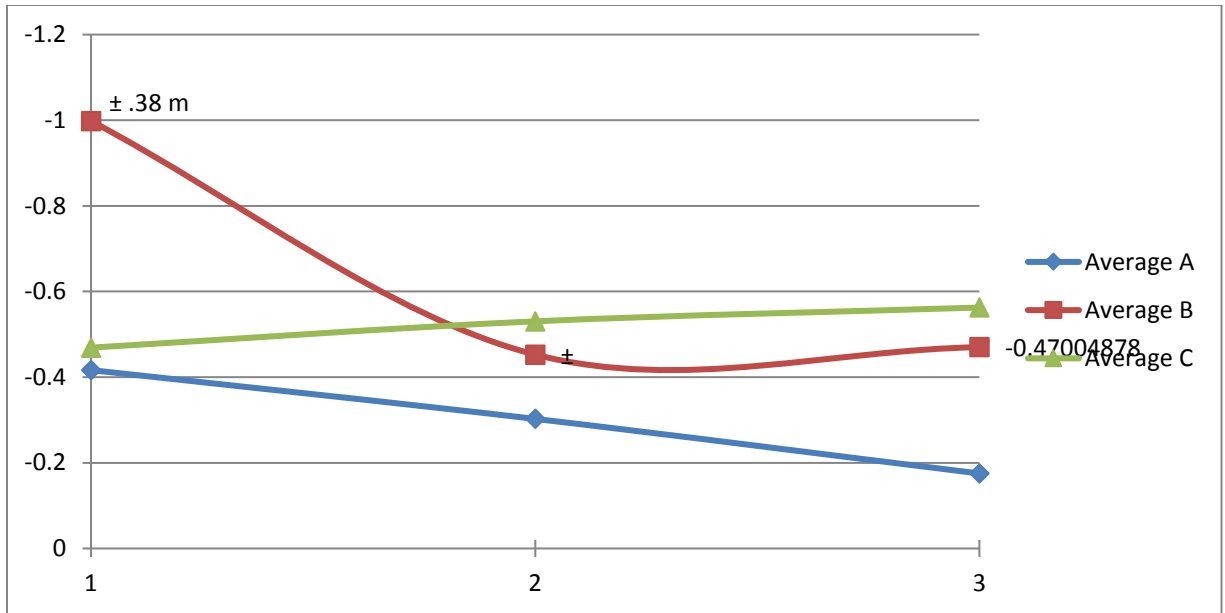
*Figure 36. Graph demonstrating average inlet width erosion rates for each zone during various time periods. Erosion rates (y-axis) are in m/yr and x-axis is time periods.*

If inlet cross sectional area is, in part, related to open water erosion rates then there will be a correlation between the erosion trends between open water and inlet erosion rates. Open water erosion rates follow a similar pattern between the three zones. Time period 1 has greater erosion rates then time period 2 and erosion rates increase in all zones from time period 2 to 3 (Figure 37). The similar nature of the trends through time within open water erosion rates seems to indicate regional variables dictate erosion of interior pond areas.
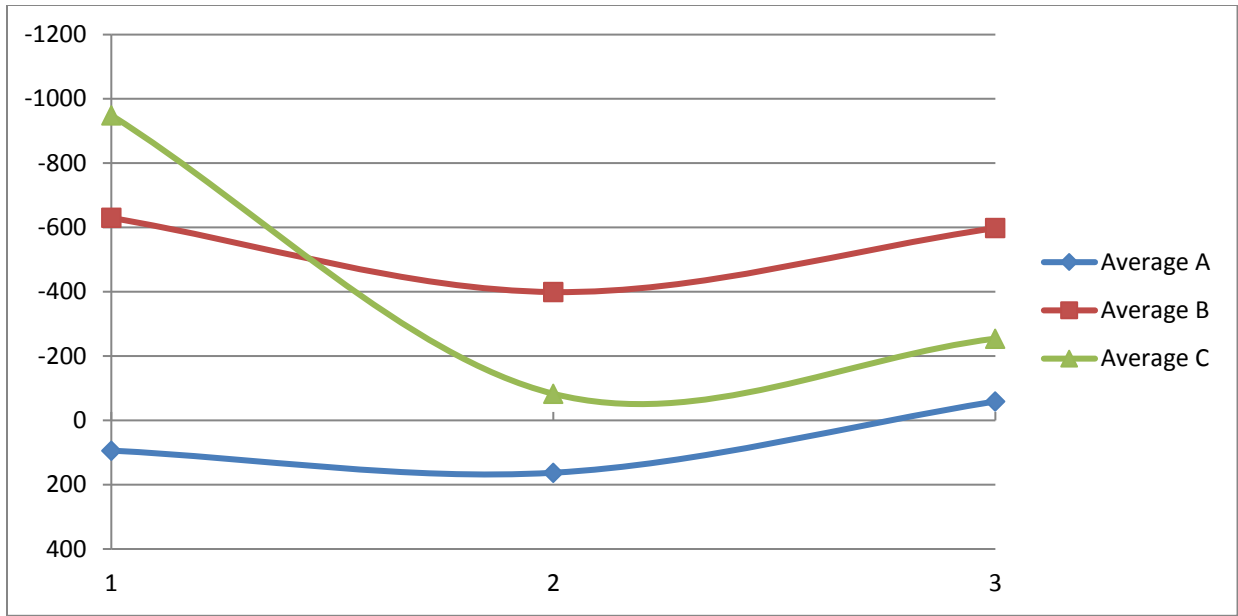
*Figure 37. Graph demonstrating average open water area erosion rates for each zone during various time periods. Erosion rates (y-axis) are in m²/yr and x-axis is time periods.*

Inlet width erosion rates for zone B most closely resemble the erosion rates to open water area in that same zone.
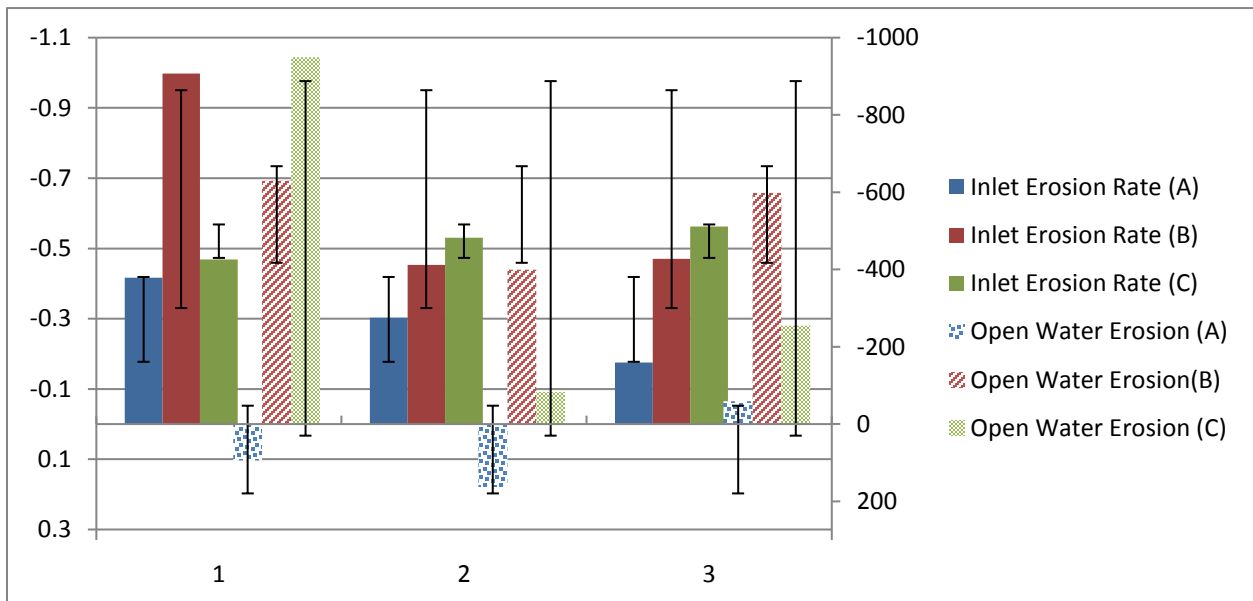


*Figure 38. Bar graph demonstrating the relationship between inlet (solid bars) erosion rates (m/yr) on the primary y-axis and open water (textured bars) erosion rates (m²/yr on the secondary y-axis). X-axis is time period. The error bars represent the standard deviation for each average erosion rate.*

## *Tide Range*

Based on data collected from CRMS stations and through deployment of YSI and RBR sensors, it is known that tide range varies from one research site to the other (Table 17). In order to evaluate the impact of tide range on the erosion rates of the sites erosion rates between sites with different tide ranges will be compared.

| Site | Tide Range Averages |
|------|---------------------|
| 4C | .28 m |
| 1C | .22 m |
| 1B | .24 m |
| 2B | .27 m |
| 1A | .36 m |

*Table 17. Average spring tide range values from 8/23/2016 to 9/12/2016.*

Inlet width erosion rates vary between these five sites but the site with the lowest erosion rate has the highest tide range value (Figure 39). The correlation between increased tide prism and increased inlet erosion seems to be reliant on factors other than tide range.
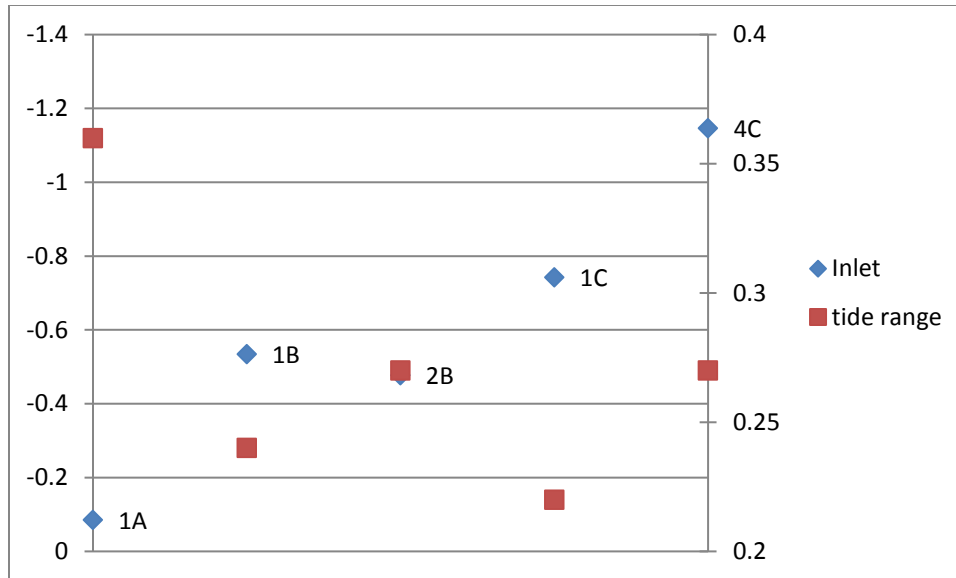
*Figure 39. Inlet erosion rate in m/yr (primary y-axis) compared to tide range in m (secondary y-axis). Varying tide range seems to have little correlation to the inlet erosion rate in that the smallest erosion rates (site 1A) has the largest tide range while the largest erosion rate is found at a site with average tide range (site 4C) and the second largest erosion rate is found at a site with the smallest tide range.*

## *Current Velocity Erosion*

Inshore tidal creeks have similar traits to oceanic inlets, in that water moves through them. Thus inshore tide current could demonstrate sufficient velocity to move sediment in order for a model to be established. Reidel and Gourlay (1980) discussed how sheltered interior inlets demonstrate larger inlet cross sectional area than similar unprotected inlets. It was argued that insufficient sediment supply due to the lack of wave driven longshore sediment transport prevented sediment infilling at the inlet. These sheltered inlets have sufficient tide current to create equilibrium with the flow entering and leaving, yet there was no sediment input to facilitate infilling (Reidel and Gourlay, 1980).

Protected tidal creeks within Barataria Bay exhibit similar traits to the protected inlets Reidel and Gourlay studied. To examine whether tide flow can determine inlet cross sectional

64

area, it must be established whether current velocities entering or leaving the creek can facilitate erosion. This study utilized a current profiler to establish current velocity at a selected research site. Aquadopp deployment revealed that current velocities from 8/23/2016 to 9/12/2016 reached sufficient speeds to scour silt and soft mud shorelines. Current velocity data from site 1C shows that ebb tide velocities reached a maximum velocity of .41 m/s (Figure 40).
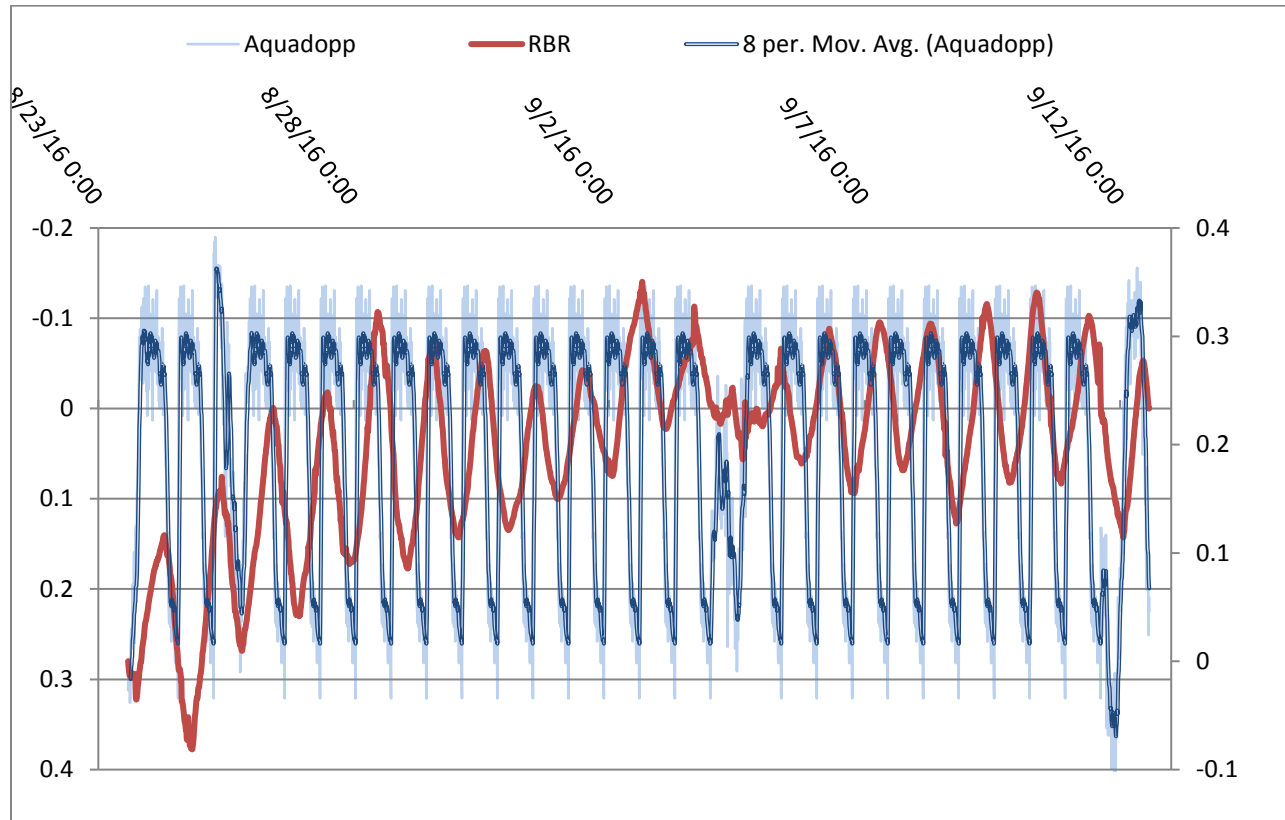


*Figure 40. This plot shows Aquadopp current velocity data (primary y-axis in m/s) with RBR tide range data (secondary y-axis in m). Negative values correlate to flood tide and positive values represent ebb tide velocities.*

During the study period the water levels at the Grand Isle data buoy were higher than predicted by NOAA. The average tide level at the gauge was .46m. Additionally, between 8/26/2016 and 9/3/2016 water levels were consistently .3m above NOAA predicted levels. It should be noted that a tropical system moved into the Gulf of Mexico during this time. Hurricane

Hermine entered the Gulf on August 27, 2016 and made land fall in the Florida Panhandle on Sept 2, 2016 (https://www.wunderground.com/hurricane/atlantic/2016/Tropical-Storm-Hermine). The impact of the storm can be seen in the tide data acquired during the event.
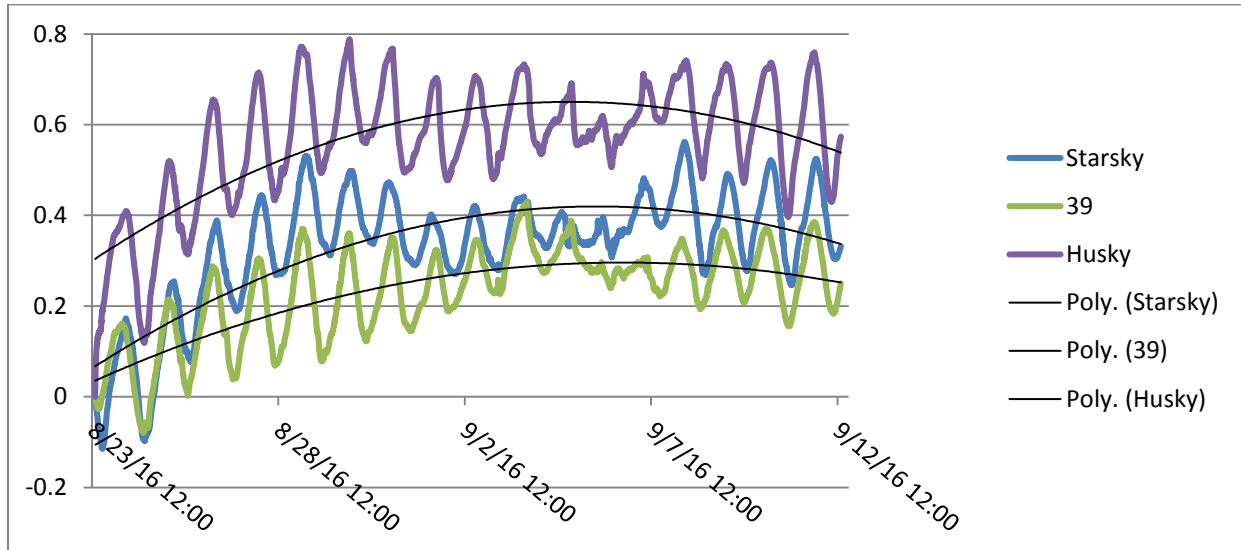


*Figure 41. Tide range data from all YSI sensors used during this study. Impact of tropical system can be seen as increases in overall water level.*

On the deployment day, the water level was approximately 0.02 m below the marsh platform, thus the first YSI and RBR measurements were below the marsh platform. After the tide data was adjusted to zero by subtracting the starting depths from the initial pressure readings, any water level above 0.02 m is above the marsh platform. Careful examination of water levels and current velocity reveals that during the only marsh platform-draining event recorded, ebb current velocities were between 0.2 m/s and 0.32 m/s for a 10-hour period. Conversely, when tropical storm conditions began to push water into the marsh there were extended periods of flood tide currents. The ebb tide current velocities are stronger, but the flood tide generally peaks for longer periods of time (Figure 40). When comparing water level data to *Aquadopp* current velocities it is apparent that the highest flood tide current velocity occurs

66

during the tide pulse event on 8/25/2016. Conversely, the highest ebb tide velocities occur in conjunction to the set down event on 9/11/2016 (Figure 40).

The increase in tide current velocity during the set down event recorded from the *Aquadopp* deployment indicates that tide currents do reach velocities capable of shaping the morphology of tidal creeks. The association of the increased tidal velocities with the passage of a storm system highlights the importance of subtidal variation to erosional events. Observing tidal velocity increases during the set down event demonstrates that similar events could occur during marsh draining events such as the passage of cold fronts. Erosion throughout Louisiana has been tied to subtidal storm events (Moeller et al., 1993; Snedden et al., 2007 and Li et al., 2011) and it seems apparent that increased tidal velocities due to tide set down play a role in the erosion of tidal creeks.

## *Tide Prism Impacts*

A review of historical data reveals that sites with large fetch distances have disproportionately high erosion rates that make assessing tidal prism impacts separate from wave erosion impossible. The higher than average erosion rates for the sites with large (>200m) fetch distances were addressed in the fetch analysis, thus to asses tidal prism impacts these sites were removed. Removing the three sites with the largest fetch distances and erosion rates (4B, 6B and 6C) from the erosion results helps to isolate the impacts of tidal prism equilibrium. When the remaining sites are plotted with respect to inlet erosion rates as they relate to open water erosion rates it is revealed that the higher the open water erosion rate does not necessarily equate to higher inlet erosion rate (Figure 42).
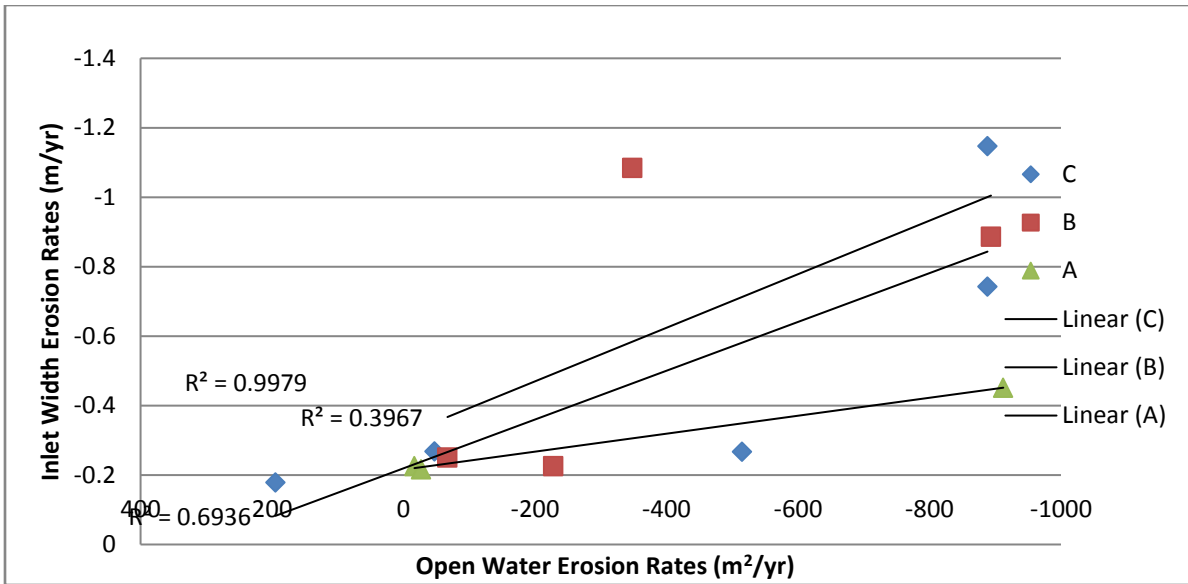
*Figure 42. Open water erosion rates (x-axis in m²/yr) compared to inlet width erosion rates (y-axis m/yr). Negative results indicate erosion while positive results indicate accretion.*

# Conclusion

The study sites selected for this study showed changes to open water area and inlet width through time. All tidal creek mouths studied underwent various rates of erosion, and the open water pond areas behind these inlets increased through time. The erosion at these sites presents an opportunity to examine whether there is a correlation between the rate of pond area increase and tidal creek expansion. This study examined open water area behind the inlets, tide range, fetch and distance from the Gulf of Mexico to assess which of these factors has the most substantial role in tidal creek mouth erosion at the research sites.

Comparing research sites to theoretical models (Jarrett, 1976) reveals that the tidal creeks cross sectional areas are much larger than oceanic inlet models would suggest. Thus, other factors must be affecting the size of tidal creeks within Barataria Bay. This study demonstrates that the correlation between the size of the open water area being serviced by a tidal creek does not necessarily determine the cross sectional area of the creek (Figure 33). An example of this is site 2B. The most consistent result of this this study is that the larger the fetch distance the higher the tide creek erosion rate (Figure 34).

Equilibrium between a tidal creek and an interior open water body can exist only where limited fetch distances allow for shorelines adjacent to the creek mouth to remain stable. An examination of historical imagery reveals that a contributing factor to inlet erosion rates is the erosion of the shoreline adjacent to the mouth. This erosion facilitates the migration of the creek mouth and ultimately shortens the distance from the mouth to the open water pond area. The equilibrium that could exist between tidal creeks and interior ponds must take into account fetch as a contributing factor to cross sectional area.

# References

Adam, P. (1990). Saltmarsh Ecology. Cambridge University Press, Cambridge.

Barbier, E. B., Georgiou, I. Y., Enchelmeyer, B., & Reed, D. J. (2013). The Value of Wetlands in Protecting Southeast Louisiana from Hurricane Storm Surges. PloS one, 8(3), e58715.

Barras, J.A., Bernier, J.C., and Morton, R.A., 2008, Land area change in coastal Louisiana--A multidecadal perspective (from 1956 to 2006): U.S. Geological Survey Scientific Investigations Map 3019, scale 1:250,000, 14 p. pamphlet.

Bruun, P., and Gerritsen, F. (1960). Stability of coastal inlets. Coastal Engineering Proceedings, 1(7), 23.

Byrne, R. J., Gammisch, R. A., and Thomas, G. R. (1980). Tidal prism-inlet area relations for small tidal inlets. Coastal Engineering Proceedings, 1(17).

Couvillion, B.R., Barras, J.A., Steyer, G., Sleavin, W., Fischer, M., Beck, H., Trahan, N., Griffin, B., and Heckman, D. (2011). Land area change in coastal Louisiana from 1932 to 2010: U.S. Geological Survey Scientific Investigations Map 3164, scale 1:265,000, 12 p. pamphlet.

Chuang, W. and Wiseman, W. (1983). Coastal sea level responses to frontal passages on the Louisiana-Texas shelf. Journal of Geophysical Research, 88, 2615-2620.

Day Jr, J. W., Reed, D., Suhayda, J. N., Kemp, G. P., Cahoon, D., Boumans, R. M., & Latif, N. (1988). Physical processes of marsh deterioration. Final Report: Critical Physical Processes of Wetland Loss, 1994(1994), 5-1.

Day Jr, J. W., Martin, J. F., Cardoch, L., & Templet, P. H. (1997). System functioning as a basis for sustainable management of deltaic ecosystems. Coastal Management, 25(2), 115-153.

Day, J. W., Britsch, L. D., Hawes, S. R., Shaffer, G. P., Reed, D. J., & Cahoon, D. (2000). Pattern and process of land loss in the Mississippi Delta: a spatial and temporal analysis of wetland habitat change. Estuaries, 23(4), 425-438.

Day, J. W., Boesch, D. F., Clairain, E. J., Kemp, G. P., Laska, S. B., Mitsch, W. J., and Whigham, D. F. (2007). Restoration of the Mississippi Delta: lessons from hurricanes Katrina and Rita. Science, 315(5819), 1679-1684.

Day, J. W., Kemp, G. P., Reed, D. J., Cahoon, D. R., Boumans, R. M., Suhayda, J. M., and Gambrell, R. (2011). Vegetation death and rapid loss of surface elevation in two contrasting Mississippi delta salt marshes: The role of sedimentation, auto compaction and sea-level rise. Ecological Engineering, 37(2), 229-240.

DeLaune, R. D., Baumann, R. H., & Gosselink, J. G. (1983). Relationships among vertical accretion, coastal submergence, and erosion in a Louisiana Gulf Coast marsh. Journal of Sedimentary Research, 53(1), 147-157.

DeLaune, R. D., Nyman, J. A., & Patrick Jr, W. H. (1994). Peat collapse, ponding and wetland loss in a rapidly submerging coastal marsh. Journal of Coastal Research, 1021-1030.

DeLaune, R.D. and Pezeshki, S.R. (1994). The Influence of Subsidence and Saltwater Intrusion on Coastal Marsh Stability: Louisiana Gulf Coast, U.S.A. Journal of Coastal Research, Special Issue No. 12. Coastal Hazards: Perception, Susceptibility and Mitigation, 77-89.

Escoffier, F. F. (1977). Hydraulics and Stability of Tidal Inlets. GITI-13. U.S. Army Corp of Engineers. Coastal engineering Research Center, Fort Belvoir VA, and the U.S. Army Engineer Waterways Experiment Station, Vicksburg, MS.

Fagherazzi, S., Palermo, C., Rulli, M. C., Carniello, L., & Defina, A. (2007). Wind waves in shallow microtidal basins and the dynamic equilibrium of tidal flats. Journal of Geophysical Research: Earth Surface (2003–2012), 112(F2).

Fagherazzi, S., & Wiberg, P. L. (2009). Importance of wind conditions, fetch, and water levels on wave-generated shear stresses in shallow intertidal basins. Journal of Geophysical Research: Earth Surface (2003–2012), 114(F3).

Fagherazzi, S., & Priestas, A. M. (2010). Sediments and water fluxes in a muddy coastline: interplay between waves and tidal channel hydrodynamics. Earth Surface Processes and Landforms, 35(3), 284-293.

Fagherazzi, S., Kirwan, M. L., Mudd, S. M., Guntenspergen, G. R., Temmerman, S., D'Alpaos, A., & Clough, J. (2012). Numerical models of salt marsh evolution: Ecological, geomorphic, and climatic factors. Reviews of Geophysics, 50(1).

FitzGerald, D. M., Penland, S., and Nummedal, D. (1984). Control of barrier island shape by inlet sediment bypassing: East Friesian Islands, West Germany, Marine Geology, v. 60, 355-376.

FitzGerald, D. M., Kulp, M. A., and Penland S. (2003). Tidal prism changes within Barataria Bay and its effects on sedimentation patterns and barrier shoreline stability. Gulf Coast Association of Geological Societies Transactions Vol. 53, 243-251.

Fitzgerald, D. M.; Buynevich, I. and Argow, B. (2006). Model of tidal inlet and barrier island dynamics in a regime of accelerated sea level rise. Journal of Coastal Research, SI 39 (Proceedings of the 8th International Coastal Symposium), 789 - 795.

Gagliano, S.M., Meyer-Arendt, K.J. and Wicker, K.M., 1981. Land loss in the Mississippi River deltaic plain. Transactions—Gulf Coast Association of Geological Societies. Volume XXXI.

Georgiou, I. Y., FitzGerald, D. M. and Stone, G. W. (2005). The Impact of Physical Processes along the Louisiana Coast. Journal of Coastal Research (SPRING), 72-89.

Hatton, R. S., DeLaune, R. D., and Patrick, W. H. Jr. (1983). Sedimentation, accretion, and subsidence in marshes of Barataria Basin, Louisiana."*Limnol. Oceanogr* 28.3: 494-502.

Hume, T.M., Herdendorf, C., 1993. On the use of empirical stability relationships for characterising estuaries. *Journal of Coastal Research* 9 (2), 413– 422.

Jarrett, J. T. (1976). Tidal prism-inlet area relationships. GITI-3. U.S. Army Corp of Engineers. Coastal engineering Research Center, Fort Belvoir VA, and the U.S. Army Engineer Waterways Experiment Station, Vicksburg, MS.

Kirwan, M. L., & Murray, A. B. (2007). A coupled geomorphic and ecological model of tidal marsh evolution. Proceedings of the National Academy of Sciences, 104(15), 6118-6122.

Kraus, N.C., (1998). Inlet Cross-Sectional area Calculated by Process-Based Model. Proceedings of the 26th International Coastal Engineering Conference (American Society of Civil Engineers, New York), Vol 3, pp. 3265-3278.

Krishnamurthmy, , 1977. Tidal Prism of Equilibrium Inlets. Journal of the Waterway, Port, Coastal and Ocean Division (American Society of Civil Engineers, New York), 103(WW4), 423-432.

Kulp, M., Penland, S., Williams, S., Jenkins, C., Flocks, J., and Kindinger, J. (2005). Geologic frame work, evolution, and sediment resources for restoration of the Louisiana Coastal Zone. Journal of Coastal Research, SI(44), 56-71.

Kirwan, M. L. and Guntenspergen (2010). Influence of tidal range on the stability of coastal marshland. Journal of Geophysical Research. Vol. 115, F02009.

Kirwan, M. L., Megonial, P. J. (2013). Tidal wetland stability in the face of human impacts and sea-level rise. Nature, Vol. 504, 53-60.

Li, C., Roberts H., Stone Gregory G. W., Weeks, E., and Luo, Y. (2011). Wind surge and saltwater intrusion in Atchafalaya Bay during onshore winds prior to cold front passage. Hydrobiologia, 658, 27–39.

Mariotti, G., S. Fagherazzi, P. L. Wiberg, K. J. McGlathery, L. Carniello, & A. Defina (2010). Influence of storm surges and sea level on shallow tidal basin erosive processes, Journal of Geophysical Research., 115, C11012.

Mayor-Mora, R. E. (1977). Laboratory investigation of tidal inlets on sandy coasts. GITI-11. U.S. Army Corp of Engineers. Coastal engineering Research Center, Fort Belvoir VA, and the U.S. Army Engineer Waterways Experiment Station, Vicksburg, MS.

Moeller, C. C., Huh, O. K., Roberts, H. H., Gumley, L. E., & Menzel, W. P. (1993). Response of Louisiana coastal environments to a cold front passage. Journal of Coastal Research, 434-447.

Morris, J. T., Sundareshwar, P. V., Nietch, C. T., Kjerfve, B., & Cahoon, D. R. (2002). Responses of coastal wetlands to rising sea level. Ecology, 83(10), 2869-2877.

Mudd, S. M. (2011). The life and death of salt marshes in response to anthropogenic disturbance of sediment supply. Geology, 39(5), 511-512.

O'Brien, M. P. (1969). Equilibrium flow areas of inlets on sandy coasts. Journal of Waterways and Harbor Division, ASCE, 95(1) 43-52.

O'Brien, M. P., and Dean, R. G. (1972). Hydraulics and sedimentary stability of coastal inlets. Coastal Engineering Proceedings, 11, 761-779.

Penland, S. and Ramsey, K.E. (1990). Relative sea-level rise in Louisiana and the Gulf of Mexico: 1908-1988. Journal of Coastal Research, 6(2), 323-342.

Pethick, J. S. (1992). Saltmarsh Geomorphology. Saltmarshes: Morphodynamics, Conservation and Engineering Significance. Cambridge University Press. 41-62.

Pethick, J.S. (1993). Shoreline Adjustments and Coastal Management: Physical and Biological Processes Under Accelerated Sea-Level Rise. The Geographical Journal, 159 (2), 162-168.

Penland, S., Wayne, L. D., Britsch, L. D., Williams, S. J., Beall, A. D., & Butterworth, V. C. (2000). The Processes of Coastal Land Loss in the Mississippi River Delta Plain. New Orleans, LA: USGS. USGS Open-File Report 00-0418.

Penland, S.; Beall, A.; Britsch, L.D., III, & Williams, S.J., (2002). Geologic classification of coastal land loss between 1932 and 1990 in the Mississippi River Delta Plain, southeastern Louisiana. Gulf Coast Association of Geological Societies Transaction, 52, 799–807.

Reed, D. J. (1995). The response of coastal marshes to sea level rise: survival or submergence? Earth Surface Processes and Landforms 20:39-48.

Riedel, H.P., and Gourlay, M.R. (1980). Inlets/Estuaries Discharging into Sheltered Waters. Proc. 17th Coastal Eng. Conf., ASCE Press, NY, 2550-2562.

Sasser, CE.; Visser, J.M.; Mouton, E.; Linscombe, J., and Hartley, S.B., (2008). Vegetation types in coastal Louisiana in 2007. U.S. Geological Survey Open-File Report 2008-1224, 1 sheet, scale 1:550,000. http:// pubs.usgs.gov/oF2008/1224.

Smith, J. M., Cialone, M. A., Wamsley, T. V., & McAlpin, T. O. (2010). Potential impact of sea level rise on coastal surges in southeast Louisiana. Ocean Engineering, 37(1), 37-47.

Snedden, G. A., Cable, J. E., and Wiseman, W. J. (2007). Subtidal sea level variability in a shallow Mississippi River deltaic estuary, Louisiana. Estuaries and Coasts, 30(5), 802-812.

Stevenson, J. C., L. G. Ward, and M. S. Kearney. (1986). Vertical accretion in marshes with varying rates of sea level rise. Pages 241-259 in D. A. Wolfe, editor. Estuarine variability. Academic Press, San Diego, California, USA

Stive, M. J. F., van de Kreeke, J., Lam, N. T., Tung, T. T. and Ranasinghe, R., (2009). Empirical relationships between tidal inlet cross section and tidal prism: A review. Proceedings of Coastal Dynamics.

Törnqvist, T. E., Kidder, T. R., Autin, W. J., van der Borg, K., de Jong, A. F., Klerks, C. J., & Wiemann, M. C. (1996). A revised chronology for Mississippi River subdeltas. Science, 273(5282), 1693-1696.

Wilson, C. A., and Allison, M. A. (2008). An Equilibrium Profile Model for Retreating Marsh Shorelines in Southeast Louisiana. Estuarine, Coastal and Shelf Science, 80.4, 483-494.

Van de Kreeke, J., (1985). Stability of tidal inlets; Pass Cavallo, Texas. Estuarine Coastal Shelf Science, 21:33-43

Van de Kreeke, J., (1990). Stability of a two-inlet bay system. Coastal Engineering, 14: 481-497

Van de Kreeke, J., (1992). Stability of tidal inlets; Escoffier's analysis. Shore and Beach, 60 (1): 9-12

Van de Kreeke, J., (1998). Adaptation of the Frisian inlet to a reduction in basin area with special reference to the crosssectional area of the inlet channel. In Dronkers, J. and Scheffers , M.B.A.M. (Eds). Proc. PECS conference: 355-362

Van de Kreeke, J., (2004). Equilibrium and cross-sectional stability of tidal inlets: application to the Frisian Inlet before and after basin reduction. Coastal Engineering, 51: 337-350

Van Maanen, B., Coco, G., & Bryan, K. R. (2013). Modelling the Effects of Tidal Range and Initial Bathymetry on the Morphological Evolution of Tidal Embayments. Geomorphology, 191, 23-34.

Yuill, B., Lavoie, D., and Reed, D.J. (2009). Understanding subsidence processes in coastal Louisiana. Journal of Coastal Research, SI (54), 23–36.

Zedler, Joy B., and John C. Callaway (2001). "Tidal wetland functioning." *Journal of Coastal Research* 38-64.

# Appendices

## Appendix A

### *Site 2A*

Site 2 is located a kilometer to the southeast of Bassa Bassa Bay approximately 10.5 km North of Grand Isle, Louisiana at N 29.3459˚W 89.9821˚(*Figure 43*). The tidal channel being studied at this site is protected on all sides by marsh platform. The mouth of the channel has the greatest fetch distance of 313 m to the SSW. Open water area behind the channel is 28,214 m$^2$. The open water area and tidal channel are positioned in the center of an island that is flanked by an oil and gas pipeline to the west and Barataria Bay to the south, east and north. The channel is 25 m, straight, and provides connection between a uniform pond area to the North and open water to the South.



*Figure 43. Location and latest image available for site 2A. Image shows open water area and tidal channel (2016 image from Google Earth).*

#### *Historical Analysis*
The first satellite imagery reviewed for site 2A was10/18/2005. The initial measurement of the inlet revealed the width of the creek mouth was 10.40 m. Further measurements were taken on 3/02/2010, 10/29/2012 and 1/27/2015.

*Inlet Widths*

The final measurement indicates the inlet mouth had widened to 15.8 m (*Table 17*). The creek mouth eroded at an average rate of 0.61 m per year and experienced the greatest erosion between 2010 and 2012.

| Date | Width of Inlet (m) | Erosion Rates Inlet (m/yr) | Open Water Area (m²) | Erosion Rates Open Water Area (m2/yr) |
|---|---|---|---|---|
| 10/18/2005 | 11.10 | --- | 30660.00 | --- |
| 3/2/2010 | 12.40 | -0.29 | 29112.00 | 354.02 |
| 10/29/2012 | 14.40 | -0.75 | 27890.00 | 458.88 |
| 1/27/2015 | 15.80 | -0.62 | 28214.00 | -144.22 |

*Table 18. Inlet and open water area sizes and erosion rates for site 2A.*

*Interior Pond Area*

Site 2A is unique in this study because the open water area within the study area actually decreased during the time frame of analysis. The site shows an average decrease in open water area of 222.89 m²/ year and an inspection of the satellite imagery reveals that land was created within the interior pond. Along the southern shoreline of the pond, separating the open water area from Barataria Bay, there appears to have been a washover event that occurred between images from 2005 and 2010. The washover fan extends into the pond area creating new marsh platform. The progradation of the marsh platform into the open water area connected to the tidal creek at site 2A explains the decrease in open water area between 2005 and 2010, additionally, the same washover fan appears to prograde further between 2010 and 2012 (*Figure 44*). Open water area of the pond is once again increased from 2012 to 2015, indicating that the washover fan had not increased in size between these dates.
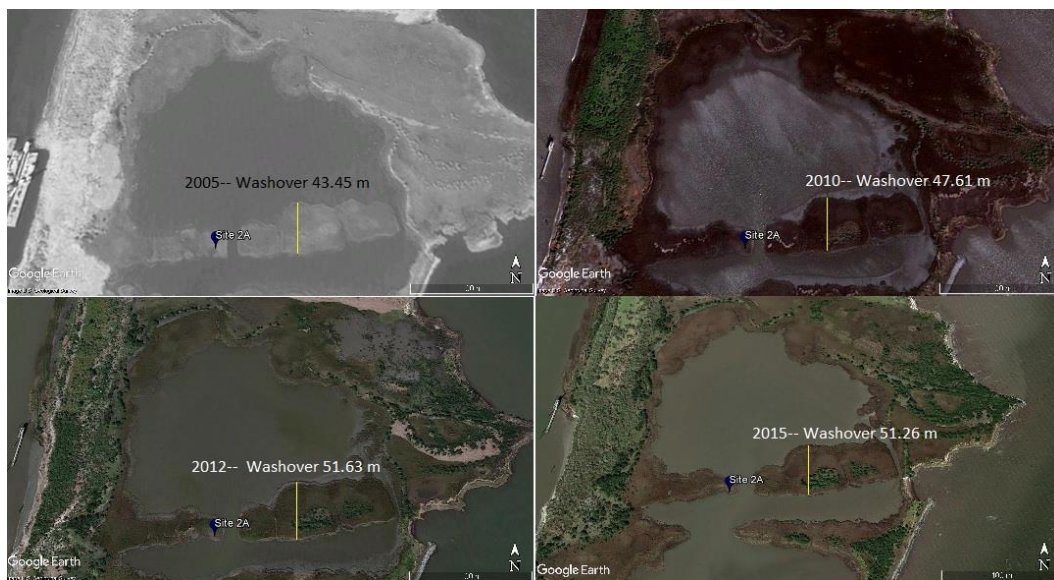


*Figure 44. Backfilling of the shoreline separating site 2A from open water resulted in a decrease of tidal prism from 2005 through 2012. The washover area decreased in size from 2012 to 2015 and open water area at the site also increased (2016 image from Google Earth).*

### Tidal Prism

The average tide range based on measurements from CRMS station 0178 is .36m. Using open water area multiplied by the average tide range reveals tidal prism values ranging from 11037.60 m$^3$ (2005) to 10480.32 (2010) (Table 5).

| Date | Tidal Prism (m$^3$) |
| --- | --- |
| 10/18/2005 | 11037.60 |
| 3/2/2010 | 10480.32 |
| 10/29/2012 | 10040.40 |
| 1/27/2015 | 10157.04 |

*Table 19. Tidal prism calculation for site 2A. Calculations were based on tide range data from CRMS station 0178.*

### Fetch Measurements

Beginning from the center of the creek mouth fetch measurements were taken to the closest land mass that would disrupt wave action (*Figure 45*). This site has an average fetch distance of 123.48 m and has the longest stretch of open water to the SSW at 313 m.
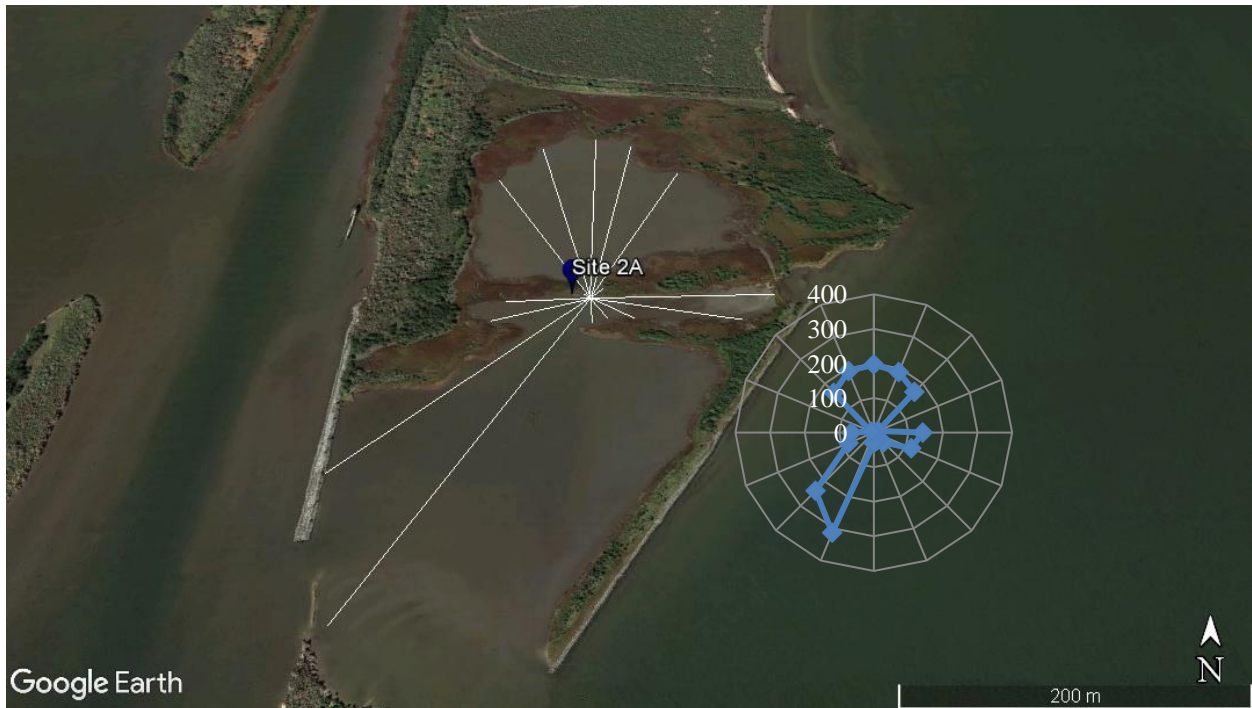


*Figure 45. This image depicts Fetch distances and directions as they relate to the mouth of the inlet located at site 2A. Distance (in meters) from the center of the inlet mouth to the nearest shoreline is depicted as the blue line in the inset graph. The largest fetch distance is to the SSW (2016 image from Google Earth).*

*Site 3A*

Site 3 is located in an island complex situated between Bay Long and Lake Grand Ecaille at N 29.3515° W 89.8171° (*Figure 46*). The site is 3.5 km NW of Quatre Bayou Pass, an inlet that connects Barataria Bay to the Gulf of Mexico. The site is protected by marsh platform on all sides and is most unprotected to the SW with a fetch distance of 158 m. This creek is serviced by a natural bayou that connects an oil and gas pipeline canal to a section of broken marsh/pond areas. The channel meanders approximately 30 m until it enters the open water area.



*Figure 46. Location and latest image available for site 3A. Image shows open water area and tidal channel (2016 image from Google Earth).*

*Historical Analysis*

The first historical imagery used to analyze site 3A is from September of 2008. Additional images were measured from 2010, 2012 and 2015 (*Table 19*).

*Inlet Width*

Initial measurements (2008) show the inlet to be 6.9 m wide. This site had the largest rates of erosion for inlet width between 2008 and 2010. The average rate of erosion through the study period (2008-2015) was -.22 m/yr. Analyzing satellite imagery reveals that erosion to this inlet mouth occurred most along the eastern shoreline. This shoreline retreated and the structure of the point along the eastern edge of the inlet changed through time to become more rounded. Conversely, the shoreline along the western edge of the inlet mouth comes to a point that has remained unchanged through time.

*Open Water Area*

Initial measurements reveal an interior pond open water area of 1449 m². Changes occurred at an average of -15.17 m²/yr of erosion (*Table 19*). While the average through the

78

study period indicates the open water area increased, there was actually very little change between the imagery measurements (< 6 % change). This is the least amount of change in open water area to any site being studied.

| Date | Width of Inlet (m) | Erosion Rates Inlet (m/yr) | Open Water Area (m²) | Erosion Rates Open Water Area (m²/yr) |
|---|---|---|---|---|
| 9/4/2008 | 6.9 | --- | 1449 | --- |
| 7/28/2010 | 7.8 | -0.47 | 1558 | -57.49 |
| 10/29/2012 | 8.1 | -0.13 | 1543 | 6.64 |
| 1/27/2015 | 8.2 | -0.04 | 1531 | 5.34 |

*Table 20. Inlet and open water area sizes and erosion rates for site 3A.*

### Tidal Prism

Tidal prism values were calculated based on average tide range from CRMS site 0178. Open water area multiplied by the average tide range of .36 m results in tidal prism figures listed in *Table 20*.

| Date | Tidal Prism (m³) |
|---|---|
| 9/4/2008 | 436.31 |
| 7/28/2010 | 455.232 |
| 10/29/2012 | 462.67 |
| 1/27/2015 | 490.51 |

*Table 21. Tidal prism calculation for site 3A. Calculations were based on tide range data from CRMS station 0178.*

## Fetch Measurements

Site 3A is protected on most sides from open water. The longest fetch distance is to the west-southwest at 104 m. The average fetch for the mouth of the inlet is 28.52 m (*Figure 47*).
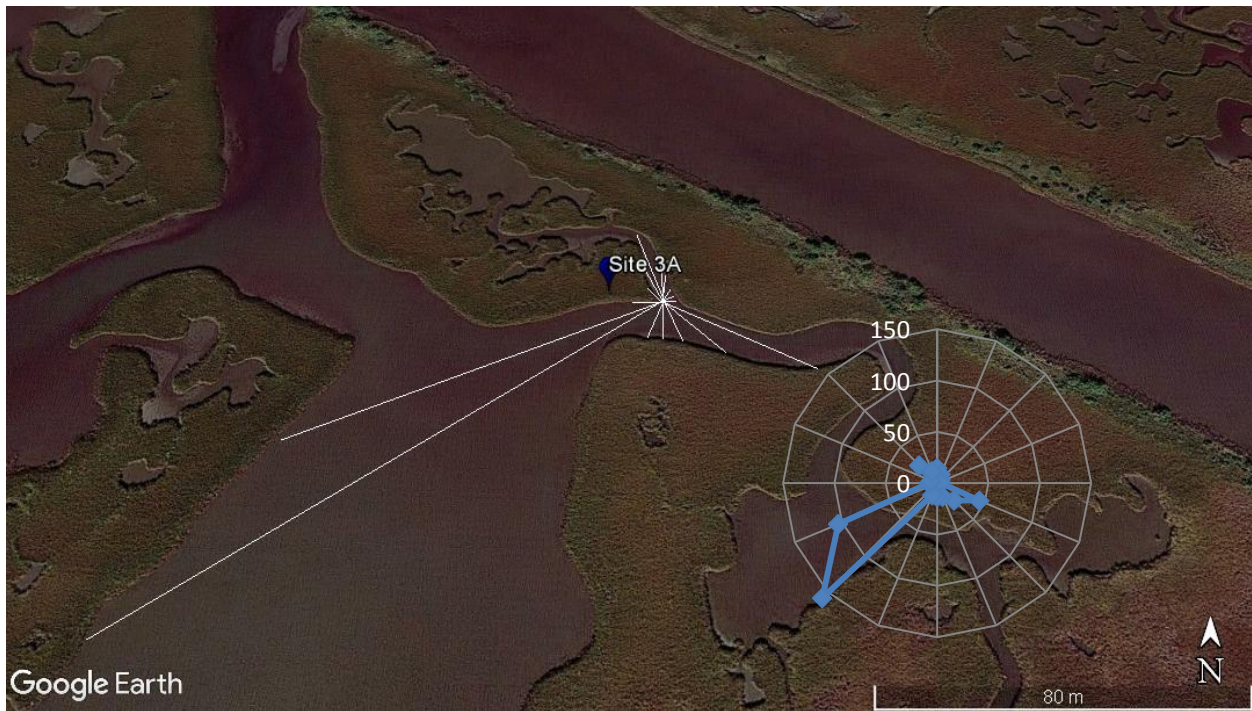


*Figure 47. This image depicts fetch distances and directions as they relate to the creek mouth at site 3A (2016 image from Google Earth).*

## Site 2B

Located 3.5 km west southwest from site 1B at N 29.5042˚ W 89.9496˚, site 2B is situated on Wilkinson Canal (*Figure 48*). The canal is a manmade waterway that connects Northern Barataria Bay and the town of Myrtle Grove, Louisiana. The tidal creek at the site services an open water pond area of 207,839 m$^2$. The greatest fetch distance at 2B is to the NNW with a fetch distance of 487 m. In addition to wind generated waves, the creek mouth at site 2B is undoubtedly impacted by boat generated wakes. During field work researchers observed 3 commercial fishing boats and 2 recreational boats using Wilkinson Canal. An *YSI* pressure sensor was deployed at this site 35 m SE of the mouth of the creek to collect tide range data. ADCP instrumentation was also used to calculate the cross sectional area of this creek mouth. The open water area behind the channel is a narrow (<150 m) series of pond structures connected by a shallow (< 1 meter) channel.

*Figure 48. Site 2B and the location of YSI deployment. The YSI instrumentation was positioned in the thalweg of the inlet mouth (2016 image from Google Earth).*

### Historical Analysis

#### Inlet Width

The earliest satellite imagery reviewed for site 2B was 10/18/2005 during this time the width of the creek mouth measured 40.1 m. Additional measurements were taken on 10/11/2007, 10/29/2012 and 1/27/2015. The latest image date measurement indicated the inlet mouth had widened to 46.8 m (*Table 21*). Site 2B eroded between each image date with the highest erosion occurring between 2012 and 2015. The inlet mouth opens to the north and is flanked to the east and west by pointed shorelines. The erosion to the inlet mouth has occurred through the retreat of these points.

#### Interior Pond Area

The open water pond area behind the inlet at site 2B is meandering series of oblong open water structures. Conversion of land to open water has occurred between each image researched. The largest rate of erosion occurred between 2012 and 2015. The open water area at this site increased due to widespread shoreline retreat.

| Date | Width of Inlet (m) | Erosion Rates Inlet (m/yr) | Open Water Area (m2) | Erosion Rates Open Water Area (m²/yr) |
|---|---|---|---|---|
| 10/18/2005 | 30.8 | --- | 199329 | --- |
| 10/11/2007 | 31.4 | -0.30 | 200150 | -414.47 |

| 10/29/2012 | 31.7 | -0.06 | 204826 | -925.06 |
| 1/27/2015 | 34.1 | -1.07 | 207839 | -1341.15 |

*Table 22. Inlet and open water area sizes and erosion rates for site 2B.*

### Tidal Prism

Tidal prism for site 2B was calculated based on data acquired during YSI pressure sensor deployment. Based on tide range averages during the deployment it is known that tide range at this site was .28 m. Multiplying this tide range value by historical open water measurements reveals tidal prism ranging from 63, 185.70 to 65,883.30 $m^3$ (*Table 22*).

| Date | Tidal Prism ($m^3$) |
|---|---|
| 10/18/2005 | 63185.70 |
| 10/11/2007 | 63445.95 |
| 10/29/2012 | 64928.20 |
| 1/27/2015 | 65883.30 |

*Table 23. Tidal prism calculation for site 2B. Calculations were based on tide range data from YSI sensor 'Starsky'.*

### Fetch Measurements

Site 2B is situated on a main canal connecting Myrtle Grove Marina to Northern Barataria Bay. Boat wakes and human activity may also play a role in erosion rates for site 2B. Fetch distances are greatest to the west-northwest and the average fetch distance is 120.98 m.

*Figure 49. This image depicts Fetch distances and directions as they relate to the mouth of the inlet located at site 2B. Distance (in meters) from the center of the inlet mouth to the nearest shoreline is depicted as the blue line in the inset graph (2016 image from Google Earth).*

### Hydrology—ADCP

ADCP transects taken at site 2B highlighted the fact that this inlet maintains a consistent depth across the mouth and has an average depth of 1.07 m. The cross sectional area of the inlet mouth averaged to 36.41 m (*Table 23*).

| Transect # | 003 | 004 |
|---|---|---|
| Q (m³/s) | 3.60 | 3.26 |
| Average Depth (m) | 1.08 | 1.06 |
| Transect Length (m) | 26.03 | 27.96 |
| Cross Sectional Area (m²) | 36.79 | 36.02 |
| Avg. Cross Sectional Area (m²) | 36.41 | |

*Table 24. This table includes data from ADCP transects run at site 2B. Cross sectional area and averages were also calculated.*

### Hydrology—YSI and RBR

YSI deployment from August 23, 2016 until September 12, 2016 provided necessary data to calculate an average tide range for this site. The average of the spring tide cycles during the deployment time was .28 m (*Figure 50*).
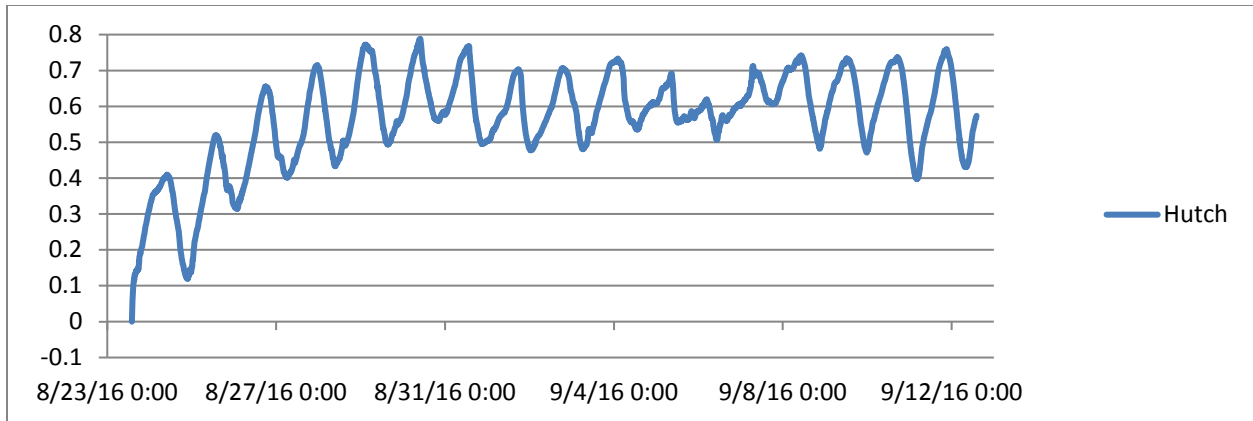
*Figure 50. YSI 'Hutch' data from 8/23/2016 through 9/12/201. Y-axis is tide range (m) x-axis is the date and time.*

### Site 3B

Site 3B is located 1.6 km SW from site 2B at N 29.4944°W 89.9615°and is situated in the bend of a natural bayou. The tide creek connects this bayou to a 12,596 $m^2$ open water pond structure (*Figure 51*). The site lies approximately 26 km north of Barataria Pass. The mouth of the tidal creek is protected on all side from open water with the greatest fetch distances being 450 m to the NE. ADCP transects were taken at this location to calculate the cross sectional area of the channel mouth. Also of note, the latest satellite imagery makes the mouth of the channel appear to stretch from a point to the west of the inlet to an area east of the inlet along the shoreline of the natural bayou. Upon inspection during field work that area had eroded; thus, inlet width dimension and ADCP transects were taken from inside the channel mouth (*Figure 52*).



84
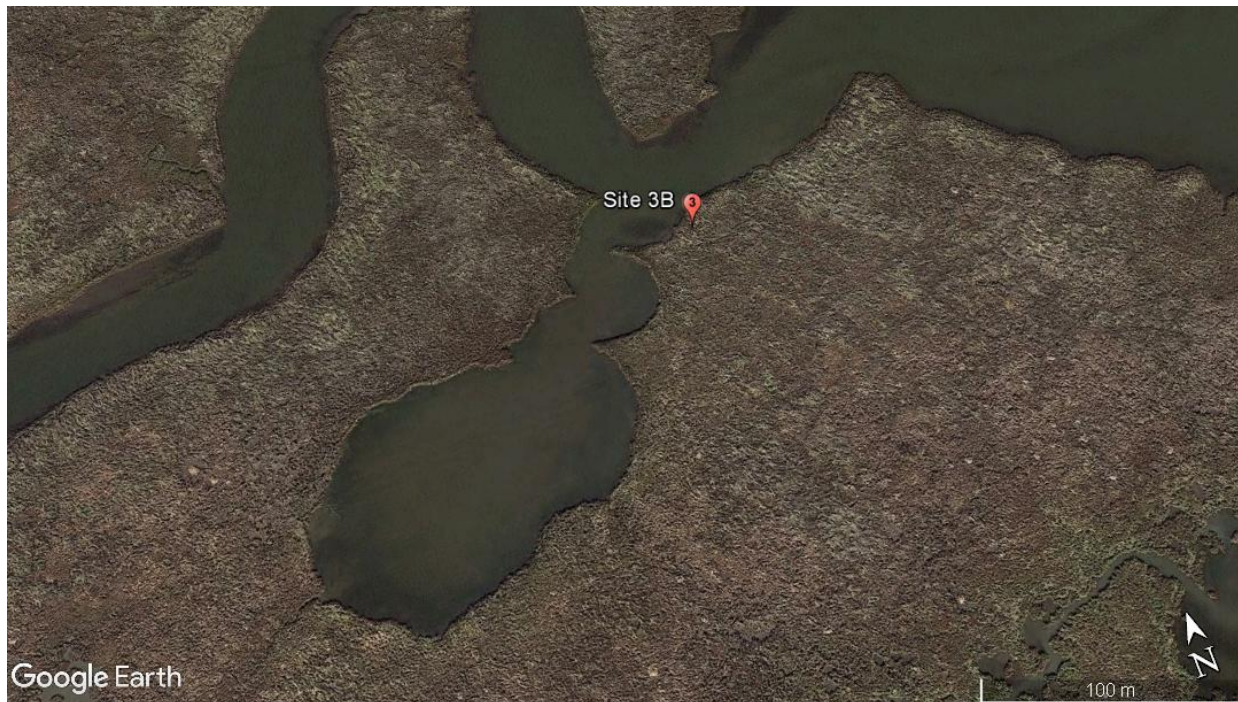
*Figure 51 Location and latest image available for site 3B. Image shows open water area and tidal channel (2016 image from Google Earth).*



*Figure 52. Image of changes made to historical evolution of the channel inlet at site 3B after field work revealed the erosion of landmarks used for original historical evolution measurements (2016 image from Google Earth).*

### Historical Analysis

#### Inlet Width
The earliest satellite imagery reviewed for site 3B was 10/18/2005 during this time measurement of the inlet revealed the width of the creek mouth was 22.3 m. Further measurements were taken on 7/28//2010, 10/29/2012 and 1/27/2015. The final measurement indicates the inlet mouth had widened to 10.5 m (*Table 24*). Site 3B continued to erode between image analysis dates, however, the rate of erosion decreased through time.

#### Interior Pond Area
Erosion rates for the interior pond area followed a similar pattern to the inlet width rates for the time period between 2005 and 2012. The open water area increased at the highest rates between 2005 and 2010 then the rate slowed from 2010 to 2012 (similar to slowing rates at the inlet mouth). The open water area rates of erosion increased from 2012 to 2015, whereas rates continued to decrease at the inlet (*Table 24*).

| Date | Width of Inlet (m) | Erosion Rates Inlet (m/yr) | Open Water Area (m2) | Erosion Rates Open Water Area (m2/yr) |
|---|---|---|---|---|

| 10/18/05 | 22.3 | --- | 11891 | --- |
| 7/28/10 | 24.2 | -0.40 | 12371 | -100.45 |
| 10/29/12 | 24.7 | -0.22 | 12473 | -45.18 |
| 1/27/15 | 25 | -0.13 | 12596 | -54.75 |

*Table 25. Inlet and open water area sizes and erosion rates for site 3B.*

### Tidal Prism

The tide range average from YSI sensor 'Hutch' was used to calculate tide prism at site 3B. Open water area multiplied by the average tide range of .28 m results in tidal prism values ranging from 3769.35 m$^3$ (2005) to 3992.83 m$^3$ (2015) (*Table 25*).

| Date | Tidal Prism |
|---|---|
| 10/18/05 | 3769.35 |
| 7/28/10 | 3921.51 |
| 10/29/12 | 3953.84 |
| 1/27/15 | 3992.83 |

*Table 26. Tidal prism calculation for site 3B. Calculations were based on tide range data from YSI sensor 'Hutch'.*

### Fetch Measurements

Site 3B had the largest fetch distance to east-northeast at 451 m and southwest at 211 m. Average fetch distance is 85.32 m (*Figure 53. This image depicts fetch distances and directions as they relate to the mouth of the inlet located at site 3BFigure 53*).
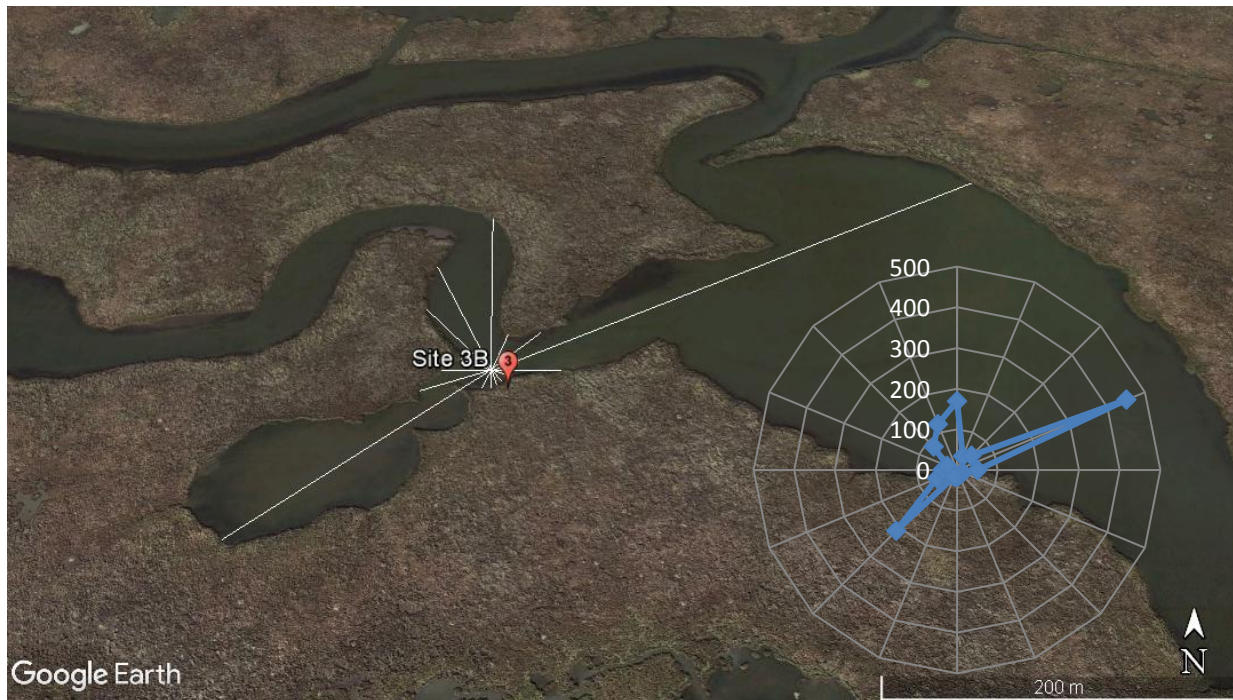
86

*Figure 53. This image depicts fetch distances and directions as they relate to the mouth of the inlet located at site 3B. Distance (in meters) from the center of the inlet mouth to the nearest shoreline is depicted as the blue line in the inset graph (2016 image from Google Earth).*

### ADCP

ADCP transects taken at site 3B ranged from 22.63 m to 24.74 m. The historical analysis inlet width measurements had to be adjusted after physical inspection of site 3B due to erosion along the shoreline to the east of the creek mouth.

| Transect # | 000 | 001 | 002 |
|---|---|---|---|
| Q (m$^3$/s) | 0.25 | 0.49 | 0.385 |
| Average Depth (m) | 0.76 | 0.86 | 0.86 |
| Transect Length (m) | 24.74 | 24.24 | 22.63 |
| Cross Sectional Area (m$^2$) | 19.10 | 21.61 | 21.381 |
| Avg. Cross Sectional Area (m$^2$) | 20.70 | | |

*Table 27. ADCP transect data from site 3B. Transect length was adjusted from historical measurements due to erosion of inlet mouth since 2015 imagery.*

### Site 4B

Site 4B is approximately 10 km SE from site 3B and 50 m west of Bay Batiste on the northern shoreline of Barataria Bay at N 29.4534˚W 89.8715˚(*Figure 54*). This site has the largest open water area of sites within zone 'B' at 678,095 m$^2$. A short (70 m), wide inlet (450 m) connects the open water area of site 4B to Bay Jimmy. This inlet is unprotected, particularly

to the South where it has fetch distances of 14 km. This site is the closest site to coastal inlets in zone 'B'. No ADCP or tide range data was acquired at this location.



*Figure 54. Location and latest image available for site 4B. Image shows open water area and tidal channel (2016 image from Google Earth).*
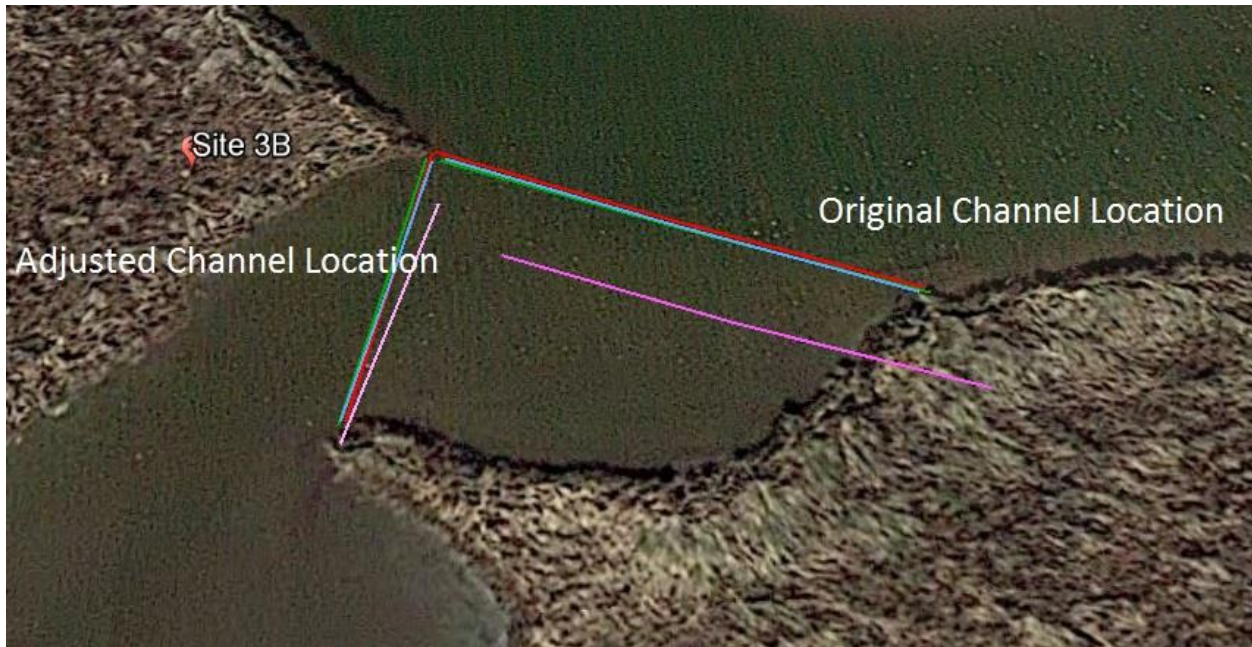
### *Historical Analysis*

#### *Inlet Width*

The earliest satellite imagery measured for site 4B was 10/18/2005 and the latest was 1/27/2015 during this time measurements of the inlet ranged from 425 m to 450 m. The inlet mouth at 4B opens to the Southwest and is flanked by shoreline points to the east and west (*Figure 54*). Erosion to the inlet mouth occurred at both the eastern and western shorelines of the inlet.

#### *Interior Pond Area*

Open water area during this time increased from 665, 814 m$^2$ to 678,095 m$^2$. The measurement of each inlet width can be seen in *Table 27*. Site 4B is distinct from other sites in this study by its large size and fetch. Expansion of the open water area at 4B occurred primarily due to retreat of shorelines surrounding the open water area at the site.

| Date | Width of Inlet (m) | Erosion Rates Inlet (m/yr) | Open Water Area (m$^2$) | Open Water (m$^2$/yr) |
|---|---|---|---|---|
| 5/20/2006 | 425 | --- | 665814 | --- |
| 12/30/2010 | 435 | -2.17 | 669233 | -740.614 |
| 10/29/2012 | 437.5 | -1.36 | 671967 | -1491.64 |

| 1/27/2015 | 450 | -5.56 | 678095 | -2727.71 |

*Table 28. Inlet and open water area sizes and erosion rates for site 4B.*

### Tidal Prism

The average tide range during the time being studied at the closest CRMS data site (CRMS 0178) is .36 m. Using open water area multiplied by the average tide range reveals tidal prism values ranging from 246297.91 m$^3$ (2005) to 250840.90 m $^3$ (2015) ( *Table 28*).

| Date | Tidal Prism (m$^3$) |
|---|---|
| 5/20/2006 | 246297.91 |
| 12/30/2010 | 247562.67 |
| 10/29/2012 | 248574.03 |
| 1/27/2015 | 250840.90 |

*Table 29. Site 4B tidal prism calculations used average tide range from CRMS site 0178.*

### Fetch Measurements

Site 4B has the greatest fetch distances from any site in this study. The largest fetch is to the south –southwest to the southeast and there is an average fetch of 4,317.50 m.



*Figure 55. This image depicts Fetch distances and directions as they relate to the mouth of the inlet located at site 4B. Distance (in meters) from the center of the inlet mouth to the nearest shoreline is depicted as the blue line in the inset graph (2016 image from Google Earth).*

*Site 5B*

Site 5B is located approximately 8 km WSW of site 3B and due north of Bayou Dosgris at N 29.4781˚ W 90.0438˚ (*Figure 56*). The channel mouth lies approximately 25 km NNW of Barataria Pass. This site is the furthest western site in zone 'B'. The channel located at site 5B connects a natural bayou (Bayou Dosgris) to an open water pond area of 29,407 m². The inlet is protected from all direction except to the W where it has a fetch distance of 1.8 km.
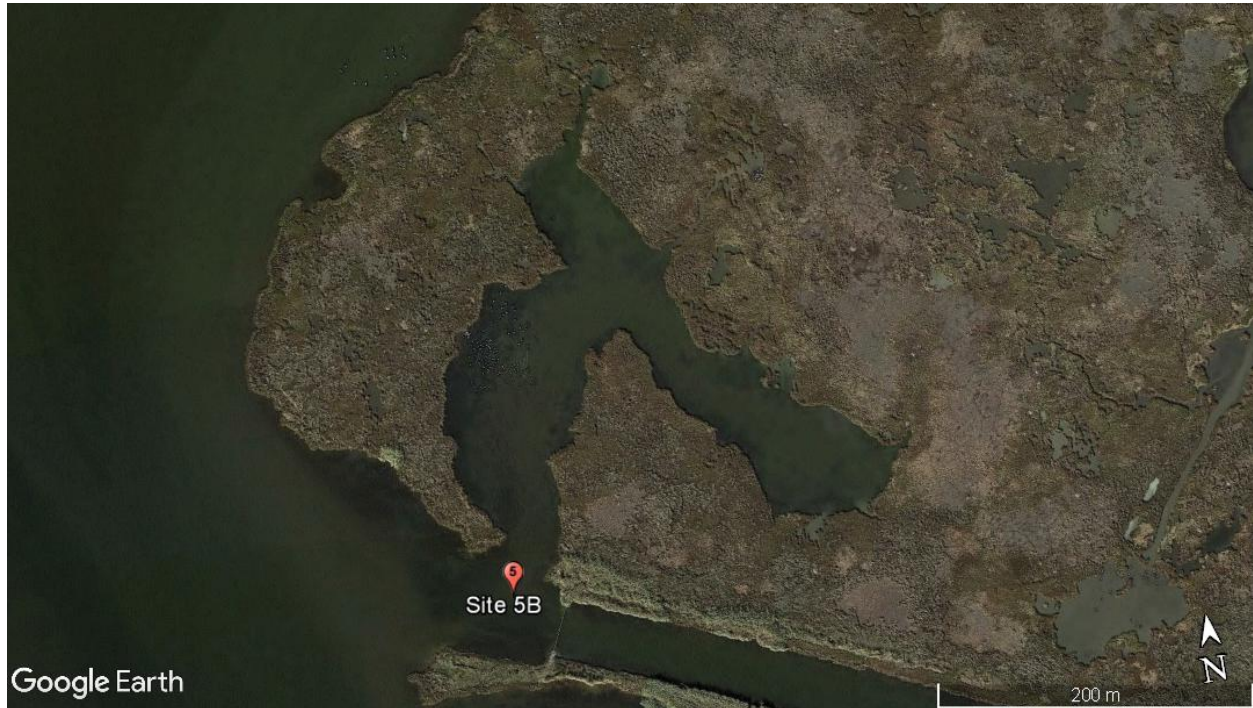


*Figure 56. Location and latest image available for site 5B. Image shows open water area and tidal channel (2016 image from Google Earth).*

*Historical Analysis*

*Inlet Width*

The width of the inlet at 5B widened between each satellite image measured. The largest rates of erosion at the mouth of the inlet occurred between 2012 and 2015, while the largest erosion rates for the open water area occurred between 2005 and 2010 (*Table 29*). This inlet face to the south and is exposed to open water in that direction. The widening of this inlet occurred as a result of erosion to the eastern point of the inlet mouth.

*Interior Pond Area*

The open water area of this site increased between each image date. The historical analysis revealed that conversion of land to open water at this site was a result of shoreline retreat. While there was erosion along most shorelines surrounding this pond, comparing image measurements indicates that the northern shoreline underwent the largest amount of erosion.

90

| Date | Width of Inlet (m) | Erosion Rates Inlet (m/yr) | Open Water Area (m2) | Erosion Rates Open Water Area (m²/yr) |
|---|---|---|---|---|
| 10/18/2005 | 35.4 | --- | 27097 | --- |
| 7/28/2010 | 35.7 | -0.06 | 28553 | -304.72 |
| 10/29/2012 | 36.3 | -0.27 | 28855 | -133.77 |
| 1/27/2015 | 37.08 | -0.347 | 29407 | -245.70 |

*Table 30. Inlet and open water area sizes and erosion rates for site 5B.Dashes in this table indicate no rate was avaiable prior to the first image date.*

### Tidal Prism

The average tide range during the time being studied at the closest CRMS data site (CRMS 0178) is .36 m. Using open water area multiplied by the average tide range reveals tidal prism values ranging from 8589.53 m$^3$ (2005) to 9321.78 m$^3$ (2015) (*Table 30*)..

| Date | Tidal Prism (m$^3$) |
|---|---|
| 10/18/05 | 8589.53 |
| 7/28/10 | 9051.07 |
| 10/29/12 | 9146.80 |
| 1/27/15 | 9321.78 |

*Table 31. Tidal prism calculation for site 5B. Calculations were based on tide range data from CRMS station 0178.*

### Fetch Measurements

The inlet at site 5B is protected from all sides except the west and west-northwest. The largest fetch distance is to the WNW at 638 m and there is an average fetch of 135.6 m (*Figure 57*).
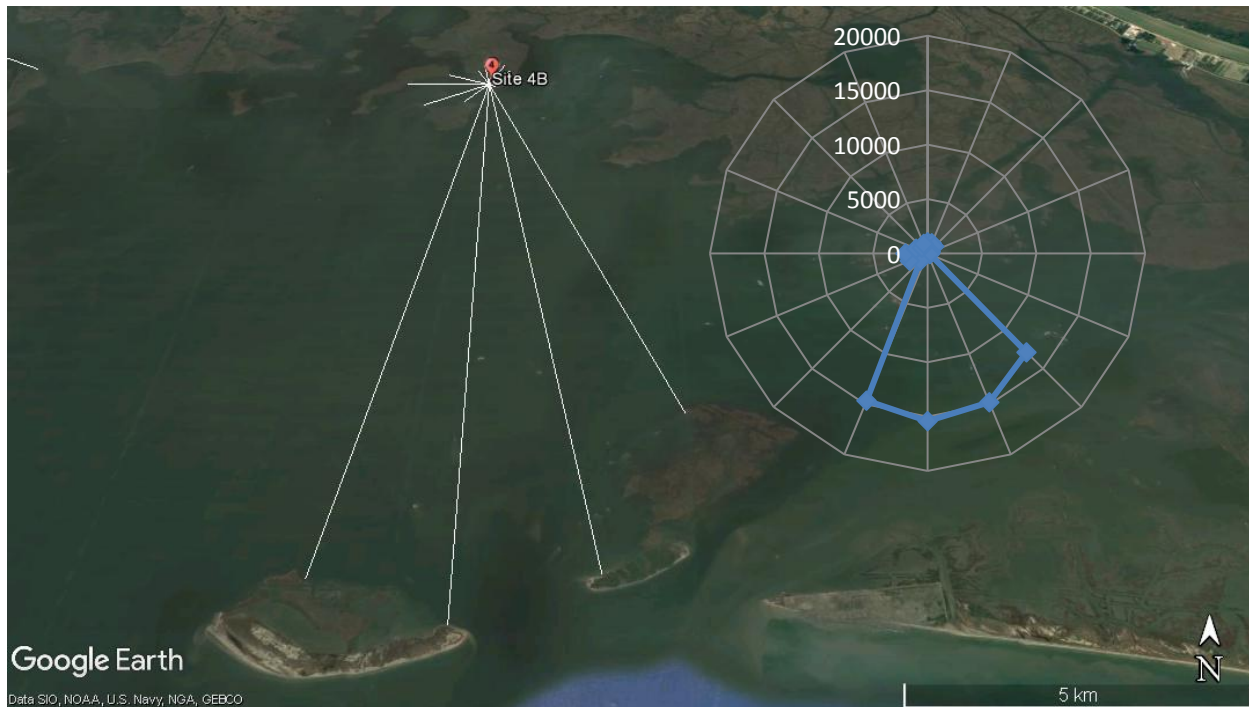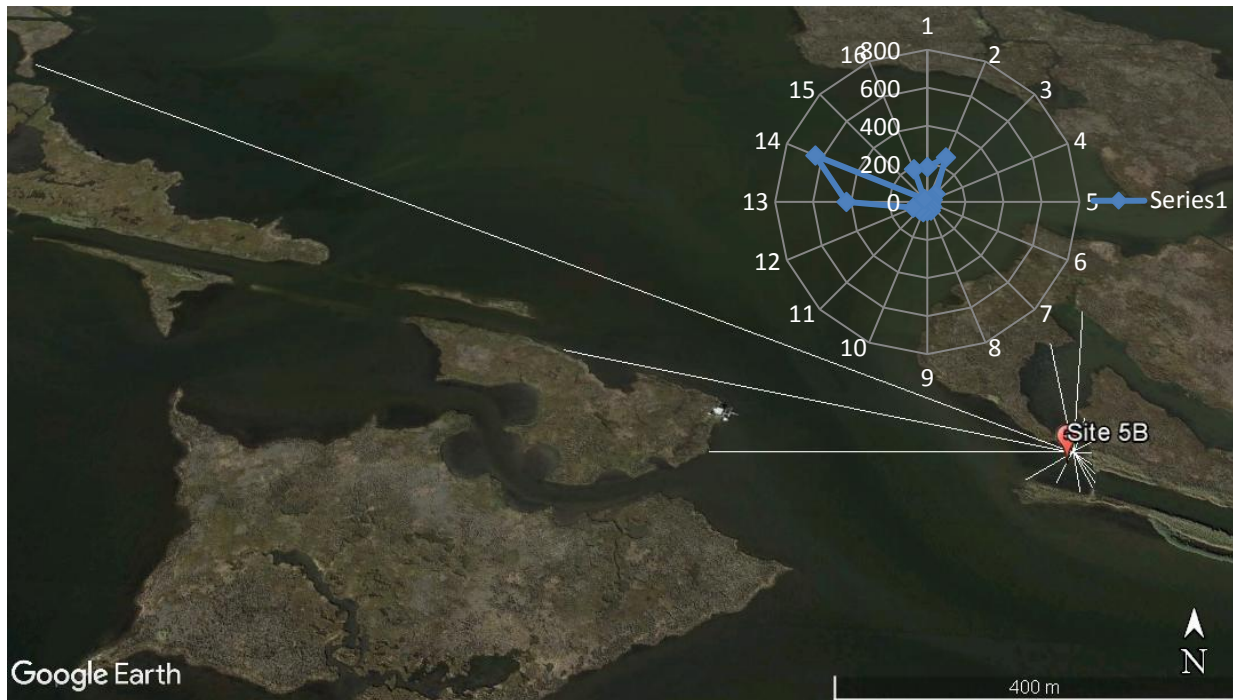
*Figure 57. This image depicts Fetch distances and directions as they relate to the mouth of the inlet located at site 5B (2016 image from Google Earth).*

### Site 6B

Site 6B is 1.5 km east of site 5B on the northwestern shoreline of Mud Lake at N 29.4772°W 90.0284°(*Figure 58*). This site is 25 km NNW of Barataria Pass. The open water pond area serviced by the channel at site 6B is the second largest in this study at 405,658 m$^2$. The site is unprotected from the SW to the ESE with the greatest fetch distance coming from the ESE at 3.9 km. There are two other inlets that feed into this system, both of which are on the northern reaches of the open water pond area.

*Figure 58. Location and latest image available for site 6B. Image shows open water area and tidal channel (2016 image from Google Earth).*

### Historical Analysis

The earliest image date used for historical analysis of site 6B was 10/18/2005. Erosion occurred between each image date at both the inlet mouth width and open water area.

### Inlet Width

The greatest erosion to the inlet width occurred between 2010 and 2012. This inlet faces open water to the southeast. Both the eastern and western points flanking this inlet underwent erosion that contributed to the widening of the inlet. As the flanking shorelines retreat wider portions of inlet were exposed.

### Interior Pond Area

The greatest rate of increase in open water area occurred from 2005 to 2010 (Table 31). Open water increases are attributed to shoreline erosion. The most noticeable changes to pond facing shorelines are along the western and northern shorelines.

| Date | Width of Inlet (m) | Erosion Rates Inlet (m/yr) | Open Water Area (m²) | Erosion Rates Open Water Area (m²/yr) |
|---|---|---|---|---|
| 10/18/2005 | 96.30 | --- | 395466.00 | --- |
| 7/28/2010 | 97.250 | -0.19 | 402384.00 | -1447.86 |
| 10/29/2012 | 99.70 | -1.08 | 403584.00 | -531.553 |
| 1/27/2015 | 101.90 | -0.97 | 405658.00 | -923.183 |

*Table 32. Inlet and open water area sizes and erosion rates for site 6B.*

*Tidal Prism*

The average tide range during the time being studied at the closest CRMS data site (CRMS 0178) is .36 m. Using open water area multiplied by the average tide range reveals tidal prism values ranging from 569.6 m$^3$ (2005) to 728.4 (2010) (Table 3). The fluctuation of tidal prism values follows a similar pattern as the creek mouth width. Tidal prism increases from 2005 to 2010 then decreases from 2012 to 2015.

| Date | Tidal Prism |
|---|---|
| 10/18/2005 | 125359.56 |
| 7/28/2010 | 127552.51 |
| 10/29/2012 | 127932.89 |
| 1/27/2015 | 128590.34 |

*Table 33. Tide prism values for site 6B using tide range values from CRMS site 0178.*

*Fetch Measurements*

Site 6B is unprotected from the southeast and east-southeast with fetch distance of 3166 m and 3943 m respectfully. The average fetch distance from the center of the inlet at site 6B is 802.28 m (*Figure 69*).

## Site 2C

Site 2C is approximately 5 km SW from site 1C adjacent to the western side of the Barataria Waterway at N 29.5331˚W 90.0384˚(*Figure 59*). The site is approximately 31 km from Barataria Pass. This site has an open water area of 2,674 m$^2$. The meandering tidal creek opens into a series of ponds approximately 75 meters from its mouth. The creek connects the ponds to a natural bayou. The site is protected on all sides with the greatest fetch distance occurring to the west at 500 m. No ADCP or tide range data was acquired at this location.
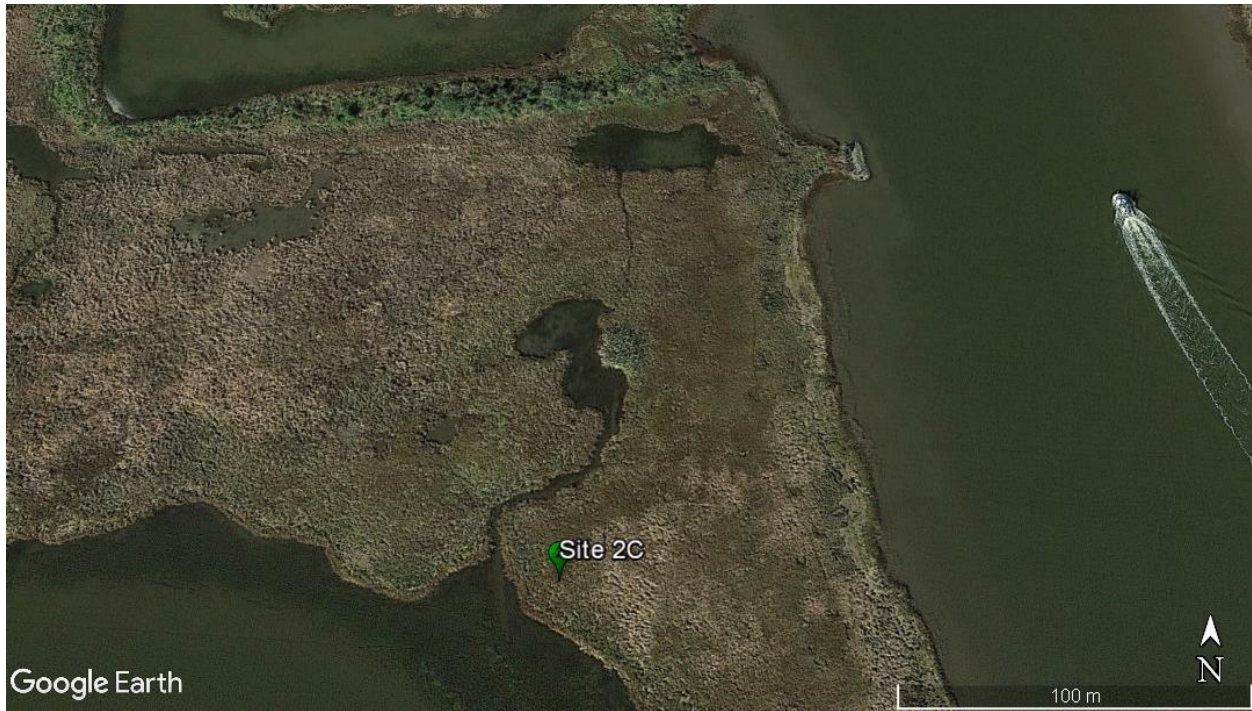
*Figure 59. Location and latest image available for site 2C. Image shows open water area and tidal channel (2016 image from Google Earth).*

### Historical Analysis

The earliest image measured for inlet width and open water area for site 2C was 10/18/2005. Subsequent measurements were taken from images in 2011, 2012 and 2015 (*Table 33*).

### Inlet Width

The mouth of the inlet at the site widened between each satellite image. The widening of the inlet mouth occurred at an average rate of -0.18 m/yr. The greatest rate of erosion occurred during the time between images in 2011 and 2012. This inlet is distinct to this study, in that, there is a wide entrance which narrows within 25 m of open water. Erosion to the inlet mouth occurred most to the eastern shoreline of the mouth.

### Interior Pond Area

The open water area, unlike the inlet mouth, did not erode between image dates. Measurements from satellite images in 2011, 2012 and 2015 indicate that the open water area of the site actually diminished between the image dates (*Table 33*). The interior pond at site 2C consist of two distinct areas that are connected by a thin (<5 m), straight channel. Through time this channel has narrowed, contributing to open water increases. In addition, shorelines in the northern portion of the pond, prograded, therefore, decreased open water area.

| Date | Width of Inlet (m) | Erosion Rates Inlet (m/yr) | Open Water Area (m²) | Erosion Rates Open Water Area (m²/yr) |
|---|---|---|---|---|
| 10/18/2005 | 30.6 | --- | 4023 | ---- |
| 4/15/2011 | 31.5 | -0.16 | 3596 | 77.73 |

| | | | | |
|---|---|---|---|---|
| 10/29/2012 | 31.8 | -0.19 | 3125 | 305.35 |
| 1/27/2015 | 32.2 | -0.18 | 2674 | 200.75 |

*Table 34. Inlet and open water area sizes and erosion rates for site 2C.*

### Tidal Prism

Tidal prism calculation for site 2C used tide range data from YSI 'Starsky' that was deployed at site 4C. Average tide range during deployment of SI sensors was .27 m (*Table 34*).

| Date | Tidal Prism |
|---|---|
| 10/18/2005 | 1086.21 |
| 4/15/2011 | 970.92 |
| 10/29/2012 | 843.75 |
| 1/27/2015 | 721.98 |

*Table 35. Tidal prism calculation for site 2C. Tide range data was used from YSI 'Starsky' that was deployed at site 4C.*

### Fetch Measurements

Site 2C is located along the bend of a natural bayou and is protected along most sides. The positioning of the inlet mouth in the bend of the bayou results in the greatest fetch distances coming from the west and south-southeast at 504 m and 313 m respectfully. The average fetch distance at this site is 108.42 m (*Figure 60*).
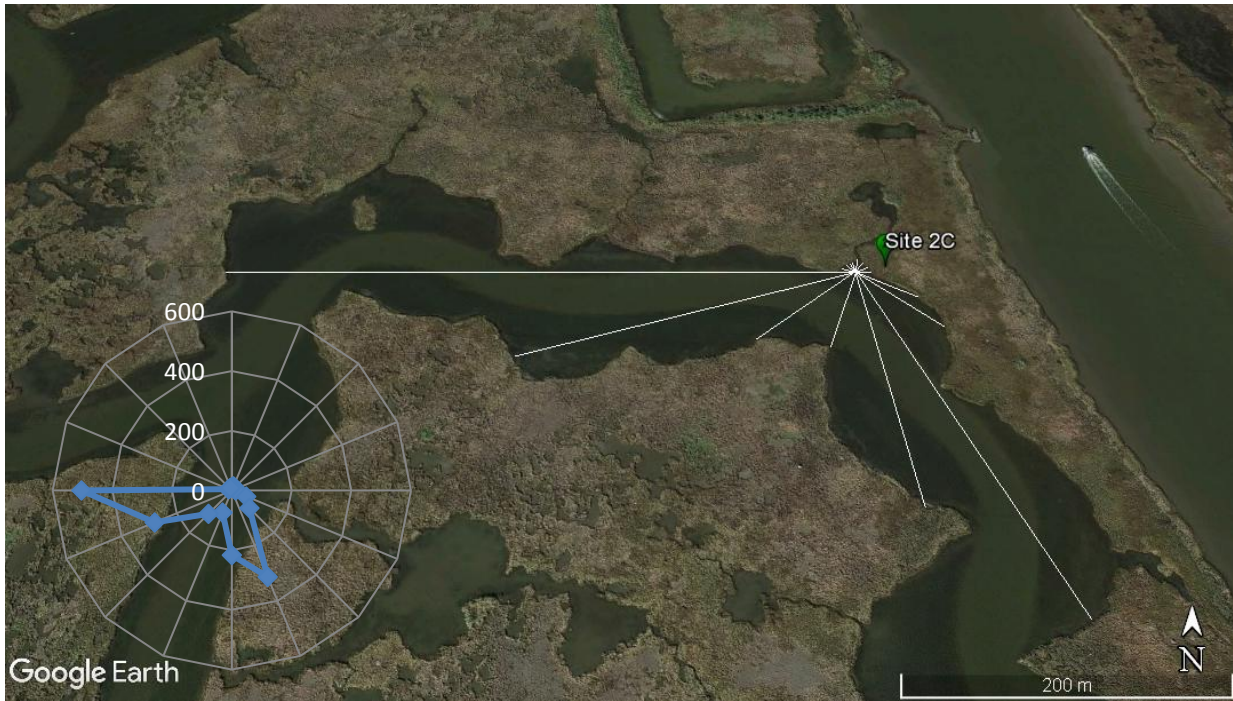
*Figure 60. This image depicts Fetch distances and directions as they relate to the mouth of the inlet located at site 2C. Distance (in meters) from the center of the inlet mouth to the nearest shoreline is depicted as the blue line in the inset graph (2016 image from Google Earth).*

### Site 3C

Site 3C is approximately 2.1 km NE from site 2C and 1 km from the eastern side of the Barataria Waterway at N 29.5510˚ W 90.0300˚ (*Figure 61*). This site has an open water area at 5,957m$^2$ and lies approximately 30 km to Barataria Pass. The tidal creek is 18 m long and connects a series of open water ponds and broken marsh to oil and gas pipelines that meander approximately 1 km to the Barataria Waterway. No ADCP or tide range data was acquired at this location.

*Figure 61. Location and latest image available for site 3C. Image shows open water area and tidal channel (2016 image from Google Earth).*

### Historical Analysis

Erosion occurred at both the inlet mouth and open water area located at site 3C. The greatest erosion occurred from 2005 to 2010 for both the inlet and open water area (*Table 35*).

### Inlet Width

The inlet at site 3C eroded through time. The greatest rates of erosion occurred between 2005 and 2010. When the satellite images from the chosen dates are reviewed, in can be seen that the shorelines flanking the inlet have eroded. The erosion of the inlet mouth continues through time and the inlet mouth migrates north as the shoreline flanking it retreats.

### Interior Pond Area

The open water area behind the inlet at site 3C is two distinct open water bodies attached by a meandering creek system. Expansion of the open water area at his site occurs as a result of shoreline retreat within the interior pond area. The most noticeable erosion took place along the northern shoreline the largest open water area.

| Date | Width of Inlet (m) | Erosion Rates Inlet (m/yr) | Open Water Area (m²) | Erosion Rates Open Water Area (m²/yr) |
|---|---|---|---|---|
| 10/18/2005 | 7.3 | --- | 5466 | --- |
| 3/13/2010 | 9.3 | -0.45 | 5788 | -73.13 |

| 10/29/2012 | 9.4 | -0.038 | 5895 | -40.64 |
| 1/27/2015 | 10.1 | -0.31 | 5957 | -27.60 |

*Table 36. Inlet and open water area sizes and erosion rates for site 3C.*


### Tidal Prism

Tide prism for site 3C was calculated using tide range data from YSI sensor 'Starsky'. The average spring tide range during the YSI deployment was .27 m. Multiplying open water area to .27 m results in tide prism ranging from 1472.82 m $^3$ to 1608.39 m$^3$ (*Table 36*).

| Date | Tidal Prism (m³) |
|---|---|
| 10/18/2005 | 1472.82 |
| 3/13/2010 | 1562.76 |
| 10/29/2012 | 1591.65 |
| 1/27/2015 | 1608.39 |

*Table 37. Tide prism values for site 3C. The averge tide range used was based on data collected from YSI sensor 'Starsky'.*


### Fetch Measurements

The inlet mouth at this site is located at the junction of a pipeline canal and a pond area. The straight pipeline to the west-southwest of the inlet mouth creates the greatest fetch distance at 502 m. The average fetch distance is 80.42 m (*Figure 62*).

*Figure 62. This image depicts Fetch distances and directions as they relate to the mouth of the inlet located at site 3C. Distance (in meters) from the center of the inlet mouth to the nearest shoreline is depicted as the blue line in the inset graph (2016 image from Google Earth).*

### Site 4C

Located approximately 5 km west from Wilkinson Canal and 1 km north of site 1C at N 29.5727 W 90.0080˚, site 4C can be found in the northwest corner of the open water area behind site 1C (*Figure 63*). This tidal creek services an open water area of 167763 m². 4C is protected from wave action in most directions, the greatest fetch distance of 190 m can be found to the WSW. The open water area behind the channel is a uniform pond structure with an alternative tide channel in the southeast corner. YSI instrumentation was deployed in the deepest portion of the channel to record tide range data.
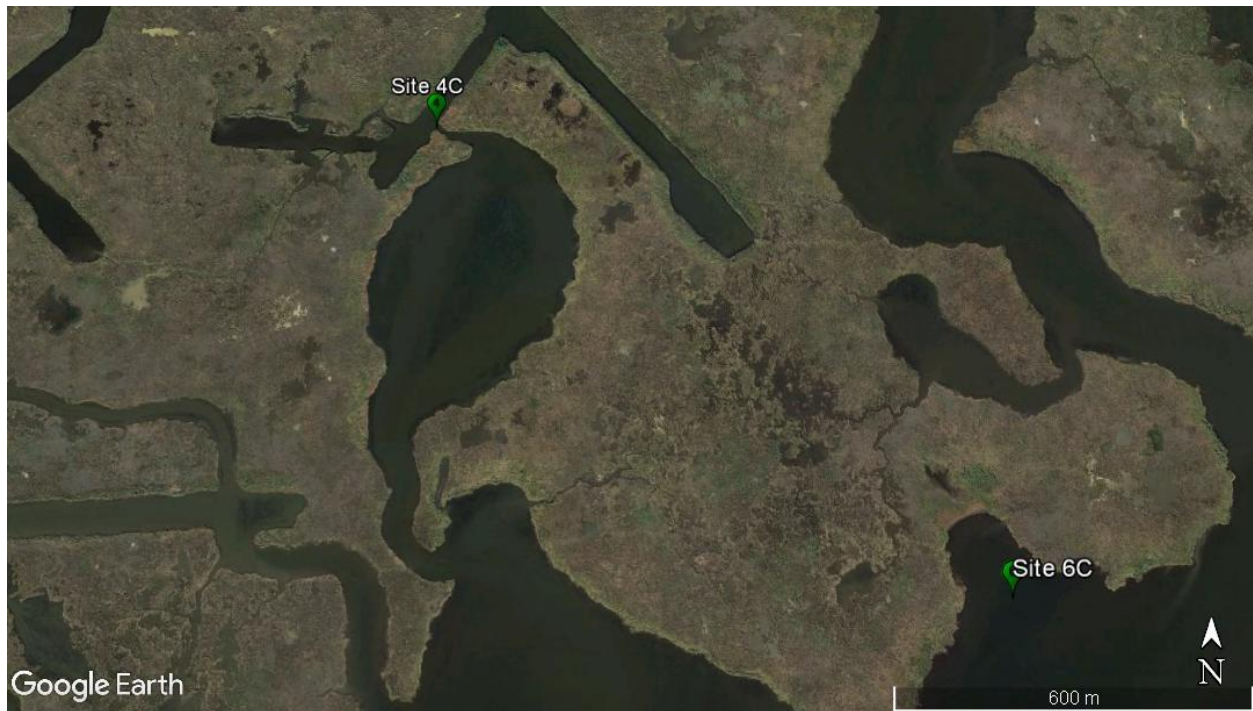
*Figure 63. Location and latest image available for site 4C. Image shows open water area and tidal channel (2016 image from Google Earth).*

### Historical Analysis

Site 4C was analyzed from images taken in 2005, 2010, 2012 and 2015. Both inlet width and open water area eroded through the study time period.

#### Inlet Width

The earliest image date for site 4C is 10/18/2005. The inlet had the greatest erosion from 2010 until 2012. Historical satellite imagery analysis revealed that this inlet was not identifiable on images prior to 2005.

#### Interior Pond Area

The open water area of site 4C also eroded between satellite image dates. The greatest erosion occurred from 2005 to 2010 (*Table 37*). This site shares interior pond area with site 1C and, therefore, underwent the same expansion of open water.

| Date | Width of Inlet (m) | Erosion Rates Inlet (m/yr) | Open Water Area (m2) | Erosion Rates Open Water Area (m²/yr) |
|---|---|---|---|---|
| 10/18/2005 | 0.95 | --- | 156956 | --- |
| 3/13/2010 | 1.17 | -0.05 | 166619 | -2194.77 |
| 10/29/2012 | 6.44 | -2.00 | 167220 | -228.26 |
| 1/27/2015 | 9.56 | -1.39 | 167763 | -241.70 |

*Table 38. Inlet and open water area sizes and erosion rates for site 2A.*

### Tidal Prism

The average tide range during the time being studied at YSI sensor 'Hutch' was  Using open water area multiplied by the average tide range reveals tidal prism values ranging from 49753.80 m$^3$ (2005) to 53179.53 m$^3$ (2015) (Table 34).

| Date | Tidal Prism |
|---|---|
| 10/18/2005 | 49753.80 |
| 3/13/2010 | 52816.89 |
| 10/29/2012 | 53007.40 |
| 1/27/2015 | 53179.53 |

*Table 39. Tide Prism data from site 4C.*

### Fetch Measurements
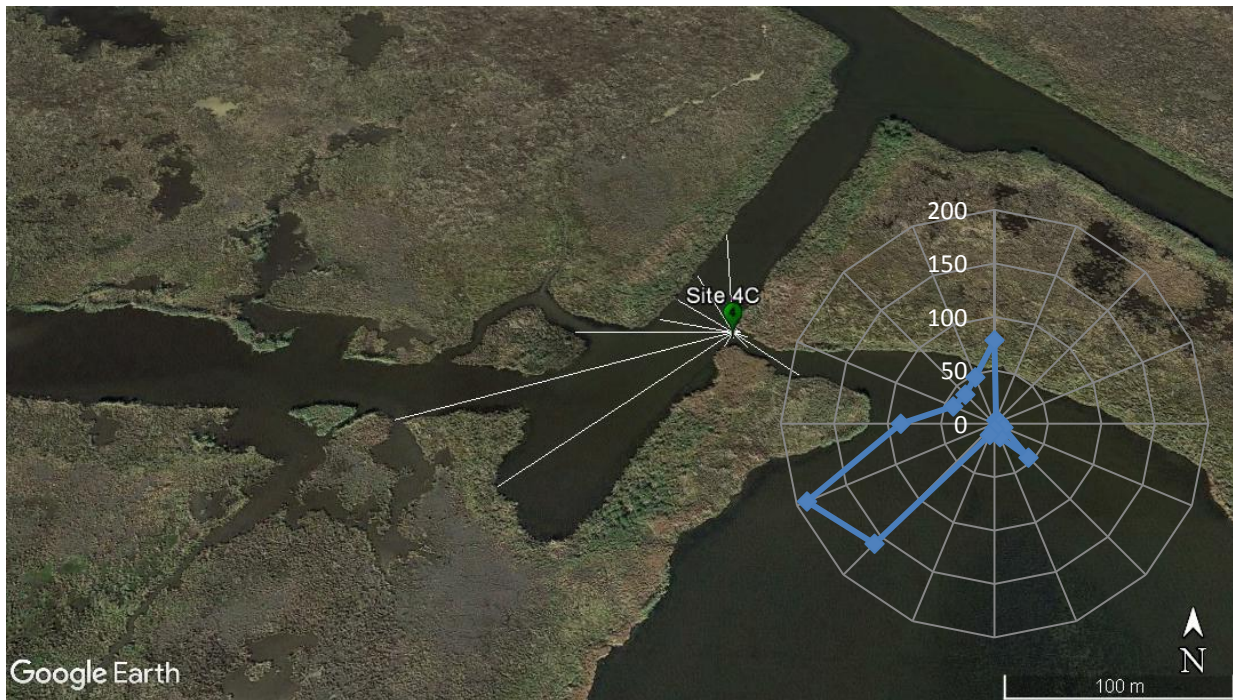


*Figure 64. This image depicts Fetch distances and directions as they relate to the mouth of the inlet located at site 4C. Distance (in meters) from the center of the inlet mouth to the nearest shoreline is depicted as the blue line in the inset graph (2016 image from Google Earth).*

### YSI and RBR

**Site 5C**

Located 5.4 km SE of site 1C and 1.1 km W of Wilkinson Canal at N 29.5327˚ W 89.9651˚ site 5C is the furthest south research site in zone 'C' (*Figure 65*). The site lies 29 km north of Barataria Pass. The channel entrance is protected from each direction from wave action

with the greatest fetch distances coming from WNW at 789 m. The open water area serviced by this channel is 33,934m$^2$. This meanders in a northerly direction for approximately 235 m before entering a series of pond structures. The channel connects these ponds to a natural bayou to the south. ADCP equipment was used to determine channel mouth depths and this data was used to calculate cross sectional area of the creek.



*Figure 65. Location and latest image available for site 5C. Image shows open water area and tidal channel (2016 image from Google Earth).*

### Historical Analysis
The earliest image date measured for site 5C was 10/18/2005. From 2005 until 2015 the inlet mouth widened at an average rate of .26 m/yr. Similarly, the open water area behind the inlet eroded between each measure image date.

### Inlet Width
The inlet at this site opens to the west into a natural bayou. The mouth of the inlet widened through time an average of -0.27 m/yr. The mouth of the inlet widened as a result of erosion that caused the migration of the mouth to the east. Field work at this location revealed a shallow (<.5m) entrance to the inlet.

### Interior Pond Area
The average erosion rate for this open water area was -515.03 m$^2$/yr and occurred between 2012 and 2015 (*Table 39*). Open water area increased at this location as a result of shoreline erosion throughout the pond area.

| Date | Width of Inlet (m) | Erosion Rates Inlet (m/yr) | Open Water Area (m²) | Erosion Rates Open Water Area (m²/yr) |
|---|---|---|---|---|
| 10/18/2005 | 11.7 | --- | 29547 | --- |
| 7/28/2010 | 13.2 | -0.31 | 31271 | -360.81 |
| 10/29/2012 | 13.8 | -0.27 | 31773 | -222.37 |
| 1/27/2015 | 14.3 | -0.22 | 33934 | -961.91 |

*Table 40. Inlet and open water area sizes and erosion rates for site 5C.*

### Tidal Prism

The average tide range during the time being studied at the RBR sensor at site 1C is .22m. Using open water area multiplied by the average tide range reveals tidal prism values ranging from 7091.28 m³ (2005) to 8144.16 m³ (2015) (*Table 40*).

| Date | Tidal Prism (m³) |
|---|---|
| 10/18/2005 | 7091.28 |
| 7/28/2010 | 7505.04 |
| 10/29/2012 | 7625.52 |
| 1/27/2015 | 8144.16 |

*Table 41. Tide prism calculations from site 5C.*

### Fetch Measurements

Site 5C is located at the bend of a natural bayou that provides protection from open water at all sides. The longest fetch distance is to the northwest at 789 m. and the average fetch distance is 118.21 m.
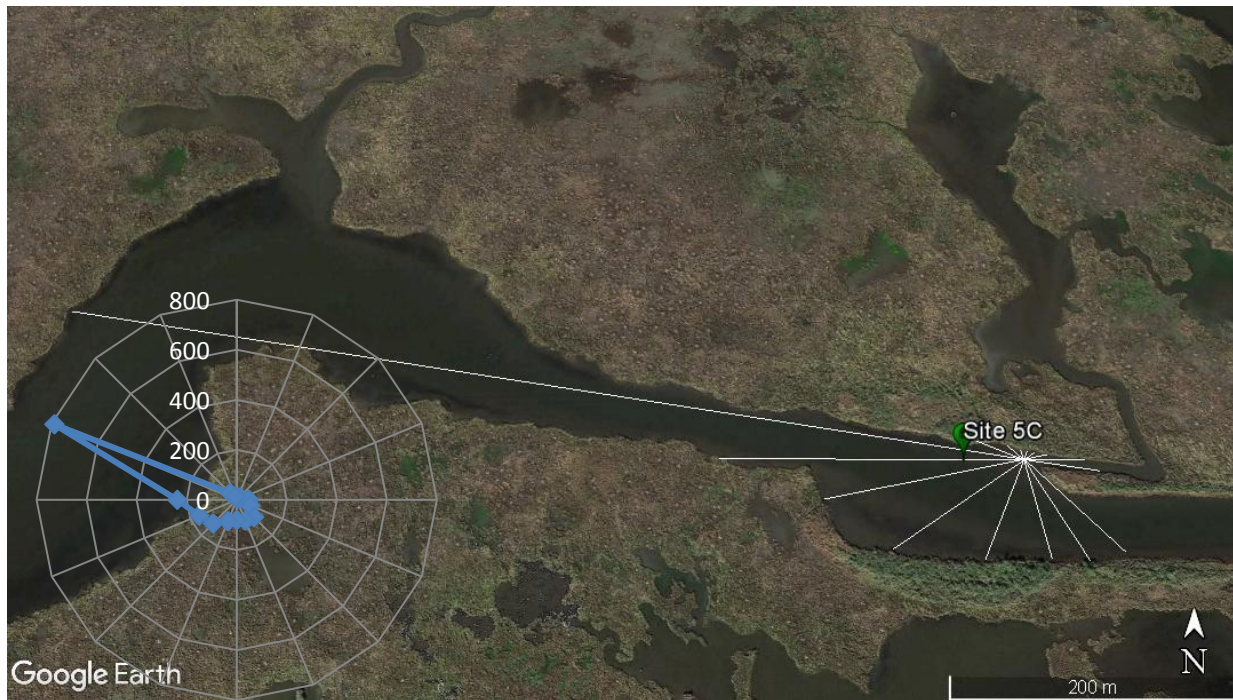
*Figure 66. This image depicts Fetch distances and directions as they relate to the mouth of the inlet located at site 5C (2016 image from Google Earth).*

### Hydrology—ADCP

Two transects were measured at site 5C. The average depth for both measurements was .68 m and the average length of the inlet mouth was 43.52 m (*Table 41*). The inlet mouth location was adjusted for the purpose of taking these transects. Shallow water limited the boats ability to access the inlet mouth location measured from satellite imagery.

| Transect # | 000 | 001 |
|---|---|---|
| Average Depth (m) | 0.74 | 0.62 |
| Transect Length (m) | 39.78 | 47.25 |
| Actual Cross Sectional Area (m2) | 29.29 | 29.10 |

*Table 42. ADCP transects from site 5C.*

### Site 6C

Site 6C is approximately 5 km NE from site 5C on the northern shoreline of Bay Round at N 29.5647°W 89.9976° (*Figure 67*). This site lies approximately 35 km from Barataria Pass. The connection of the open water area behind site 6C to Bay Round did not occur until 2009. This research will evaluate the historical evolution of the channel as it transforms from a small opening/channel to the opening that can be seen today. The open water area behind the inlet is 19,898 $m^2$. This inlet is unprotected, particularly to the south where it has fetch distances of over 3.2 km. ADCP data was acquired at this site and was used to calculate the cross sectional area of the inlet.

*Figure 67. Location and latest image available for site 6C. Image shows open water area and tidal channel (2016 image from Google Earth).*

### Historical Analysis

Site 6C is unique to this research because the inlet did not show up in satellite imagery prior to 2010. The historical analysis of satellite imagery measures the creation of the inlet and the effects on the open water area of the site. The greatest erosion to the inlet and the open water area occurred between 2011 and 2012.

### Inlet Width

Satellite imagery revealed that the inlet at this site did not show up until 2010. The rapid expansion of the inlet from 2010 until 2015 began as a small (5.5m) inlet that eventually developed into an open cove on the northern shoreline of Bay Round.

### Interior Pond Area

The open water area behind the inlet increased as the inlet width grew. The erosion rate for the open water area follows closely with the expansion of the inlet mouth. Most land loss conversion to open water occurred as the result of shoreline retreat along then northern shoreline of the pond at site 6C.

| Date | Width of Inlet (m) | Erosion Rates Inlet (m/yr) | Open Water Area (m²) | Erosion Rates Open Water Area (m²/yr) |
|------|--------------------|----------------------------|----------------------|----------------------------------------|

| | | | | |
|---|---|---|---|---|
| 3/13/2010 | 5.50 | --- | 14495 | --- |
| 4/15/2011 | 11.84 | -5.81 | 14572 | -70.62 |
| 10/29/2012 | 95.53 | -54.26 | 19081 | -2923.24 |
| 1/27/2015 | 106.42 | -4.85 | 19898 | -363.67 |

*Table 43. Inlet and open water area sizes and erosion rates for site 6C.*

### Tidal Prism

The average tide range during the time being studied at the closest tide sensor is from the RBR deployed at site 1C. Average tide range of .22 m was used to calculate tidal prism. Using open water area multiplied by the average tide range reveals tidal prism values ranging from 3188.9 $m^3$ (2010) to 4377.56 $m^3$ (2015) (Table 39).

| Date | Tidal Prism ($m^3$) |
|---|---|
| 3/13/2010 | 3188.90 |
| 4/15/2011 | 3205.84 |
| 10/29/2012 | 4197.82 |
| 1/27/2015 | 4377.56 |

*Table 44. Tidal prism values based on average tide range from RBR sensor at site 1C.*

### Fetch Measurements

Site 6C is located on the northern shoreline of Bay Round and is unprotected to the south. The greatest fetch distances are to the south-southeast (3286 m), southeast (2354 m) and east-southeast (3280 m). The average fetch distance from the center of the inlet at site 6C is 895.48 m (*Figure 68*).

*Figure 68. This image depicts Fetch distances and directions as they relate to the mouth of the inlet located at site 6C. Distance (in meters) from the center of the inlet mouth to the nearest shoreline is depicted as the blue line in the inset graph (2016 image from Google Earth).*

### ADCP

| Transect # | 002 | 004 | 005 |
|---|---|---|---|
| Depth (m) | 1.08 | 0.67 | 0.98 |
| Transect Length (m) | 108.5 | 103.23 | 108.82 |
| Actual Cross Sectional Area (m2) | 117.11 | 68.94 | 106.62 |

*Table 45. Transect data taken during ADCP instrument deployment.Transect direction and location affected the depth between #002 and #004. The larger cross sectional area calculated from transects #002 and #005 were derived from transects taken closer to the open water bay to the south of site 6C.*
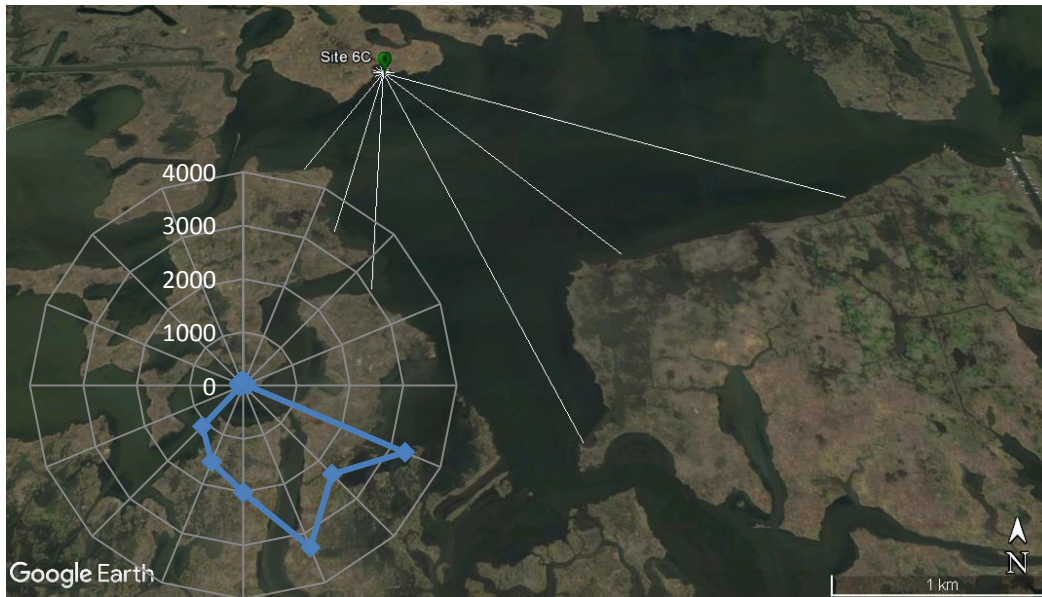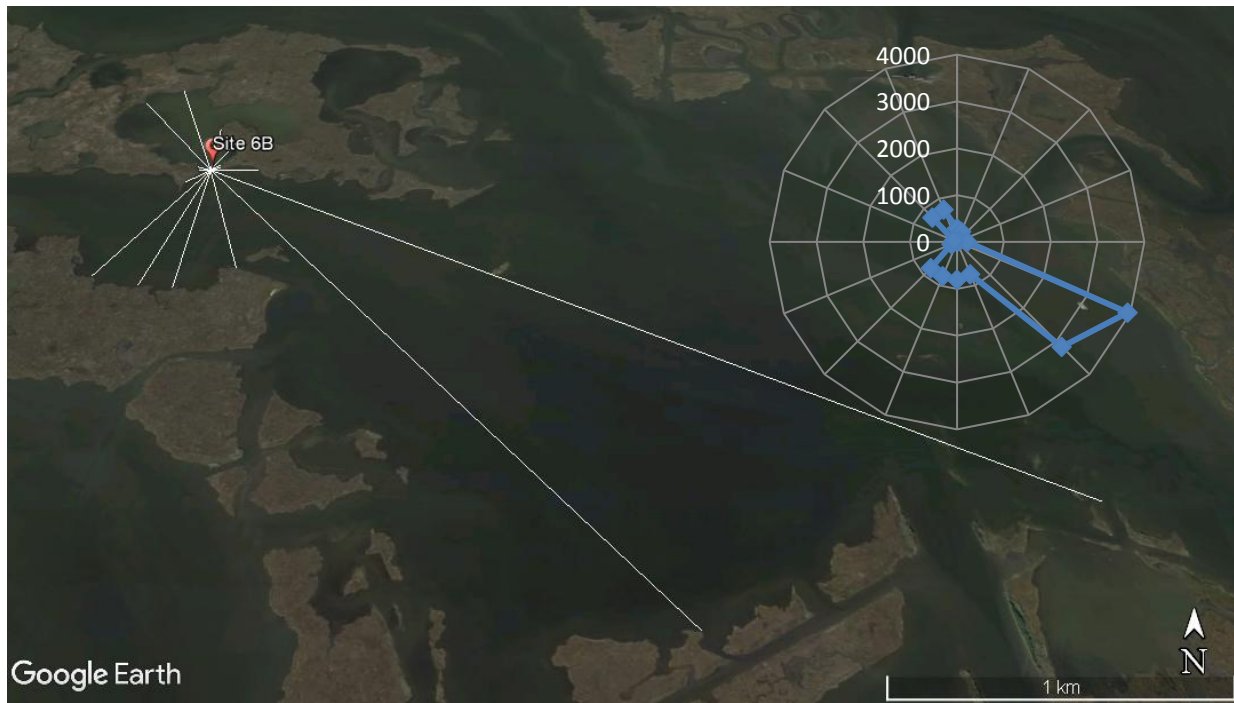
*Figure 69. This image depicts Fetch distances and directions as they relate to the mouth of the inlet located at site 6B. Distance (in meters) from the center of the inlet mouth to the nearest shoreline is depicted as the blue line in the inset graph (2016 image from Google Earth).*

# Appendix B

Wind data from New Orleans International Airport during instrument deployment period (8/23/2016-9/13/2016).

| Dir | 0-3 | 3-6 | 6-9 | 9-12 | 12-15 | >15 | Grand Total |
|---|---|---|---|---|---|---|---|
| 0-9 | 0.29% | 0.22% | 0.13% | 0.05% | 0.02% | 0.00% | 0.71% |
| 10-19 | 0.36% | 0.45% | 0.13% | 0.13% | 0.14% | 0.00% | 1.21% |
| 20-29 | 0.22% | 0.33% | 0.63% | 0.58% | 0.25% | 0.00% | 2.01% |
| 30-39 | 0.25% | 0.38% | 0.51% | 0.71% | 0.31% | 0.00% | 2.16% |
| 40-49 | 0.31% | 0.76% | 1.05% | 0.69% | 0.04% | 0.00% | 2.84% |
| 50-59 | 0.36% | 0.47% | 0.67% | 0.47% | 0.20% | 0.00% | 2.17% |
| 60-69 | 0.33% | 1.54% | 1.59% | 0.76% | 0.56% | 0.04% | 4.82% |
| 70-79 | 0.43% | 1.25% | 1.92% | 2.12% | 1.87% | 0.42% | 8.01% |
| 80-89 | 0.34% | 1.59% | 2.43% | 1.45% | 0.29% | 0.00% | 6.11% |
| 90-99 | 0.62% | 2.12% | 3.46% | 1.54% | 0.25% | 0.02% | 8.01% |
| 100-109 | 0.63% | 3.19% | 4.46% | 1.45% | 0.20% | 0.02% | 9.95% |
| 110-119 | 0.91% | 4.29% | 2.50% | 0.36% | 0.04% | 0.00% | 8.10% |
| 120-129 | 0.94% | 3.82% | 0.74% | 0.18% | 0.02% | 0.00% | 5.71% |
| 130-139 | 0.76% | 3.08% | 1.76% | 0.09% | 0.04% | 0.00% | 5.72% |
| 140-149 | 0.69% | 2.39% | 1.54% | 0.14% | 0.11% | 0.02% | 4.89% |
| 150-159 | 0.63% | 2.70% | 0.80% | 0.07% | 0.05% | 0.00% | 4.26% |
| 160-169 | 0.74% | 2.16% | 0.45% | 0.05% | 0.00% | 0.00% | 3.41% |
| 170-179 | 0.82% | 1.18% | 0.18% | 0.04% | 0.00% | 0.02% | 2.23% |
| 180-189 | 0.92% | 0.76% | 0.04% | 0.04% | 0.00% | 0.00% | 1.76% |
| 190-199 | 1.07% | 1.21% | 0.07% | 0.00% | 0.00% | 0.00% | 2.36% |
| 200-209 | 0.69% | 0.83% | 0.18% | 0.00% | 0.00% | 0.00% | 1.70% |
| 210-219 | 0.91% | 0.56% | 0.09% | 0.00% | 0.00% | 0.00% | 1.56% |
| 220-229 | 0.98% | 0.20% | 0.00% | 0.00% | 0.00% | 0.00% | 1.18% |
| 230-239 | 0.78% | 0.33% | 0.00% | 0.00% | 0.00% | 0.00% | 1.11% |
| 240-249 | 0.82% | 0.27% | 0.02% | 0.00% | 0.00% | 0.00% | 1.11% |
| 250-259 | 0.60% | 0.18% | 0.04% | 0.00% | 0.00% | 0.00% | 0.82% |
| 260-269 | 0.45% | 0.42% | 0.11% | 0.00% | 0.00% | 0.00% | 0.98% |
| 270-279 | 0.25% | 0.04% | 0.09% | 0.00% | 0.00% | 0.00% | 0.38% |
| 280-289 | 0.22% | 0.04% | 0.16% | 0.00% | 0.00% | 0.00% | 0.42% |
| 290-299 | 0.25% | 0.11% | 0.04% | 0.00% | 0.00% | 0.00% | 0.40% |
| 300-309 | 0.43% | 0.00% | 0.09% | 0.02% | 0.00% | 0.00% | 0.54% |
| 310-319 | 0.38% | 0.07% | 0.07% | 0.00% | 0.00% | 0.04% | 0.56% |
| 320-329 | 0.24% | 0.16% | 0.13% | 0.00% | 0.02% | 0.05% | 0.60% |
| 330-339 | 0.18% | 0.16% | 0.42% | 0.02% | 0.00% | 0.02% | 0.80% |
| 340-349 | 0.34% | 0.14% | 0.18% | 0.05% | 0.02% | 0.00% | 0.74% |
| 350-359 | 0.38% | 0.24% | 0.05% | 0.02% | 0.00% | 0.00% | 0.69% |
| >360 | 0.02% | 0.00% | 0.00% | 0.00% | 0.00% | 0.00% | 0.02% |
| Grand Total | 19.55% | 37.64% | 26.72% | 11.03% | 4.42% | 0.63% | 100.00% |

# Appendix C

## Fetch Measurements

| Direction | 1A | 2A | 3A | 1B | 2B | 3B | 4B | 5B | 6B | 1C | 2C | 3C | 4C | 5C | 6C |
|---|---|---|---|---|---|---|---|---|---|---|---|---|---|---|---|
| N | 38.1 | 197 | 14.8 | 34.2 | 221 | 169 | 1023 | 183 | 287 | 58.2 | 10.6 | 4.9 | 78 | 9.1 | 85.5 |
| NNE | 57.7 | 189 | 9.2 | 41.9 | 66.9 | 36.5 | 1018 | 253 | 243 | 132 | 14.8 | 10.9 | 3.54 | 9 | 72.4 |
| NE | 4.63 | 166 | 4.89 | 284 | 16 | 49.9 | 890 | 60.8 | 55.3 | 170 | 14.1 | 41.8 | 3.5 | 12 | 65.5 |
| ENE | 5.22 | 12.9 | 3.48 | 372 | 13 | 451 | 323 | 30.1 | 44.4 | 155 | 11.5 | 29.5 | 4.4 | 19.7 | 50.4 |
| E | 6.23 | 142 | 3.9 | 94.4 | 20.4 | 50.6 | 227 | 20 | 223 | 170 | 13.4 | 7.31 | 4.9 | 48.4 | 80.7 |
| ESE | 6.74 | 117 | 44.6 | 129 | 95.4 | 15.7 | 218 | 22.6 | 3943 | 688 | 52.1 | 5.92 | 9.1 | 58.4 | 3280 |
| SE | 65.3 | 40 | 23.5 | 226 | 36.1 | 13.8 | 12859 | 35.3 | 3166 | 2910 | 83.6 | 9.2 | 44.9 | 97.4 | 2354 |
| SSE | 25.1 | 24.5 | 13.9 | 83.3 | 29.7 | 14.5 | 14821 | 48 | 745 | 1146 | 313 | 11.9 | 13.5 | 89.4 | 3286 |
| S | 17.5 | 30.5 | 12.9 | 77.3 | 25.2 | 17.3 | 15424 | 49.3 | 805 | 25 | 216 | 211 | 4.9 | 80 | 2012 |
| SSW | 19.1 | 313 | 12.2 | 71.2 | 130 | 17.6 | 14643 | 58.8 | 791 | 28.8 | 80.2 | 287 | 11.5 | 92 | 1555 |
| SW | 30 | 238 | 158 | 55.1 | 107 | 211 | 953 | 58.3 | 787 | 43 | 110 | 127 | 159 | 133 | 1082 |
| WSW | 67.8 | 78.6 | 104 | 62.4 | 170 | 53.3 | 1795 | 79.5 | 127 | 55.7 | 280 | 502 | 190 | 163 | 70 |
| W | 55.7 | 64.4 | 7.7 | 107 | 147 | 36 | 2044 | 426 | 57.5 | 76.7 | 504 | 26.1 | 87.9 | 238 | 69 |
| WNW | 4.5 | 7.85 | 6.3 | 153 | 150 | 25.8 | 1146 | 638 | 75.2 | 104 | 11.5 | 5.7 | 42 | 789 | 91.3 |
| NW | 4.57 | 163 | 24.4 | 63 | 221 | 81.2 | 744 | 21.5 | 741 | 28.9 | 10 | 3.2 | 38.4 | 38 | 86.3 |
| NNW | 7.22 | 192 | 12.5 | 27.7 | 487 | 122 | 952 | 186 | 746 | 32.2 | 9.9 | 3 | 46.8 | 15 | 87.6 |
| | 25.96313 | 123.4844 | 28.51688 | 117.5938 | 120.9813 | 85.325 | 4317.5 | 135.6375 | 802.275 | 363.9688 | 108.4188 | 80.40188 | 46.39625 | 118.2125 | 895.4813 |

# Vita

Bryan T. Carter received his Bachelor of Arts in History and Religious Studies at Millsaps College in Jackson, Mississippi in 1999. An avid outdoorsmen and fly-fishing guide, Carter has owned and operated his charter fishing business in the greater New Orleans area since 2002. During his time as a fly-fishing guide, Carter served as the regional ambassador for the outdoor company Patagonia.  Since returning to academia to complete his Master of Science**,** Carter has worked with national non-profits such as the Ocean Conservancy.